Sodium [^{18}F]Fluoride positron emission tomography for non-invasive identification of micro-calcifications as marker of atherosclerotic plaque vulnerability

Von der Medizinischen Fakultät
der Rheinisch-Westfälischen Technischen Hochschule Aachen
zur Erlangung des akademischen Grades eines Doktors der Theoretischen Medizin
genehmigte Dissertation

vorgelegt von

Dr. med.

Alexandru Florea

aus Bukarest (Rumänien)

Berichter: Universitätsprofessor Dr. med. Felix Mottaghy
Universitätsprofessor Dr. med. Fabian Kiessling

Tag der mündlichen Prüfung: 16.02.2023

Sodium [^{18}F]Fluoride positron emission tomography

for non-invasive identification of micro-calcifications

as marker of atherosclerotic plaque vulnerability

DISSERTATION

To obtain the degree of Doctor at Maastricht University and Doctor rerum medicinalium (Dr. rer. medic.) at the RWTH Aachen University on the authority of the Rector Magnifici Prof. dr. Pamela Habibović and Univ.-Prof. Dr. rer. nat. Dr. h. c mult. Ulrich Rüdiger, in accordance with the decision of the Board of Deans to be defended in public

on Wednesday 8th, March 2023, at 16:00 hours

By

Alexandru Florea

Approved after corrections

Prof. dr. Pamela Habibović

Rector Magnificus

Medizinische Fakultät | RWTH AACHEN UNIVERSITY

Maastricht UMC+

Maastricht University

Supervisors:

Prof. Dr. F. M. Mottaghy, RWTH Aachen University

Prof. Dr. M. E. Kooi, Maastricht University

Prof. Dr. L. J. Schurgers, Maastricht University

Co-supervisor:

Prof. Dr. J. Bucerius, RWTH Aachen University

Assessment Committee:

Prof. Dr. Chris P. Reutelingsperger, Maastricht University (Chair)

Prof. Dr. Ingrid Dijkgraaf, Maastricht University

Prof. Dr. Fabian Kiessling, RWTH Aachen University

Dr. Hein J. Verberne, UC Louvain Brussels, Belgium

Prof. Dr. Olivier Gheysens, Amsterdam University Medical Centers

Printing: Ridderprint | www.ridderprint.nl

The research presented in this dissertation was financed by a grant from the European Union's Horizon 2020 research and innovation programme under the Marie Skłodowska-Curie grant "INTRICARE" (722609).

INTRICARE

"*A new scientific truth does not triumph by convincing its opponents and making them see the light, but rather because its opponents eventually die, and a new generation grows up that is familiar with it.*" — MAX PLANCK, SCIENTIFIC AUTOBIOGRAPHY AND OTHER PAPERS

Parts of this dissertation were pre-published in:

- Florea A, Morgenroth A, Bucerius J, Schurgers LJ, Mottaghy FM. Locking and loading the bullet against micro-calcification. *Eur J Prev Cardiol*. 2020;28(12):1370-1375.
- Florea A, Sigl JP, Morgenroth A, Vogg A, Sahnoun S, Winz OH, Bucerius J, Schurgers LJ, Mottaghy FM. Sodium [^{18}F]Fluoride PET Can Efficiently Monitor In Vivo Atherosclerotic Plaque Calcification Progression and Treatment. *Cells*. 2021;10(2):275.
- Florea A, Kooi ME, Mess W, Schurgers LJ, Bucerius J, Mottaghy FM. Effects of Combined Vitamin K2 and Vitamin D3 Supplementation on Na[^{18}F]F PET/MRI in Patients with Carotid Artery Disease: The INTRICATE Rationale and Trial Design. *Nutrients*. 2021;13(3):994.

Table of content

List of abbreviations

Scientific abbreviations

ApoE – Apolipoprotein E

$ApoE^{-/-}$ – Apolipoprotein E knock-out

BGP – Bone Gla protein

CAC – Coronary artery calcification

CT – Computed tomography

CVD – Cardiovascular disease

CXCL-12 – CXC ligand 12

CXCR-4 – CXC receptor 4

dp-ucMGP – Dephosphorylated uncarboxylated Matrix Gla protein

Gla – Carboxyglutamic acid

Glu – Glutamic acid

GRP – Gla-rich protein

HDL – High-density lipoprotein

HE – Haematoxylin eosin

HU – Hounsfield units

IDL – Intermediate-density lipoprotein

IGF-1 – Insulin-like growth factor 1

INR – International normalized ratio

KH_2 – Reduced vitamin K

KO – Vitamin K 2,3-epoxide

LDL – Low-density lipoprotein cholesterol

MGP – Matrix Gla protein

MK – Menaquinone

MK-7 – Menaquinone-7

MRI – Magnetic resonance imaging

$Na[^{18}F]F$ – Sodium [^{18}F]Fluoride

OC – Osteocalcin

PET – Positron emission tomography

PT – Prothrombin time

SPECT – Single-photon emission computed tomography

TBRmax – Maximum target-to-background ratio

TNF-α – Tumor necrosis factor alpha

US – Ultrasound

VKA – Vitamin K antagonist

VKDP – Vitamin K dependent protein

VKOR – Vitamin K epoxide reductase

VLDL – Very low-density lipoprotein cholesterol

VOI – Volume of interest

γGCX – γ-glutamyl carboxylase

Linguistic abbreviations

e.g. – for example (lat. *exempli gratia*)

et al. – and others (lat. *et alia*)

i.e. – in other words (lat. *id est*)

vs. – as opposed to, in contrast to (lat. *versus*)

Chapter I: General introduction

Cardiovascular disease is an ancient foe of human health, that can be traced back to a 5.300 year old mummy found in Austria, in the Tyrolean Alps (Murphy et al., 2003). Despite the recent advances in interventional medicine, cardiovascular disease is the leading cause of death worldwide, exceeding even cancer mortality (European Heart Network, 2017; World Health Organization, 2017) (Fig. 1). In addition, it is associated with significant health consequences for the individual and results in high medical costs for society.

Almost 90% of cardiovascular diseases have as an underlying pathophysiological process atherosclerosis (Planer et al., 2014). In atherosclerosis the arterial wall develops lesions, which initially consist of macrophage cells, cell debris, lipids, and a variable amount of connective tissue. In the 90's, Ross *et al.* proved that atherosclerosis is a chronic inflammatory disease (Ross, 1999); a process which the body usually resolves through either fibrosis or through calcification. The appearance of micro-calcifications in an atherosclerotic plaque is generally regarded as a feature of vulnerability and of high-risk for the patient.

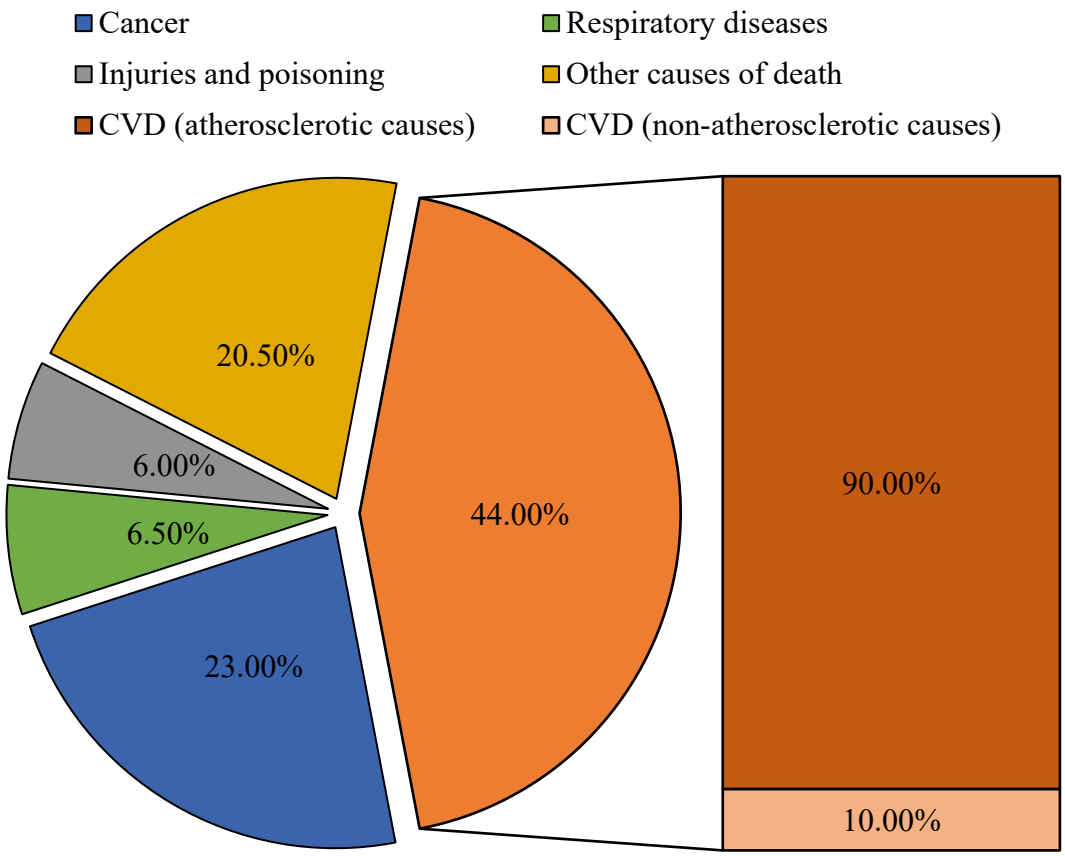

Figure 1. Deaths by cause in Europe. Cardiovascular disease (CVD) is the main cause of death in Europe (Planer et al., 2014; European Heart Network, 2017) and atherosclerosis the main culprit of this high mortality.

Atherosclerotic plaque development

The atherogenic process starts with the sub-endothelial retention of cholesterol-containing plasma lipoproteins, which initiate a cascade of pro-inflammatory responses. In the initial stages, vascular permeability is increased, allowing for infiltration and retention of low and very low-density lipoprotein cholesterol (LDL and VLDL), and peripheral monocytes are drawn into the intimal layer and transformed into macrophages. As these lipoproteins oxidize, they are phagocytised by macrophages, forming "foam cells" that subsequently undergo apoptosis and necrosis. The resulting breakdown products, including oxidized lipids and cellular debris, make up a highly thrombogenic lipid core covered by a collagen-rich fibrous cap. These plaques can expand with further accumulation of lipids and eventually rupture with the weakening of the fibrous cap, causing life-threatening events such as myocardial infarction and ischemic stroke.

The understanding of atherosclerotic plaque formation has evolved tremendously since Ross stated it is an inflammatory disease. Nowadays, atherosclerosis is considered to be a 6-stage disease (Gargiulo et al., 2016), with lesions that occur at predicted sites, where blood flow is turbulent (Figure 2):

1. Local accumulation and oxidation of lipids with slight thickening of the intima. The most notably lipids, which participated in this stage, can be found in LDL and VLDL.
2. Local infiltration of inflammatory cells. During this stage, macrophages try to eat the oxidized lipids, thus they become abundant in intra-cytoplasmic lipid inclusions, hence their name "foam cells". This stage is also known as "fatty streaks".
3. Local activation of the inflammasome. This is the body's failed attempt to clear the site of lipids.

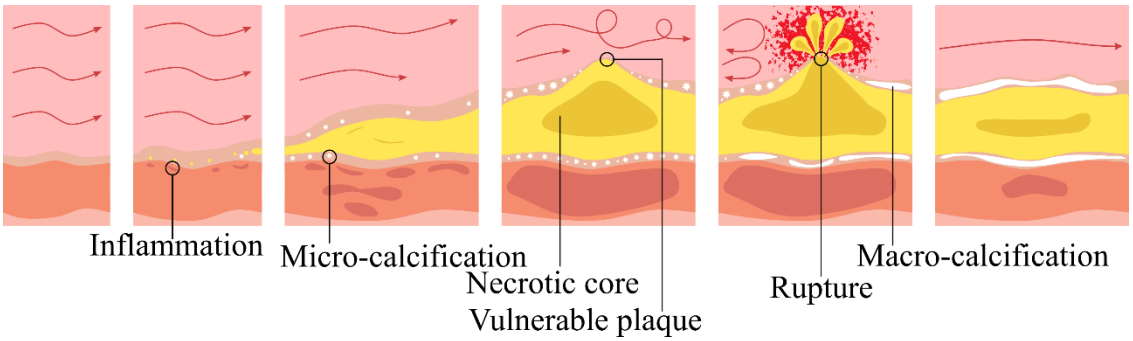

Figure 2. Atherosclerotic plaque development.

4. The disease progresses and the plaque has a lipid core, surrounded by (i) inflammatory cells, which try to eat the lipids, (ii) fibroblasts, which secrete extracellular matrix to limit the expansion of the process, and (iii) vascular smooth muscle cells and osteoblast-like cells, which start to promote calcification around the lipid core to localize and delimit the process. Because of the start of micro-calcifications, from this stage onwards, the plaque is prone to rupture.
5. Fibroblasts finished forming the fibrous "cap" of the plaque, thus further expanding the plaque into the lumen of the vessel, and so destabilising it. This stage is also known as "fibrous plaque".
6. The final stage is named "complicated", because now the plaque has ruptured, exposing the thrombogenic core to the blood and to platelets, with subsequent thrombi formation, that may generate and acute event (*e.g.,* heart attack, stroke).

Thus, from stage 4 onwards, the plaque is called "vulnerable" because it can rupture and create a thrombus, that can completely obstruct the vessel, leaving the down-stream tissue without any blood supply (Figure 2); and so, in a matter of minutes, or even seconds, the cells of the tissue will die (*i.e.,* necrosis).

The initiation of inflammation triggers the calcification of the vascular wall (W. Chen & Dilsizian, 2013). In the early stages of plaque progression, cytokines released by inflammatory cells, such as TNF-α and IGF-1, induce the formation of lipid-laden plaques as well as the osteogenic transformation of the surrounding vascular smooth muscle cells. These changes create a positive feedback loop that causes further osteogenic differentiation and gives rise to micro-calcifications that coalesce and ultimately pervade the atherosclerotic plaque, intimal layer (N. X. Chen & Moe, 2015). Calcifications under 50 μm in size are generally considered microcalcifications, which are a marker of cell death and inflammation and carry an increased risk of plaque rupture and associated complications (McKenney-Drake et al., 2018). Macrocalcifications, on the other hand, measure greater than 50 μm and may actually impart plaque stability (Irkle et al., 2015).

From a clinical point of view, macro-calcified plaques are considered to be irreversible (McKenney-Drake et al., 2018); furthermore, macro-calcification is suggested to be beneficiary for its stability. Once a micro-calcified plaque becomes macro-calcified, it is supposed to be stable, because the fibrous cap is thick enough to withstand erosion. The most often used parallelism, is with the calcification that occurs around the tuberculosis granuloma. In a desperate attempt to stop the infection, the body isolates the *bacterium via* a calcified membrane and lets it die by depriving it of nutrients from the blood.

However, in the case of atherosclerosis, this strategy does not seem to be helpful, as plaque vulnerability and its complications are a greater risk to human health. This is the reason why, current research is concentrated on correctly identifying, as soon as possible, the micro-calcified state and to try to delay as much as possible the appearance of calcifications.

Vitamin K

Despite having a long history, vitamin K is probably the most understudied vitamin. It was discovered in 1934 by the Danish researcher H. Dam, who observed a tendency to large haemorrhages to chicks eating a fat-free diet (Dam, 1935). Shortly after, his colleague, F. Schönheyder, asserted that vitamin K deficiencies decrease the efficiency of the coagulation cascade (Schönheyder, 1935). In spite of this early research, only in the 1970's, biological inactive clotting factors (factors II, VII, IX and X) were found after treatment with Dicumarol, a vitamin K antagonist (VKA) (Nelsestuen & Suttie, 1972; Stenflo et al., 1974). These abnormal factors lacked the γ-carboxyglutamate (Gla) residues from Ca^{2+}-binding site (Nelsestuen & Suttie, 1972; Stenflo et al., 1974) that was present in the untreated animals. Thus, it became common knowledge that vitamin K is a cofactor in the post-translational γ-carboxylation of the glutamate (Glu) residues from most liver-derived clotting factors, hence transforming them into Gla residues.

Over the years, many other vitamin K dependent proteins (VKDPs), which require vitamin K to become biologically active, have been discovered (Berkner & Runge, 2004), such as protein C (Stenflo, 1976), protein S (Maillard et al., 1992), protein Z (Prowse & Esnouf, 1977), osteocalcin (OC) (*i.e.,* BGP, from bone Gla protein) (P A Price, Otsuka, et al., 1976; P A Price, Poser, et al., 1976), matrix Gla protein (MGP) (Paul A. Price et al., 1983) and Gla-rich protein (GRP) (Viegas et al., 2008). Therefore, VKDPs can be divided into two categories: (i) liver derived VKDPs that participate in haemostasis and (ii) extra-hepatic VKPDs, which are synthetized in other organs (*e.g.,* bone, blood vessels). However, no matter the origin, their common feature is that they activate only

after binding calcium free ions (*i.e.,* Ca^{2+}) *via* their Gla-rich domain. This led to the assertion that the presence of vitamin K is paramount for the biological activation of VKDPs.

The structure of vitamin K

Actually, the term vitamin K refers to a family of vitamers. All of them share a common 2-methyl-1,4-naphthoquinone (*i.e.,* Menadione) nucleus, to which different side chains are linked to the 3-position (Figure 3). This family of vitamers include:

i. one naturally occurring Phylloquinone (*i.e.,* vitamin K1),
ii. several naturally occurring Menaquinones *(i.e.,* vitamin K2) and
iii. some synthetic compounds: Menadione (*i.e.,* vitamin K3), Acetomenaphthone (*i.e.,* vitamin K4), and vitamin K5.

Depending on the length and the saturation of the side chain, naturally occurring vitamins K are classified into Phylloquinone and Menaquinones (MKs). Mostly plants and cyanobacteria produce Phylloquinone (Collins & Jones, 1981; Ogawa et al., 2007; Martin J. Shearer & Newman, 2008), which has the same phytyl side chain as in chlorophyll (Figure 3). MKs are characterized by a variable number of repeating prenyl units attached to 3-position of the nucleus (Figure 3). For purposes of nomenclature, MKs are further

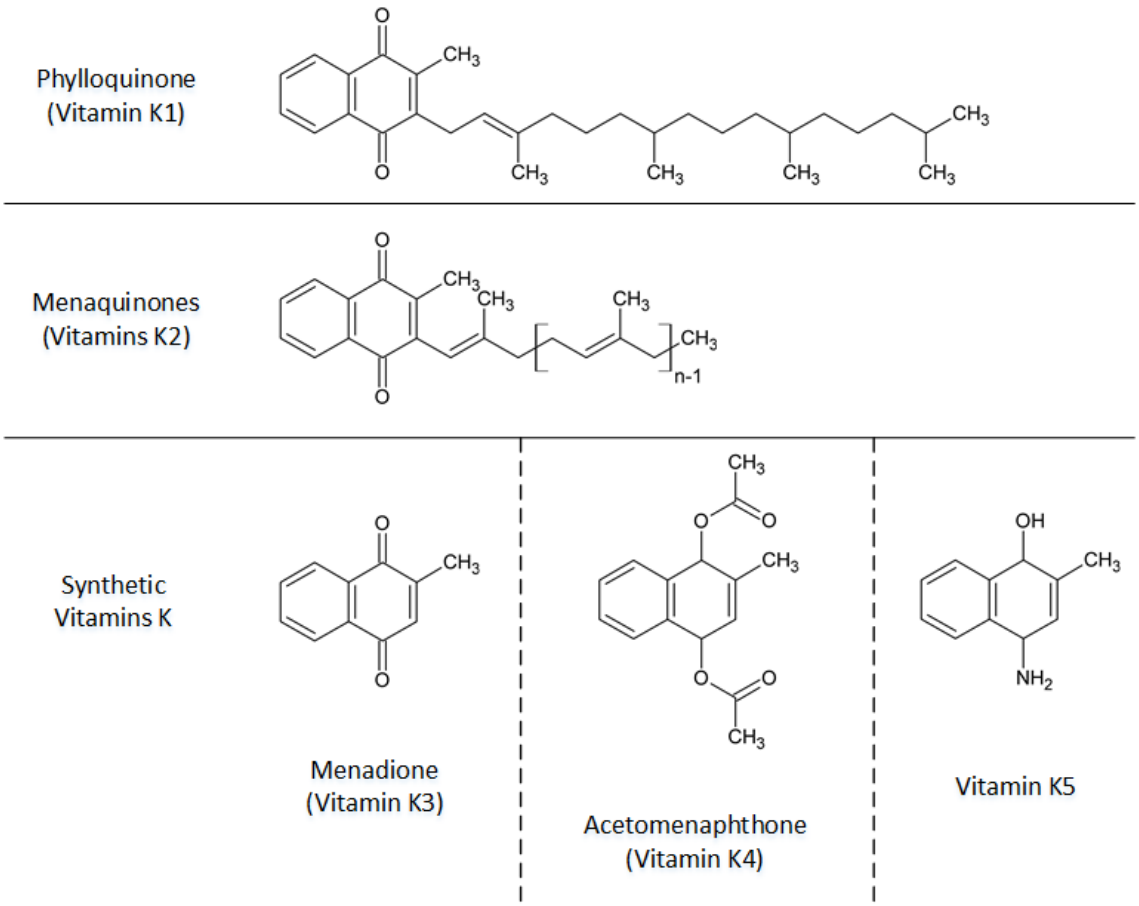

Figure 3. Chemical structure of all vitamins K.

sub-classified according to the number of prenyl units (*i.e.,* n) and this number is given as a suffix to the name (*i.e.,* MK-n) (Martin J. Shearer & Newman, 2008). The longer the side chain of repeating units, the more lipophilic the MK is. Therefore, most naturally occurring vitamins K (including Phylloquinone) are not soluble in water; for this reason, synthetic vitamins K were produced, that lack the side chain.

Vitamin K3 is composed only of the common Menadione nucleus (Figure 3), after which it is also named. By having no side chain at the 3-position, K3 is the first water soluble member of the vitamin K family. Within the liver, K3 is converted into MK-4 (Sato et al., 2012), thus it is considered a pro-vitamin K (Ogawa et al., 2007). K4 is a vitamin K diacetate, with two acetyl groups linked to the Menadione nucleus, while K5 has one of the carbonyl groups (*i.e.,* oxygen double bounds) replaced with an amino group and the other with a hydroxyl group, further increasing its hydrophilicity.

Dietary sources of vitamins K

Phylloquinone is almost invariably synthetized by cyanobacteria and plants (Collins & Jones, 1981; Ogawa et al., 2007; Martin J. Shearer & Newman, 2008), where it serves as a light-dependent electron carrier from the chlorophyll (Fromme & Grotjohann, 2006; Sakuragi & Bryant, 2006). Therefore, high concentrations of Phylloquinone can be found in green leafy vegetables, but also in several vegetable oils, fruits and dairy products (Booth et al., 1993; M.J. Shearer & Bolton-Smith, 2000; Martin J. Shearer & Newman, 2008). But, by being tightly bound to the chloroplast membrane (Chatrou et al., 2011), there is a poor absorption of Phylloquinone from vegetables (Gijsbers et al., 1996; Schurgers & Vermeer, 2000).

On the other hand, most bacteria possess the enzymatic equipment required to produce a variety of MKs that have different prenyl polymers in the 3-position (*i.e.,* from 3 to 13 repeating units within the side chain) (Collins & Jones, 1981). Thus, they are mostly found in animal liver, meat, and fermented foods (from bacteria, not fungi) (Schurgers & Vermeer, 2000; Martin J. Shearer & Newman, 2008). The richest food in MKs are represented by cheeses and sauerkraut (*i.e.,* MK-8 and MK-9) in Western diets and by natto (*i.e.,* MK-7) in Japan (Schurgers & Vermeer, 2000; Martin J. Shearer & Newman, 2008). The absorption of MKs is much better than that of Phylloquinone (Schurgers, Teunissen, et al., 2007).

By being synthetic, there are no naturally occurring sources of vitamins K3, K4, or K5. Nevertheless, dietary sources of vitamin K5 could be represented by processed foods,

which have this vitamin as an added preservative, due to its bacteriostatic and fungistatic properties (Merrifield & Yang, 1965a, 1965b).

The physiological function of vitamins K

Since the discovery of naturally occurring vitamins K in 1935 (Schönheyder, 1935), until 1976, when the first VKDP that is synthetized outside the liver (*i.e.,* OC) was found (P A Price, Otsuka, et al., 1976; P A Price, Poser, et al., 1976), there is a 40-year gap, while this vitamin have been falsely assumed of activating only the liver-derived clotting factors. Fortunately, nowadays, two more extra-hepatic VKDPs are completely characterised. The most recent one was characterised in 2008 by Viegas *et al.* (Viegas et al., 2008) and, because it has the highest Gla percent of all known proteins, it was named Gla-rich protein (GRP).

Nevertheless, the common feature of all VKDPs is that they become biologically active only after the post-translational γ-carboxylation of the Glu residues into Gla. With the discovery of the first Gla-containing proteins, the dependency of this process on vitamins K has been elucidated (M.J. Shearer, 1995).

The vitamin K cycle

The Gla-rich domains of the nowadays-well-characterised VKDPs range from 3 to 16 Glu residues (Laizé et al., 2005; Viegas et al., 2008) that need to be successively γ-carboxylated during a multi-step process (Berkner & Runge, 2004; Morris et al., 1995; Stenina et al., 2001), called the vitamin K cycle. Like the absorption and bio-distribution, most of the knowledge regarding the metabolism and catabolism of vitamins K comes from studies done with Phylloquinone. The exact mechanism by which vitamin K is involved in the γ-carboxylation of VKDP remained a puzzle until 1999, when Furie *et al.* published a review (Furie et al., 1999) that became the foundation of explaining the vitamin K cycle.

All dietary forms of vitamin K enter the cells as quinones, but the active form required for the γ-carboxylation is the reduced vitamin K (KH_2), *i.e.,* the hydroquinone form (Figure 4A). In most tissues, KH_2 is recycled from the already used vitamin K 2,3-epoxide (KO) *via* vitamin K epoxide reductase (VKOR) (Martin J. Shearer & Newman, 2008; Suttie, 1985). The first evidence of this recycling was the high rate of Glu to Gla conversion, compared to the low dietary intake of vitamins K (Suttie, 1985). Subsequently, KH_2 is used by γ-glutamyl carboxylase (γGCX) to carboxylate Glu into Gla. In 1995, Dowd *et al.* (Dowd et al., 1995) proposed the "base strength amplification" to explain this conversion. To KH_2, which is a weak base, is added oxygen to produce a short-lived alkoxide form that is a strong base (Dowd et al., 1995). This active oxygenated specie of vitamin K is able to abstract a hydrogen from the γ-carbon of Glu, with subsequent collapse into KO (Furie et al., 1999); thus, γGCX is also a vitamin K epoxidase. Carbon dioxide is then subsequently added to the same γ-carbon to form Gla (Furie et al., 1999). Under normal conditions, for each Gla-residue generated, a molecule of KO is also created (Figure 4A). The cycle is finally closed, as KO is recycled into KH_2, by VKOR (Figure 4A). In the liver, there is an alternate pathway that can activate dietary vitamins K to KH_2 *via* NAD(P)H-dependent quinone reductase (Berkner & Runge, 2004) (Figure 4B). This enzyme has such a high affinity for vitamins K, that is relatively insensitive to VKAs (Berkner & Runge, 2004) (Figure 4B). This accounts for an efficient hepatic synthesis of clotting factors when VKAs are co-administered with vitamins K. This mechanism has been used in animal studies where the vascular influences of Warfarin were of interest (Krüger et al., 2013; Paul A. Price et al., 1998; Schurgers et al., 2012).

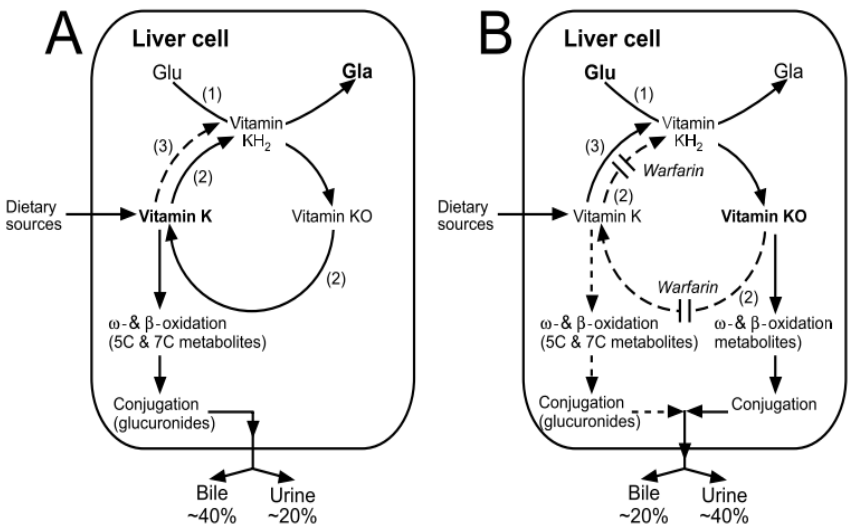

Figure 4. The vitamin K cycle (Martin J. Shearer & Newman, 2008; Stenina et al., 2001)

The short-lived vitamin K alkoxide is highly reactive and potentially toxic (Furie et al., 1999). Therefore, the affinity of γGCX for KH_2 is turned off until it is bound to the carboxylase recognition signal of a VKDP (Jorgensen et al., 1987; Sugiura et al., 1997). With the notable exception of MGP (Berkner & Runge, 2004), all other VKDPs have their recognition signal in the pro-peptide region, upstream to the Gla-rich domain (Furie et al., 1999). By being bound to the inner layer of the endoplasmic reticulum membrane (Furie et al., 1999), γGCX is able to bind un-carboxylated VKDPs that pass through the lumen. Moreover, the recognition signal also has the role of allosterically activating the γGCX (Knobloch & Suttie, 1987) to bind KH_2. Strangely enough, even though γGCX was found also in the Golgi apparatus *via* immunostaining, the carboxylation appears to be completed in the endoplasmic reticulum (Furie et al., 1999). Emphasizing even more the efficiency of γGCX, is the fact that VKDPs require multiple carboxylations to become biologically active but the mean half-time of a γGCX/VKDP interaction is 63,5min (Morris et al., 1995). The speed of γGCX is explained by the "tethered" mechanism (Stenina et al., 2001). During the γ-carboxylation, the proteins are bound to γGCX throughout the reaction *via* the carboxylase recognition signal, with the Gla-rich domain undergoing a rapid intramolecular movement to reposition Glu residues for catalysis (Stenina et al., 2001). Furthermore, this mechanism shows how the Gla-rich domain is not sterically constrained by the rest of the VKDP during γ-carboxylation (Stenina et al., 2001).

VKDPs require also other post-translational modifications. While in the endoplasmic reticulum, they also undergo N- or O-linked glycosylation, sulfation, phosphorylation, asparagine- or aspartate-β-hydroxylation and limited proteolysis (Berkner & Runge, 2004).

Vitamin K dependent proteins (VKDPs)

There are many other VKDPs that are insufficiently characterised, such as periostin (Coutu et al., 2008), growth arrest-specific gene 6 (*i.e.,* Gas-6) (Manfioletti et al., 1993), proline-rich Gla proteins 1 and 2 (*i.e.,* PRGP1 and PRGP2) (Kulman et al., 1997), transmembrane Gla protein 3 and 4 (*i.e.,* TGP3 and TGP4) (Kulman et al., 2001) but their functions are not yet well established. Nevertheless, the Gla-rich domains of well characterised VKDPs can range up to 16 residues in GRP (Viegas et al., 2008). In 1995, Dowd *et al.* (Dowd et al., 1995) asserted that VKDPs require so many γ-carboxylated Glu residues, in order to be able to bind strongly and specifically to calcium ions that is able

to form a bride to the anionic phosphate. Indeed, the binding factors II, VII, IX and X to membrane phospholipids *via* calcium promotes the cleavage of the pro-enzymes into active enzymes. In a similar manner, OC, MGP and GRP manage to have a high affinity for calcium-based extracellular matrices (Willems et al., 2014), but the final target of each protein changes in accordance with its function.

Extra-hepatic VKDPs

OC and MGP, the most studied extra-hepatic VKDPs have proven to have a role in the protection against calcification (Ducy et al., 1996; Luo et al., 1997). This correlation is not coincidental, because, with the aging population of Europe and the USA, the need is felt for an answer to the problem of vascular calcification; and the solution seems to be the so-called anti-calcification proteins, which include OC, MGP and the non-vitamin K dependent fetuin-A (Jahnen-Dechent et al., 1997), but many other proteins have the potential to enter this group.

Aim and outline of the thesis

Main objective

Recent clinical trials have proven the cardiovascular and renal benefits of vitamin K supplementation, especially against ectopic-calcification on chronic kidney disease patients (Aoun et al., 2017; Caluwe et al., 2014; Westenfeld et al., 2012).

We hypothesise that the same effect could be seen in patients with a normal renal function. Therefore, this project will assess the influence of vitamin K2 supplementation on arterial micro-calcification and plaque development. This will be achieved by determining the difference in the uptake of the positron emission tomography (PET) tracer Sodium [^{18}F]Fluoride (Na[^{18}F]F) between the intervention and control groups. An introduction of the molecular imaging of atherosclerosis, but also its treatment is made in Chapter II. Additionally, an inflammation tracer (*i.e.*, [^{68}Ga]Ga-Pentixafor) is assessed for its ability to determine differences between the intervention and control groups in a preclinical mouse model.

Outline

In order to test several radiolabelled tracers at the same time, a translational dual-phase setup (preclinical and clinical) was planned.

The aim of the preclinical phase was to answer the question whether vitamin K is protective against vulnerable plaque formation, while vitamin K antagonist drugs, which are given in the current medical practice in the treatment of atherosclerotic caused CVD, are detrimental. To answer this question in an immediately human-trial applicable way, plaques were *in vivo* assessed *via* a small animal PET/computer tomography (PET/CT). The results of this study are presented in Chapter III.

The results from the preclinical phase were afterwards translated into the assessment of vitamin K supplementation on of human carotid and coronary arteries using Na[^{18}F]F hybrid PET/magnetic resonance imaging (PET/MRI). The clinical protocol of the established trial is available in Chapter IV.

Lastly, the ability of [^{68}Ga]Ga-Pentixafor, an inflammation marker, to determine differences in the inflammatory status of different stages of atherosclerotic plaque development will be assessed in Chapter V.

The ultimate goal of this thesis is to improve knowledge on micro-calcification and inflammation during atherosclerotic plaque development and how vitamin K is able to influence this process in the aforementioned group of patients.

References

Aoun M., Makki M., Azar H., Matta H., Chelala D. N.: High Dephosphorylated-Uncarboxylated MGP in Hemodialysis patients: risk factors and response to vitamin K2, A pre-post intervention clinical trial. BMC Nephrol. (2017) 18:191

Berkner K. L., Runge K. W.: The physiology of vitamin K nutriture and vitamin K-dependent protein function in atherosclerosis. J. Thromb. Haemost. (2004) 2:2118–2132

Booth S. L., Sadowski J. A., Weihrauch J. L., Ferland G.: Vitamin K1 (Phylloquinone) Content of Foods: A Provisional Table. J. Food Compos. Anal. (1993) 6:109–120

Caluwe R., Vandecasteele S., Van Vlem B., Vermeer C., De Vriese A. S.: Vitamin K2 supplementation in haemodialysis patients: a randomized dose-finding study. Nephrol. Dial. Transplant. (2014) 29:1385–1390

Chatrou M. L. L., Reutelingsperger C. P., Schurgers L. J.: Role of vitamin K-dependent proteins in the arterial vessel wall. Hamostaseologie (2011) 31:251–257

Chen N. X., Moe S. M.: Pathophysiology of Vascular Calcification. Curr. Osteoporos. Rep. (2015) 13:372–380

Chen W., Dilsizian V.: Targeted PET/CT Imaging of Vulnerable Atherosclerotic Plaques: Microcalcification with Sodium Fluoride and Inflammation with Fluorodeoxyglucose. Curr. Cardiol. Rep. (2013) 15:364

Collins M. D., Jones D.: Distribution of isoprenoid quinone structural types in bacteria and their taxonomic implication. Microbiol. Rev. (1981) 45:316–354

Coutu D. L., Wu J. H., Monette A., Rivard G.-É., Blostein M. D., Galipeau J.: Periostin, a Member of a Novel Family of Vitamin K-dependent Proteins, Is Expressed by Mesenchymal Stromal Cells. J. Biol. Chem. (2008) 283:17991–18001

Crosier M. D., Booth S. L., Peter I., Dawson-Hughes B., Price P. A., O'Donnell C. J., … Ordovas J. M.: Matrix Gla protein polymorphisms are associated with coronary artery calcification in men. J. Nutr. Sci. Vitaminol. (Tokyo). (2009) 55:59–65

Dalmeijer G. W., van der Schouw Y. T., Magdeleyns E. J., Vermeer C., Verschuren W. M. M., Boer J. M. A., Beulens J. W. J.: Matrix Gla Protein Species and Risk of Cardiovascular Events in Type 2 Diabetic Patients. Diabetes Care (2013) 36:3766–3771

Dalmeijer G. W., van der Schouw Y. T., Vermeer C., Magdeleyns E. J., Schurgers L. J., Beulens J. W. J.: Circulating matrix Gla protein is associated with coronary artery calcification and vitamin K status in healthy women. J. Nutr. Biochem. (2013) 24:624–628

Dam H.: The Antihæmorrhagic Vitamin of the Chick.: Occurrence And Chemical Nature. Nature (1935) 135:652–653

Delanaye P., Krzesinski J.-M., Warling X., Moonen M., Smelten N., Médart L., … Cavalier E.: Dephosphorylated-uncarboxylated Matrix Gla protein concentration is predictive of vitamin K status and is correlated with vascular calcification in a cohort of hemodialysis patients. BMC Nephrol. (2014) 15:145

Dihingia A., Ozah D., Baruah P. K., Kalita J., Manna P.: Prophylactic role of vitamin K supplementation on vascular inflammation in type 2 diabetes by regulating the NF-κB/Nrf2 pathway via activating Gla proteins. Food Funct. (2018) 9:450–462

Dowd P., Hershline R., Ham S., Naganathan S.: Vitamin K and energy transduction: a base strength amplification mechanism. Science (80-.). (1995) 269:1684–1691

Ducy P., Desbois C., Boyce B., Pinero G., Story B., Dunstan C., … Karsenty G.: Increased bone formation in osteocalcin-deficient mice. Nature (1996) 382:448–452

Farzaneh-Far A., Weissberg P. L., Proudfoot D., Shanahan C. M.: Transcriptional regulation of matrix gla protein. Z. Kardiol. (2001) 90 Suppl 3:38–42

Fromme P., Grotjohann I.: Structural Analysis of Cyanobacterial Photosystem I. In *Photosystem I* (2006) (pp. 47–69). Springer Netherlands

Furie B., Bouchard B. A., Furie B. C.: Vitamin K-dependent biosynthesis of gamma-carboxyglutamic acid. Blood (1999) 93:1798–1808

Gargiulo S., Gramanzini M., Mancini M.: Molecular Imaging of Vulnerable Atherosclerotic Plaques in Animal Models. Int. J. Mol. Sci. (2016) 17:1511

Gijsbers B. L., Jie K. S., Vermeer C.: Effect of food composition on vitamin K absorption in human volunteers. Br. J. Nutr. (1996) 76:223–229

Goiko M., Dierolf J., Gleberzon J. S., Liao Y., Grohe B., Goldberg H. A., … Hunter G. K.: Peptides of Matrix Gla Protein Inhibit Nucleation and Growth of Hydroxyapatite and Calcium Oxalate Monohydrate Crystals. PLoS One (2013) 8:e80344

Hackeng T. M.: Total chemical synthesis of human matrix Gla protein. Protein Sci. (2001)

10:864–870

Irkle A., Vesey A. T., Lewis D. Y., Skepper J. N., Bird J. L. E., Dweck M. R., … Davenport A. P.: Identifying active vascular microcalcification by 18F-sodium fluoride positron emission tomography. Nat. Commun. (2015) 6:7495

Jahnen-Dechent W., Schinke T., Trindl A., Müller-Esterl W., Sablitzky F., Kaiser S., Blessing M.: Cloning and Targeted Deletion of the Mouse Fetuin Gene. J. Biol. Chem. (1997) 272:31496–31503

Jorgensen M. J., Cantor A. B., Furie B. C., Brown C. L., Shoemaker C. B., Furie B.: Recognition site directing vitamin K-dependent γ-carboxylation resides on the propeptide of factor IX. Cell (1987) 48:185–191

Knobloch J. E., Suttie J. W.: Vitamin K-dependent carboxylase. Control of enzyme activity by the “propeptide” region of factor X. J. Biol. Chem. (1987) 262:15334–15337

Krüger T., Oelenberg S., Kaesler N., Schurgers L. J., van de Sandt A. M., Boor P., … Westenfeld R.: Warfarin Induces Cardiovascular Damage in Mice. Arterioscler. Thromb. Vasc. Biol. (2013) 33:2618–2624

Kulman J. D., Harris J. E., Haldeman B. A., Davie E. W.: Primary structure and tissue distribution of two novel proline-rich -carboxyglutamic acid proteins. Proc. Natl. Acad. Sci. (1997) 94:9058–9062

Kulman J. D., Harris J. E., Xie L., Davie E. W.: Identification of two novel transmembrane -carboxyglutamic acid proteins expressed broadly in fetal and adult tissues. Proc. Natl. Acad. Sci. (2001) 98:1370–1375

Laizé V., Martel P., Viegas C. S. B., Price P. A., Cancela M. L.: Evolution of Matrix and Bone γ-Carboxyglutamic Acid Proteins in Vertebrates. J. Biol. Chem. (2005) 280:26659–26668

Liabeuf S., Olivier B., Vemeer C., Theuwissen E., Magdeleyns E., Aubert C., … Massy Z. A.: Vascular calcification in patients with type 2 diabetes: the involvement of matrix Gla protein. Cardiovasc. Diabetol. (2014) 13:85

Luo G., Ducy P., McKee M. D., Pinero G. J., Loyer E., Behringer R. R., Karsenty G.: Spontaneous calcification of arteries and cartilage in mice lacking matrix GLA protein. Nature (1997) 386:78–81

Maillard C., Berruyer M., Serre C. M., Dechavanne M., Delmas P. D.: Protein-S, a

vitamin K-dependent protein, is a bone matrix component synthesized and secreted by osteoblasts. Endocrinology (1992) 130:1599–1604

Manfioletti G., Brancolini C., Avanzi G., Schneider C.: The protein encoded by a growth arrest-specific gene (gas6) is a new member of the vitamin K-dependent proteins related to protein S, a negative coregulator in the blood coagulation cascade. Mol. Cell. Biol. (1993) 13:4976–4985

McKenney-Drake M. L., Moghbel M. C., Paydary K., Alloosh M., Houshmand S., Moe S., … Alavi A.: 18F-NaF and 18F-FDG as molecular probes in the evaluation of atherosclerosis. Eur. J. Nucl. Med. Mol. Imaging (2018) 45:2190–2200

Merrifield L. S., Yang H. Y.: Factors affecting the antimicrobial activity of vitamin K5. Appl. Microbiol. (1965a) 13:766–770

Merrifield L. S., Yang H. Y.: Vitamin K5 as a fungistatic agent. Appl. Microbiol. (1965b) 13:660–662

Misra D., Booth S., Crosier M., Ordovas J., Felson D., Neogi T.: Matrix Gla Protein Polymorphism, But Not Concentrations, Is Associated with Radiographic Hand Osteoarthritis. J. Rheumatol. (2011) 38:1960–1965

Morris D. P., Stevens R. D., Wright D. J., Stafford D. W.: Processive Post-translational Modification. J. Biol. Chem. (1995) 270:30491–30498

Murphy W. A., Nedden D. zur, Gostner P., Knapp R., Recheis W., Seidler H.: The Iceman: Discovery and Imaging. Radiology (2003) 226:614–629

Murshed M., Schinke T., McKee M. D., Karsenty G.: Extracellular matrix mineralization is regulated locally; different roles of two gla-containing proteins. J. Cell Biol. (2004) 165:625–630

Nelsestuen G. L., Suttie J. W.: Mode of action of vitamin K. Calcium binding properties of bovine prothrombin. Biochemistry (1972) 11:4961–4964

Nishimoto S. K., Nishimoto M.: Matrix Gla protein C-terminal region binds to vitronectin. Co-localization suggests binding occurs during tissue development. Matrix Biol. (2005) 24:353–361

Ogawa M., Nakai S., Deguchi A., Nonomura T., Masaki T., Uchida N., … Kuriyama S.: Vitamins K2, K3 and K5 exert antitumor effects on established colorectal cancer in mice by inducing apoptotic death of tumor cells. Int. J. Oncol. (2007) 31:323–331

Planer D., Mehran R., Ohman E. M., White H. D., Newman J. D., Xu K., Stone G. W.: Prognosis of Patients With Non–ST-Segment–Elevation Myocardial Infarction and Nonobstructive Coronary Artery Disease. Circ. Cardiovasc. Interv. (2014) 7:285–293

Price P. A., Faus S. A., Williamson M. K.: Warfarin Causes Rapid Calcification of the Elastic Lamellae in Rat Arteries and Heart Valves. Arterioscler. Thromb. Vasc. Biol. (1998) 18:1400–1407

Price P. A., Otsuka A. A., Poser J. W., Kristaponis J., Raman N.: Characterization of a gamma-carboxyglutamic acid-containing protein from bone. Proc. Natl. Acad. Sci. (1976) 73:1447–1451

Price P. A., Poser J. W., Raman N.: Primary structure of the gamma-carboxyglutamic acid-containing protein from bovine bone. Proc. Natl. Acad. Sci. U. S. A. (1976) 73:3374–3375

Price P. A., Urist M. R., Otawara Y.: Matrix Gla protein, a new γ-carboxyglutamic acid-containing protein which is associated with the organic matrix of bone. Biochem. Biophys. Res. Commun. (1983) 117:765–771

Prowse C. V., Esnouf M. P.: The Isolation of a New Warfarin-Sensitive Protein from Bovine Plasma. Biochem. Soc. Trans. (1977) 5:255–256

Riphagen I., Keyzer C., Drummen N., de Borst M., Beulens J., Gansevoort R., … Bakker S.: Prevalence and Effects of Functional Vitamin K Insufficiency: The PREVEND Study. Nutrients (2017) 9:1334

Roijers R. B., Debernardi N., Cleutjens J. P. M., Schurgers L. J., Mutsaers P. H. A., van der Vusse G. J.: Microcalcifications in Early Intimal Lesions of Atherosclerotic Human Coronary Arteries. Am. J. Pathol. (2011) 178:2879–2887

Ross R.: Atherosclerosis — An Inflammatory Disease. N. Engl. J. Med. (1999) 340:115–126

Sakuragi Y., Bryant D. A.: Genetic Manipulation of Quinone Biosynthesis in Cyanobacteria. In *Photosystem I* (2006) (pp. 205–222). Springer Netherlands

Sato T., Schurgers L. J., Uenishi K.: Comparison of menaquinone-4 and menaquinone-7 bioavailability in healthy women. Nutr. J. (2012) 11:93

Schönheyder F.: Measurement And Biological Action. Nature (1935) 135:653–653

Schurgers L. J., Cranenburg E. C. M., Vermeer C.: Matrix Gla-protein: the calcification inhibitor in need of vitamin K. Thromb. Haemost. (2008) 100:593–603

Schurgers L. J., Joosen I. A., Laufer E. M., Chatrou M. L. L., Herfs M., Winkens M. H. M., … Reutelingsperger C. P.: Vitamin K-Antagonists Accelerate Atherosclerotic Calcification and Induce a Vulnerable Plaque Phenotype. PLoS One (2012) 7:e43229

Schurgers L. J., Spronk H. M. H., Skepper J. N., Hackeng T. M., Shanahan C. M., Vermeer C., … Proudfoot D.: Post-translational modifications regulate matrix Gla protein function: importance for inhibition of vascular smooth muscle cell calcification. J. Thromb. Haemost. (2007) 5:2503–2511

Schurgers L. J., Teunissen K. J. F., Hamulyak K., Knapen M. H. J., Vik H., Vermeer C.: Vitamin K-containing dietary supplements: comparison of synthetic vitamin K1 and natto-derived menaquinone-7. Blood (2007) 109:3279–3283

Schurgers L. J., Vermeer C.: Determination of Phylloquinone and Menaquinones in Food. Pathophysiol. Haemost. Thromb. (2000) 30:298–307

Shearer M. J.: Vitamin K. Lancet (1995) 345:229–234

Shearer M. J., Bolton-Smith C.: The UK food data-base for vitamin K and why we need it. Food Chem. (2000) 68:213–218

Shearer M. J., Newman P.: Metabolism and cell biology of vitamin K. Thromb. Haemost. (2008) 100:530–547

Simões Sato A. Y., Bub G. L., Campos A. H.: BMP-2 and -4 produced by vascular smooth muscle cells from atherosclerotic lesions induce monocyte chemotaxis through direct BMPRII activation. Atherosclerosis (2014) 235:45–55

Stenflo J.: A new vitamin K-dependent protein. Purification from bovine plasma and preliminary characterization. J. Biol. Chem. (1976) 251:355–363

Stenflo J., Fernlund P., Egan W., Roepstorff P.: Vitamin K dependent modifications of glutamic acid residues in prothrombin. Proc. Natl. Acad. Sci. U. S. A. (1974) 71:2730–2733

Stenina O., Pudota B. N., McNally B. A., Hommema E. L., Berkner K. L.: Tethered processivity of the vitamin K-dependent carboxylase: factor IX is efficiently modified in a mechanism which distinguishes Gla's from Glu's and which accounts for comprehensive carboxylation in vivo. Biochemistry (2001) 40:10301–10309

Sugiura I., Furie B., Walsh C. T., Furie B. C.: Propeptide and glutamate-containing substrates bound to the vitamin K-dependent carboxylase convert its vitamin K epoxidase function from an inactive to an active state. Proc. Natl. Acad. Sci. (1997) 94:9069–9074

Suttie J. W.: Vitamin K-Dependent Carboxylase. Annu. Rev. Biochem. (1985) 54:459–477

Venardos N., Bennett D., Weyant M. J., Reece T. B., Meng X., Fullerton D. A.: Matrix Gla protein regulates calcification of the aortic valve. J. Surg. Res. (2015) 199:1–6

Viegas C. S. B., Simes D. C., Laizé V., Williamson M. K., Price P. A., Cancela M. L.: Gla-rich Protein (GRP), A New Vitamin K-dependent Protein Identified from Sturgeon Cartilage and Highly Conserved in Vertebrates. J. Biol. Chem. (2008) 283:36655–36664

Wajih N., Borras T., Xue W., Hutson S. M., Wallin R.: Processing and Transport of Matrix γ-Carboxyglutamic Acid Protein and Bone Morphogenetic Protein-2 in Cultured Human Vascular Smooth Muscle Cells. J. Biol. Chem. (2004) 279:43052–43060

Wallin R., Cain D., Hutson S. M., Sane D. C., Loeser R.: Modulation of the binding of matrix Gla protein (MGP) to bone morphogenetic protein-2 (BMP-2). Thromb. Haemost. (2000) 84:1039–1044

Westenfeld R., Krueger T., Schlieper G., Cranenburg E. C. M., Magdeleyns E. J., Heidenreich S., … Schurgers L. J.: Effect of Vitamin K2 Supplementation on Functional Vitamin K Deficiency in Hemodialysis Patients: A Randomized Trial. Am. J. Kidney Dis. (2012) 59:186–195

Willems B. A. G., Vermeer C., Reutelingsperger C. P. M., Schurgers L. J.: The realm of vitamin K dependent proteins: Shifting from coagulation toward calcification. Mol. Nutr. Food Res. (2014) 58:1620–1635

European Cardiovascular Disease Statistics 2017 (2017) from http://www.ehnheart.org/cvd-statistics.html

WHO | Cardiovascular diseases (CVDs) (2017) from https://www.who.int/cardiovascular_diseases/en/

Chapter II: Review

Locking and loading the bullet against micro-calcification

Alexandru Florea, Agnieszka Morgenroth, Jan Bucerius, Leon J. Schurgers, and Felix M. Mottaghy

This work was published in *European Journal of Preventive Cardiology* on 17 April 2020

doi: 10.1177/2047487320911138

Locking and loading the bullet against micro-calcification

Alexandru Florea[1,2], Agnieszka Morgenroth[1], Jan Bucerius[2,3,4], Leon J. Schurgers[3,5], Felix M. Mottaghy[1,2]

Department of Nuclear Medicine, University Hospital RWTH Aachen, Aachen, Germany

Alexandru Florea: Ph.D. student, Department of Nuclear Medicine, University Hospital RWTH Aachen, Pauwelsstr. 31, Aachen 52072, Germany

Agnieszka Morgenroth: Head of preclinical research, Department of Nuclear Medicine, University Hospital RWTH Aachen, Pauwelsstr. 31, Aachen 52072, Germany

Jan Bucerius: Head of the department, Department of Nuclear Medicine, University of Göttingen, Robert-Koch-Str. 40, 37075 Göttingen, Germany

Leon J. Schurgers: Vice-chair of the department, Department of Biochemistry, CARIM, Maastricht University, Post box 616, 6200 MD Maastricht, Netherlands

Felix M. Mottaghy: Head of the department, Department of Nuclear Medicine, University Hospital RWTH Aachen, Pauwelsstr. 31, Aachen 52074, Germany

Corresponding author:

Felix M. Mottaghy

Tel: +49 241 80 88741

Fax: +49 241 80 82520

Email: fmottaghy@ukaachen.de

[1] Department of Nuclear Medicine, University Hospital RWTH Aachen, Aachen, Germany
[2] Department of Radiology and Nuclear Medicine, Academic Hospital Maastricht, Maastricht, Netherlands
[3] School for Cardiovascular Diseases (CARIM), Maastricht University, Netherlands
[4] Department of Nuclear Medicine, University of Göttingen, Göttingen, Germany
[5] Department of Biochemistry, Maastricht University, Maastricht, Netherlands

Abbreviations

^{18}F-NaF – ^{18}F-sodium fluoride

CAC – coronary artery calcification

CT – computed tomography

MGP – matrix γ-carboxyglutamate protein

MRI – magnetic resonance imaging

PET – positron emission tomography

VKDP – vitamin K dependent protein

Abstract

Aims

Despite recent medical advances, cardiovascular disease remains the leading cause of death worldwide. As (micro)-calcification is a hallmark of atherosclerosis, this review will elaborately discuss advantages of sodium fluoride PET as a reliable cardiovascular imaging technique for identifying the early onset of vascular calcification (*i.e.* locking onto the target). We assess state-of-the-art meta-analysis and clinical studies of possible treatment options and evaluate the concept of vitamin K supplementation to preserve vascular health (*i.e.* loading the bullet).

Methods and Results

After a structured PubMed search, we identified ^{18}F-NaF PET as the most suitable technique of detecting micro-calcification. Presenting the pros and cons of available treatments, vitamin K supplementation should be considered as a possible safe and cost-effective option to inhibit vascular (micro)-calcification.

Conclusion

This review demonstrates need for more extensive research in the concept of vitamin K supplementation (*i.e.* loading the bullet) and recommends monitoring the effects on vascular calcification using ^{18}F-NaF PET (*i.e.* locking onto the target).

Keywords

Vascular calcification · CAC score · CT · ^{18}F-NaF PET · Vitamin K

Introduction

Despite recent advances in interventional medicine, cardiovascular disease is still the leading cause of death worldwide, exceeding cancer mortality.[1,2] After the recognition of vascular calcification as a hallmark of atherosclerosis, emerging data agree on classifying coronary artery calcification (CAC) score as an independent cardiovascular risk factor.[3] However, the risk ratio of CAC is currently unavailable, because a large patient population falls under low levels of CAC, undetectable by conventional methods (*i.e.* low dose non-contrast CT calcium score).

Vascular calcification was considered a passive process, however recent evidence shows that it is actively regulated with a delicate balance between calcification promoting and inhibiting factors.[4] Most initiators of extracellular matrix mineralization converge to the secretion of extracellular vesicles by synthetic vascular smooth muscle cells and macrophages.[5] These sites provide the perfect nidus for nucleation and elongation of hydroxyapatite crystals, which will eventually destabilize the plaque.[6] Hence, early identification of vascular calcification may allow for a better stratification into high-risk individuals with poor outcomes.[7]

In this review, we discuss the most processing methods of vascular imaging (*i.e.* Part 1) and key emerging concepts in the treatment of vascular calcification (*i.e.* Part 2).

Part one: Micro-calcification as an independent risk factor

There is increasing evidence that (micro-)calcification is not merely a passive bystander of atherosclerosis, but actually plays an active role in plaque progression and destabilization.[8] *In vitro* studies showed that calcium phosphate crystals smaller than 1µm can activate macrophages and induce vascular smooth muscle cells to undergo programmed cell death.[9] The latter phenomenon further accelerates atherogenesis, by providing a nidus for further calcification and medial degeneration.[10] This vicious cycle increases vulnerability of atherosclerotic plaques.[11] So called “spotty calcification” on CT, which is the imaging equivalent of micro-calcification, has been associated with increased plaque vulnerability in coronary artery disease.[12] On the contrary, in patients with stable coronary artery disease, completely calcified, more solid lesions are more prevalent.[13]

Agatston *et al.* linked the sensitivity, specificity, and predictive values of total CAC score with increased age.[14] A high CAC score (≥1,000 Agatston units) in

asymptomatic patients seems a better predictor for coronary events than severe perfusion abnormalities.[15] Hence, for more than a decade, CAC score has been in clinical practice for detection of subclinical disease and for stratification of asymptomatic individuals.[7] Stratifying based on CAC score, reduces the number needed to treat to prevent one ischemic stroke or transient ischemic attack from 229 (CAC=0) to 68 (CAC>100).[16] Moreover, in an observational study of 25,253 asymptomatic patients, a CAC score higher than 1,000 was correlated with a 16% lower 10-year survival rate, even after the adjustments for risk factors, such as age, hypercholesterolemia, diabetes, smoking, hypertension, and a family history of premature coronary heart disease.[3]

However, the additional risk or the relative risk of CAC is yet unreliable.[17] This is due to the fact that the already established Agatston calcification score is able to assess CAC density, which seems to be inversely associated with cardiovascular risk.[18] Moreover, there is a current paradigm shift from CAC density to CAC volume as a positive predictor for cardiovascular events. Recent studies support the notion that molecular imaging techniques, such as ^{18}F-sodium fluoride (^{18}F-NaF) PET, are complementary in detecting vascular calcification and should be introduced to gain further information on active micro-calcification in unstable plaques.[19]

Sodium fluoride-18: Seeing the unseen

^{18}F-NaF is a PET tracer with an interesting property: the ^{18}F is able to replace the hydroxyl groups of hydroxyapatite, the very building block of (vascular) calcification. This, combined with its small size and its negligible plasma protein binding capacity results in a high target-to-background ratio (*i.e.* efficient targeting capability) shortly after i.v. injection.[20] Thin nano-sized hydroxyapatite crystals provide a higher surface area for ^{18}F-NaF to bind to, in contrast to the macroscopic counterpart, in which the tracer cannot enter the inner core.[20] Irkle *et al.* showed that fluoride is better adsorbed by micro-calcified plaques (*i.e.* nodules <50μm) when compared to macro-calcifications (*i.e.* nodules >50μm).[19] In the same study, ^{18}F-NaF PET demonstrated a higher sensitivity then CT, by detecting larger areas of active micro-calcification sites.[19] This makes ^{18}F-NaF suitable for detecting vulnerable sites by visualizing active micro-calcification in contrast to stable macro-calcified plaques, which are better detected by CT (Figure 1). Moreover, ^{18}F-NaF uptake in the coronary arteries is in close agreement with CT markers for plaque vulnerability (*e.g.* plaque attenuation < 30 Hounsfield units).[21]

Indeed, the feasibility of ^{18}F-NaF PET for *in vivo* quantification of micro-calcification in the aorta as well as in the coronary and carotid arteries as a feature of culprit plaques has already been proven (Figure 2).[22,23] In patients with myocardial infarction, ^{18}F-NaF was able to discriminate between culprit and non-culprit plaques.[22] Over the years, many studies used ^{18}F-NaF to acquire information about morphological and functional properties of calcified plaques. All of them provided increasing evidence that this technique represents a feasible option for imaging active micro-calcification.[24]

When compared with ^{18}F-fluorodeoxyglucose (*i.e.* FDG), ^{18}F-NaF showed improved detection of culprit plaques in thoracic aorta and coronary arteries.[22,25] Therefore, active micro-calcification, rather than vascular inflammation, should be associated more strongly with cardiovascular risk. This led Dweck *et al.* to conclude that ^{18}F-NaF PET as the only currently available clinical imaging approach that can non-invasively detect vascular micro-calcifications.[26]

By implementing hybrid PET/MRI, ^{18}F-NaF has the opportunity to fully exhibit its potential, by delivering data about the state of micro-calcification alongside high-resolution MR images that can give a detailed description of plaque burden (*e.g.* juxtaluminal lesions, intra-plaque haemorrhage, lipid-rich necrotic core, and fibrous cap status) (Figure 1). CT fails to detect many subtle *Pseudoxanthoma elasticum*-related

abnormalities, such as calcifications in the endo- or myocardium.[27] Although, ^{18}F-NaF PET/MRI is currently most used in studies that concern bone pathologies, cardiovascular research has adapted this technique.[28] Ongoing trials are using hybrid ^{18}F-NaF PET/MRI, *e.g.* BASIK-2 (NCT02917525), which assesses vitamin K influence on calcific aortic valve stenosis.

However, additional scientific efforts are still required until ^{18}F-NaF will enter the routine clinical practice as a tracer for vascular micro-calcification, but, as mentioned above, available studies reveal a promising future (Figure 2).[22]

Part two: Available treatment options against micro-calcification

Micro-calcifications have long been proposed as a marker for vulnerable plaques. *In silico* models predict that inclusions, located in a thin fibrous cap in an area of high circumferential stress, can double the intensity of initial stress.[29] The most likely candidate for these inclusions is micro-calcification. Bobryshev *et al.* showed by quantification in ultrathin sections that micro-calcifications are more present in vulnerable compared to stable plaques.[30] Based on data generated by studies using ^{18}F-NaF PET, active micro-calcifications are now an established hallmark of atherosclerosis and plaque vulnerability.[17]

In this context, an extensive list of potential medications that address vascular calcification has already been compiled.[31] However, almost half of the mentioned drugs have only been studied in preclinical setups or lack extensive clinical research. Of all enlisted drugs, bisphosphonates, phosphate binders, statins, and vitamin K seem to have the greatest potential (Table).

Bisphosphonates and phosphate binders are an attractive choice for their promise to attack the building blocks of micro-calcification, namely calcium and phosphate. Bisphosphonates bind free calcium, whereas phosphate binders prevent the absorption of dietary phosphate, making it unavailable for incorporation into hydroxyapatite. A systematic review suggests that bisphosphonates are able to favourably influence calcium homeostasis within the vessel wall.[32] However, long-term administration of bisphosphonates may cause severe adverse reactions, like osteonecrosis of the jaw, probably by reducing macrophage and osteoclast viability.[33] In case of phosphate binders, a meta-analysis that examined 104 studies involving 13,744 adults found no cardiovascular protection for dialysis patients and uncertain effects for the rest of chronic kidney disease population.[34]

Over the last years, the focus of potential cardiovascular protective medications was set on statins. Besides lowering cholesterol, numerous medical trials showed positive, pleiotropic, effects of statins on plaque stabilization and anti-inflammatory properties. However, several studies revealed that they seem to negatively influence the progression of calcification.[35] Moreover, recent studies suggest that statins promote formation of hydroxyapatite crystals within the plaque by inhibiting activity of vitamin K2.[36]

Considering that bisphosphonates, phosphate binders, and statins have already been extensively studied, sowing inconsistent results (*i.e.* phosphate binders) or detrimental side effects (*i.e.* bisphosphonates), vitamin K supplementation might be considered as a safe, cost-effective alternative for inhibiting vascular calcification. Therefore, research evaluating potential beneficial effects of vitamin K on vascular calcification has gained more and more interest over the last years.[37]

Vitamin K: The magic bullet to fight vascular calcification?

Vitamin K is paramount for the biological activation of an array of proteins, which are able to bind free calcium *via* their γ-carboxyglutamate-rich domains. Amongst these vitamin K dependent proteins (VKDPs) are liver-derived proteins with a significant role in haemostasis (*i.e.* factors II, VII, IX, and X and proteins C, S, and Z). In the last decade, several extra-hepatic VKDPs have been discovered, with dispersed functions, including bone metabolism (*e.g.* osteocalcin) and inhibition of ectopic calcification (*e.g.* matrix γ-carboxyglutamate protein – MGP).

Vitamin K is an unequivocal cofactor in the activation of VKDPs and it comes in two flavours: phylloquinone (*i.e.* vitamin K1) and menaquinones (MKs, *i.e.* vitamin K2). For purposes of nomenclature, MKs are further sub-classified according to the number of repeating prenyl units (*i.e.* MK-n, where n is the number of repeating units).

In case of vitamin K deficiency, a high-dose supplementation of vitamin K carboxylates (*i.e.* activates) VKDPs with anti-calcification properties. Plasma levels of dephosphorylated uncarboxylated (*i.e.* inactive) MGP rapidly change after increasing MK-7 intake.[38] It is worth mentioning that vitamin K supplementation does not induce a state of hypercoagulability.[39] Thus, a higher intake of vitamin K is not associated with any negative reaction on the coagulation cascade.

The detrimental effect of vitamin K antagonists (*e.g.* warfarin) on cardiovascular and renal systems have already been revealed.[40] A considerable number of studies over

the last two decades showed an association between vitamin K supplementation and positive outcomes in calcium metabolism. In most post-menopausal women and chronic kidney disease patients, there is a paradoxical decline in bone calcium content, paralleled by an increase in vascular calcification. Vitamin D is frequently used in combination with calcium supplementation to protect against bone disease, however, this treatment might accelerate vascular calcification.[41] By activating MGP, vitamin K supplementation may be the way out of this paradox. Indeed, supplementation with minerals (*i.e.* calcium, magnesium, and zinc), vitamin D, and K showed beneficial effects on arterial elasticity in post-menopausal women after a follow-up of 3 years.[42]

Vitamin K seems to have beneficial effects on vascular calcification and thus indirectly fights cardiovascular disease yet supporting vascular health (Figure 1). Poor vitamin K status correlated with intensive CAC in patients with high blood pressure, even when under antihypertension medication.[43] Meanwhile, when compared to control, vitamin K1 supplementation slows down the progression of calcification in the coronary arteries after 3 years and in the aortic valve after 1 year.[44,45] Moreover, as it is known that bone morphogenetic proteins promote the inflammation in atherogenic conditions, vitamin K supplementation may also improve vascular health by directly activating MGP, the natural inhibitor of the pro-apoptotic bone morphogenetic protein 2.[46]

Prospective population-based trials linked the increased consumption of MKs with a reduced relative risk of coronary heart disease mortality (RR=0.43 with a 95%CI of 0.24-0.77).[47] Moreover, a recent meta-analysis confirmed these findings and concluded that higher dietary vitamin K consumption is associated with a lower risk of coronary heart disease.[48] A more in-depth study also observed an inverse association between MK intake (but not for vitamin K1 intake) and the risk of coronary heart disease; this association was mainly due to subtypes MK-7, MK-8 and MK-9.[49] Indeed, MK-7 supplementation was also associated with improved MGP levels in chronic kidney disease patients and with decreased arterial stiffness in healthy postmenopausal women.[50,51] Moreover, MK-7 supplementation showed a beneficial effect on arterial stiffness in renal transplant recipients with stable graft function.[52] However, available data from randomised clinical trials is insufficient to argue in favour of an increase in the recommended daily dose of vitamin K or its introduction in clinical practice. With progress in ongoing clinical trials new supporting information will come to light on how beneficial vitamin K supplementation (*i.e.* vitamin K1 and MK-7) is in cardiovascular

disease (*i.e.* VitaK-CAC NCT01002157, iPACK-HD NCT01528800, VitaVasK NCT01742273, and BASIK2 NCT02917525).

Conclusion: Locking with ^{18}F-NaF and loading with vitamin K

Currently, the significant impact of ^{18}F-NaF PET in non-invasively identifying the early onset of vascular calcification is gaining more and more attention. In addition, emerging data are positive about the up-and-coming concept of vitamin K supplementation to combat micro-calcification. Here, we raise awareness for the need of more extensive clinical trials using vitamin K to promote vascular health. These studies should consider the use of ^{18}F-NaF PET for monitoring active micro-calcifications.

Vitamin K emerges as a suitable, cost-effective, bullet that can and should be loaded after targeting micro-calcification with ^{18}F-NaF PET.

Acknowledgements

This work was supported by no financial means to the authors involved.

Dr. Alexandru Florea, Prof. Leon Schurgers, and Prof. Felix Mottaghy receive research funding from the ITN INTRICARE of European Union's Horizon 2020 research and innovation program under the Marie Skłodowska-Curie (grant 722609). Prof. Leon Schurgers receives research funding from the ITN EVOluTION of European Union's Horizon 2020 research and innovation program under the Marie Skłodowska-Curie (grant 675111). Dr. Agnieszka Morgenroth and Prof. Felix Mottaghy receive research funding from the RTG 2375 of the German Research Foundation (grant 331065168).

All authors declare no conflict of interest.

Authorship

AF, AM, JB, LJS, and FMM contributed to the conception or design of the work. AF drafted the manuscript. AM, JB, LJS, and FMM critically revised the manuscript. All gave final approval and agree to be accountable for all aspects of work ensuring integrity and accuracy.

References

1. World Health Organization. WHO | Cardiovascular diseases (CVDs). *WHO*, https://www.who.int/cardiovascular_diseases/en/ (2017, accessed January 31, 2019).
2. Bray F, Ferlay J, Soerjomataram I, et al. Global cancer statistics 2018: GLOBOCAN estimates of incidence and mortality worldwide for 36 cancers in 185 countries. *CA Cancer J Clin* 2018; 68: 394–424.
3. Budoff MJ, Shaw LJ, Liu ST, et al. Long-Term Prognosis Associated With Coronary Calcification. *J Am Coll Cardiol* 2007; 49: 1860–70.
4. Johnson RC, Leopold JA, Loscalzo J. Vascular Calcification. *Circ Res* 2006; 99: 1044–59.
5. Schurgers LJ, Akbulut AC, Kaczor DM, et al. Initiation and Propagation of Vascular Calcification Is Regulated by a Concert of Platelet- and Smooth Muscle Cell-Derived Extracellular Vesicles. *Front Cardiovasc Med* 2018; 5: 36.
6. Hasegawa T. Ultrastructure and biological function of matrix vesicles in bone mineralization. *Histochem Cell Biol* 2018; 149: 289–304.
7. Faggiano P, Dasseni N, Gaibazzi N, et al. Cardiac calcification as a marker of subclinical atherosclerosis and predictor of cardiovascular events: A review of the evidence. *Eur J Prev Cardiol* 2019; 26: 1191–1204.
8. Chatrou MLL, Cleutjens JP, van der Vusse GJ, et al. Intra-Section Analysis of Human Coronary Arteries Reveals a Potential Role for Micro-Calcifications in Macrophage Recruitment in the Early Stage of Atherosclerosis. *PLoS One* 2015; 10: e0142335.
9. Ewence AE, Bootman M, Roderick HL, et al. Calcium Phosphate Crystals Induce Cell Death in Human Vascular Smooth Muscle Cells. *Circ Res* 2008; 103: 205–18.

10. Clarke MCH, Littlewood TD, Figg N, et al. Chronic Apoptosis of Vascular Smooth Muscle Cells Accelerates Atherosclerosis and Promotes Calcification and Medial Degeneration. *Circ Res* 2008; 102: 1529–38.

11. Bentzon JF, Otsuka F, Virmani R, et al. Mechanisms of Plaque Formation and Rupture. *Circ Res* 2014; 114: 1852–66.

12. Motoyama S, Kondo T, Sarai M, et al. Multislice Computed Tomographic Characteristics of Coronary Lesions in Acute Coronary Syndromes. *J Am Coll Cardiol* 2007; 50: 319–26.

13. Pundziute G, Schuijf JD, Jukema JW, et al. Evaluation of plaque characteristics in acute coronary syndromes: non-invasive assessment with multi-slice computed tomography and invasive evaluation with intravascular ultrasound radiofrequency data analysis. *Eur Heart J* 2008; 29: 2373–81.

14. Agatston AS, Janowitz WR, Hildner FJ, et al. Quantification of coronary artery calcium using ultrafast computed tomography. *J Am Coll Cardiol* 1990; 15: 827–32.

15. Wayhs R, Zelinger A, Raggi P. High coronary artery calcium scores pose an extremely elevated risk for hard events. *J Am Coll Cardiol* 2002; 39: 225–30.

16. Osawa K, Trejo MEP, Nakanishi R, et al. Coronary artery calcium and carotid artery intima-media thickness for the prediction of stroke and benefit from statins. *Eur J Prev Cardiol* 2018; 25: 1980–1987.

17. Nakahara T, Dweck MR, Narula N, et al. Coronary Artery Calcification: From Mechanism to Molecular Imaging. *JACC Cardiovasc Imaging* 2017; 10: 582–93.

18. Criqui MH, Knox JB, Denenberg JO, et al. Coronary Artery Calcium Volume and Density: Potential Interactions and Overall Predictive Value: The Multi-Ethnic Study of Atherosclerosis. *JACC Cardiovasc Imaging* 2017; 10: 845–54.

19. Irkle A, Vesey AT, Lewis DY, et al. Identifying active vascular microcalcification by 18F-sodium fluoride positron emission tomography. *Nat Commun* 2015; 6: 7495.

20. Joshi N V., Vesey A, Newby DE, et al. Will 18F-Sodium Fluoride PET-CT Imaging Be the Magic Bullet for Identifying Vulnerable Coronary Atherosclerotic Plaques? *Curr Cardiol Rep* 2014; 16: 521.

21. Kwiecinski J, Cadet S, Daghem M, et al. Whole-vessel coronary 18F-sodium

fluoride PET for assessment of the global coronary microcalcification burden. *Eur J Nucl Med Mol Imaging*. Epub ahead of print January 2, 2020. DOI: 10.1007/s00259-019-04667-z.

22. Joshi N V., Vesey AT, Williams MC, et al. 18F-fluoride positron emission tomography for identification of ruptured and high-risk coronary atherosclerotic plaques: a prospective clinical trial. *Lancet* 2014; 383: 705–13.

23. Hop H, de Boer SA, Reijrink M, et al. 18F-sodium fluoride positron emission tomography assessed microcalcifications in culprit and non-culprit human carotid plaques. *J Nucl Cardiol*. Epub ahead of print June 25, 2018. DOI: 10.1007/s12350-018-1325-5.

24. Sorci O, Batzdorf AS, Mayer M, et al. 18F-sodium fluoride PET/CT provides prognostic clarity compared to calcium and Framingham risk scoring when addressing whole-heart arterial calcification. *Eur J Nucl Med Mol Imaging*. Epub ahead of print November 16, 2019. DOI: 10.1007/s00259-019-04590-3.

25. Blomberg BA, de Jong PA, Thomassen A, et al. Thoracic aorta calcification but not inflammation is associated with increased cardiovascular disease risk: results of the CAMONA study. *Eur J Nucl Med Mol Imaging* 2017; 44: 249–58.

26. Dweck MR, Aikawa E, Newby DE, et al. Noninvasive Molecular Imaging of Disease Activity in Atherosclerosis. *Circ Res* 2016; 119: 330–40.

27. Vos A, Kranenburg G, de Jong PA, et al. The amount of calcifications in pseudoxanthoma elasticum patients is underestimated in computed tomographic imaging; a post-mortem correlation of histological and computed tomographic findings in two cases. *Insights Imaging* 2018; 9: 493–8.

28. Marchesseau S, Seneviratna A, Sjöholm AT, et al. Hybrid PET/CT and PET/MRI imaging of vulnerable coronary plaque and myocardial scar tissue in acute myocardial infarction. *J Nucl Cardiol* 2018; 25: 2001–11.

29. Vengrenyuk Y, Carlier S, Xanthos S, et al. A hypothesis for vulnerable plaque rupture due to stress-induced debonding around cellular microcalcifications in thin fibrous caps. *Proc Natl Acad Sci* 2006; 103: 14678–83.

30. Bobryshev Y V., Killingsworth MC, Lord RSA, et al. Matrix vesicles in the fibrous cap of atherosclerotic plaque: possible contribution to plaque rupture. *J Cell Mol Med* 2008; 12: 2073–82.

31. Wu M, Rementer C, Giachelli CM. Vascular Calcification: An Update on Mechanisms and Challenges in Treatment. *Calcif Tissue Int* 2013; 93: 365–73.

32. Caffarelli C, Montagnani A, Nuti R, et al. Bisphosphonates, atherosclerosis and vascular calcification: update and systematic review of clinical studies. *Clin Interv Aging* 2017; 12: 1819–28.

33. Patntirapong S, Phupunporn P, Vanichtantiphong D, et al. Inhibition of macrophage viability by bound and free bisphosphonates. *Acta Histochem* 2019; 121: 400–6.

34. Ruospo M, Palmer SC, Natale P, et al. Phosphate binders for preventing and treating chronic kidney disease-mineral and bone disorder (CKD-MBD). *Cochrane Database Syst Rev* 2018; CD006023.

35. Banach M, Serban C, Sahebkar A, et al. Impact of statin therapy on coronary plaque composition: a systematic review and meta-analysis of virtual histology intravascular ultrasound studies. *BMC Med* 2015; 13: 229.

36. Chen Z, Qureshi AR, Parini P, et al. Does statins promote vascular calcification in chronic kidney disease? *Eur J Clin Invest* 2017; 47: 137–48.

37. Lees JS, Chapman FA, Witham MD, et al. Vitamin K status, supplementation and vascular disease: a systematic review and meta-analysis. *Heart* 2018; 105: heartjnl-2018-313955.

38. Dalmeijer GW, van der Schouw YT, Magdeleyns E, et al. The effect of menaquinone-7 supplementation on circulating species of matrix Gla protein. *Atherosclerosis* 2012; 225: 397–402.

39. Asakura H, Myou S, Ontachi Y, et al. Vitamin K Administration to Elderly Patients with Osteoporosis Induces No Hemostatic Activation, Even in Those with Suspected Vitamin K Deficiency. *Osteoporos Int* 2001; 12: 996–1000.

40. Chatrou MLL, Winckers K, Hackeng TM, et al. Vascular calcification: The price to pay for anticoagulation therapy with vitamin K-antagonists. *Blood Rev* 2012; 26: 155–166.

41. Wasilewski GB, Vervloet MG, Schurgers LJ. The Bone—Vasculature Axis: Calcium Supplementation and the Role of Vitamin K. *Front Cardiovasc Med* 2019; 6: 6.

42. Braam L, Hoeks A, Brouns F, et al. Beneficial effects of vitamins D and K on the

elastic properties of the vessel wall in postmenopausal women: a follow-up study. *Thromb Haemost* 2004; 91: 373–80.

43. Shea MK, Booth SL, Miller ME, et al. Association between circulating vitamin K1 and coronary calcium progression in community-dwelling adults: the Multi-Ethnic Study of Atherosclerosis. *Am J Clin Nutr* 2013; 98: 197–208.

44. Shea MK, O'Donnell CJ, Hoffmann U, et al. Vitamin K supplementation and progression of coronary artery calcium in older men and women. *Am J Clin Nutr* 2009; 89: 1799–807.

45. Brandenburg VM, Reinartz S, Kaesler N, et al. Slower Progress of Aortic Valve Calcification With Vitamin K Supplementation. *Circulation* 2017; 135: 2081–83.

46. Yao Y, Bennett BJ, Wang X, et al. Inhibition of Bone Morphogenetic Proteins Protects Against Atherosclerosis and Vascular Calcification. *Circ Res* 2010; 107: 485–494.

47. Geleijnse JM, Vermeer C, Grobbee DE, et al. Dietary Intake of Menaquinone Is Associated with a Reduced Risk of Coronary Heart Disease: The Rotterdam Study. *J Nutr* 2004; 134: 3100–5.

48. Chen H-G, Sheng L-T, Zhang Y-B, et al. Association of vitamin K with cardiovascular events and all-cause mortality: a systematic review and meta-analysis. *Eur J Nutr* 2019; 58: 2191–2205.

49. Gast GCM, de Roos NM, Sluijs I, et al. A high menaquinone intake reduces the incidence of coronary heart disease. *Nutr Metab Cardiovasc Dis* 2009; 19: 504–10.

50. Aoun M, Makki M, Azar H, et al. High Dephosphorylated-Uncarboxylated MGP in Hemodialysis patients: risk factors and response to vitamin K2, A pre-post intervention clinical trial. *BMC Nephrol* 2017; 18: 191.

51. Knapen MHJ, Braam LAJLM, Drummen NE, et al. Menaquinone-7 supplementation improves arterial stiffness in healthy postmenopausal women. *Thromb Haemost* 2015; 113: 1135–44.

52. Mansour AG, Hariri E, Daaboul Y, et al. Vitamin K2 supplementation and arterial stiffness among renal transplant recipients—a single-arm, single-center clinical trial. *J Am Soc Hypertens* 2017; 11: 589–97.

Figures

Figure 1: The superiority of locking with ^{18}F-NaF and loading with vitamin K

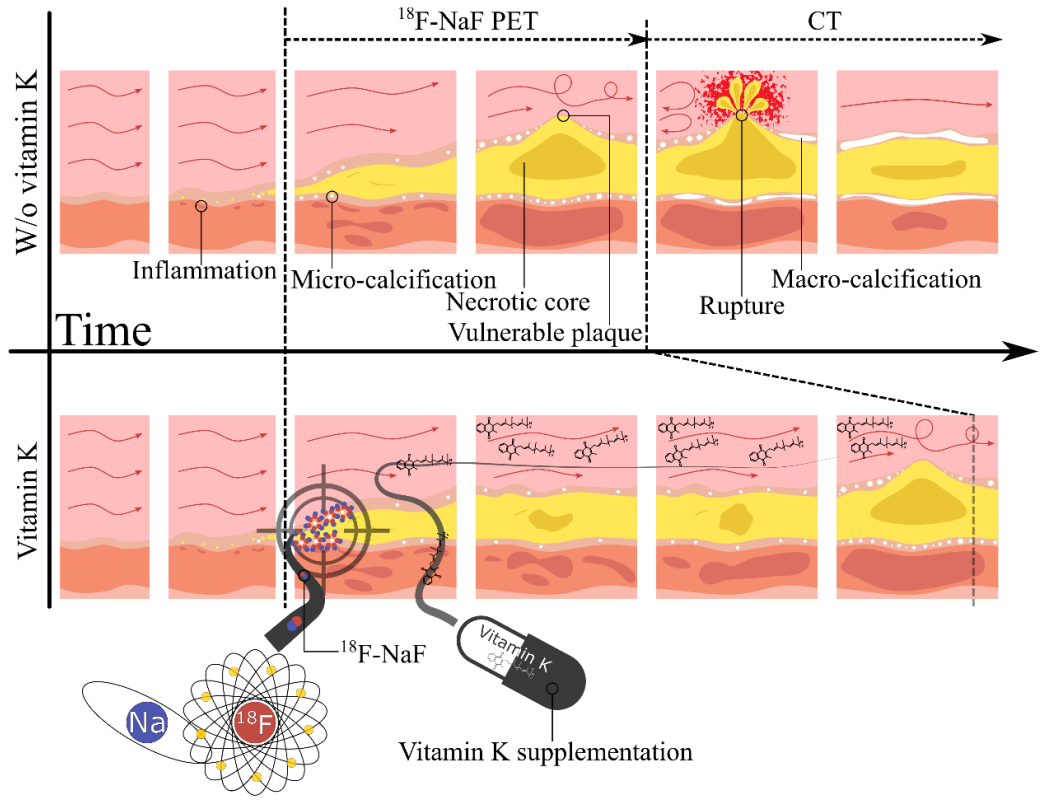

^{18}F-NaF PET is able to identify earlier stages of atherosclerotic development (*i.e.* micro-calcification) in contrast to conventional CT scans, which are detecting macro-calcifications. This micro-calcified state is ideal to start vitamin K supplementation, in order to indirectly fight against calcification and to reduce cardiovascular risk.

Figure 2: Increased ^{18}F-NaF uptake in culprit coronary artery lesion

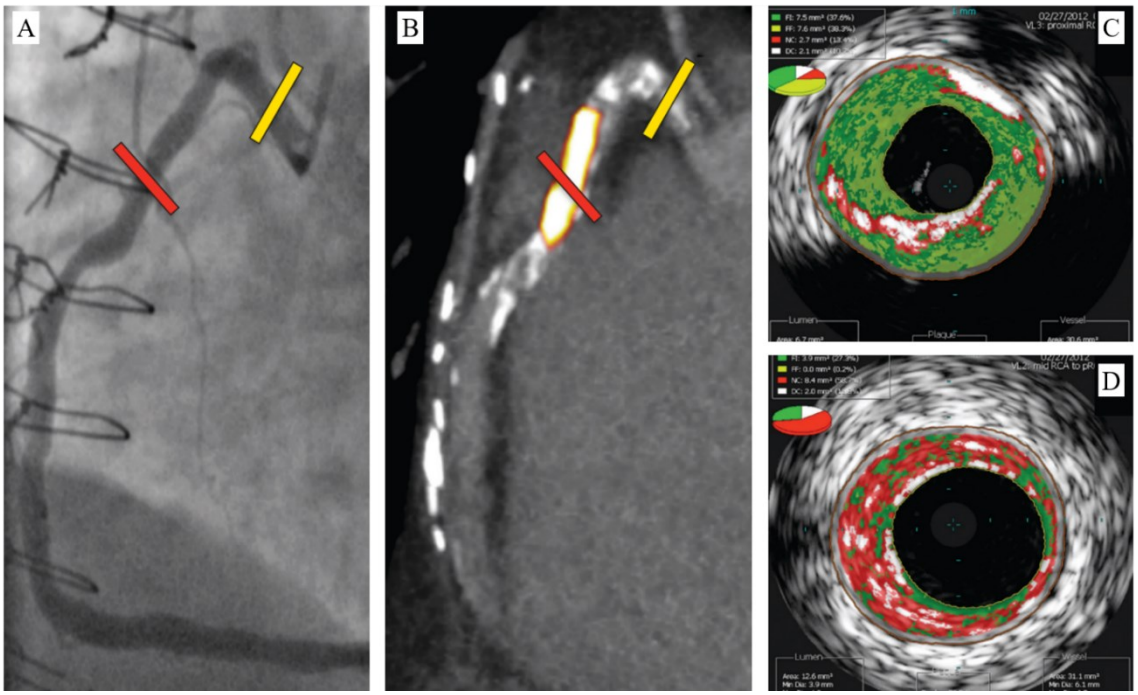

Adapted from Joshi *et. al.* [22] with permission. In a patient with coronary artery disease, invasive coronary angiography (A) showed non-obstructive disease in the right coronary artery. Corresponding ^{18}F-NaF PET/CT (B) showed a region of increased ^{18}F-NaF activity (positive lesion, red line) in the mid-right coronary artery (tissue-to-background ratio, 3.13) and a region without increased uptake in the proximal vessel (negative lesion, yellow line). Radiofrequency intravascular ultrasound shows that the ^{18}F-NaF negative plaque (C) is principally composed of fibrous and fibro-fatty tissue (green) with confluent calcium (white with acoustic shadow) but little evidence of necrosis. On the contrary, the ^{18}F-NaF positive plaque (D) shows high-risk features such as a large necrotic core (red) and micro-calcification (white).

Permissions information

The authors do hereby declare that Figure 1 in the manuscript is entirely original and does not require reprint permission.

Figure 2 in the manuscript is used with permission from Dr. Nikhil V. Joshi, the corresponding author of the article in question.

One-sentence Summary

Vitamin K emerges as a suitable, cost-effective, bullet that can and should be loaded after targeting micro-calcification with ^{18}F-NaF PET.

Table

Table: Promising therapies for the future of treatment of vascular calcification

Medication	**Mechanism of action**	**Benefits against calcification**	**References**
Bisphosphonates	Inhibit calcium metabolism	Positive (detrimental side effects)	[32]
Phosphate binders	Prevent absorption of dietary phosphate	Questionable	[34]
Statins	HMG-CoA reductase inhibitor	Positive	[35,36]
Vitamin K	cofactor in γ-carboxylation of glutamate	Promising (cost-effective)	[43,44,47,49–52]

Chapter III: Preclinical study

Sodium [^{18}F]Fluoride PET can efficiently monitor in vivo atherosclerotic plaque calcification progression and treatment

Alexandru Florea, Julius P. Sigl, Agnieszka Morgenroth, Andreas Vogg, Sabri Sahnoun, Oliver H. Winz, Jan Bucerius, Leon J. Schurgers, and Felix M. Mottaghy

This work was published in *Cells* on 30 January 2021

doi: 10.3390/cells10020275

Article

Sodium [^{18}F]Fluoride PET Can Efficiently Monitor *In Vivo* Atherosclerotic Plaque Calcification Progression and Treatment

Alexandru Florea [1,2,3], Julius P. Sigl [1], Agnieszka Morgenroth [1], Andreas Vogg [1], Sabri Sahnoun [1], Oliver H. Winz [1], Jan Bucerius [2,3,4], Leon J. Schurgers [3,5,6] and Felix M. Mottaghy [1,2,3,*]

[1] Department of Nuclear Medicine, University Hospital RWTH Aachen, 52074 Aachen, Germany; aflorea@ukaachen.de (A.F.); julius.sigl@googlemail.com (J.P.S.); amorgenroth@ukaachen.de (A.M.); avogg@ukaachen.de (A.V.); ssahnoun@ukaachen.de (S.S.); owinz@ukaachen.de (O.H.W.)

[2] Department of Radiology and Nuclear Medicine, Maastricht University Medical Center, 6229 HX Maastricht, Netherlands;

[3] School for Cardiovascular Diseases (CARIM), Maastricht University Medical Center, 6229 HX Maastricht, Netherlands; l.schurgers@maastrichtuniversity.nl (L.J.S.)

[4] Department of Nuclear Medicine, University of Göttingen, 37075 Göttingen, Germany: jan.bucerius@med.uni-goettingen.de (J.B.)

[5] Department of Biochemistry, Maastricht University Medical Center, 6229 HX Maastricht, Netherlands

[6] Institute of Experimental Medicine and Systems Biology, RWTH Aachen University, 52074 Aachen, Germany

***** Correspondence: fmottaghy@ukaachen.de; Tel.: +49-241-80-88741

Abstract

Given the high sensitivity and specificity of sodium [^{18}F]Fluoride (Na[^{18}F]F) for vascular calcifications and positive emerging data of vitamin K on vascular health, the aim of this study is to assess the ability of Na[^{18}F]F to monitor therapy and disease progression in a unitary atherosclerotic mouse model. ApoE$^{-/-}$ mice were placed on a Western-type diet for 12-weeks and then split into four groups. The early stage atherosclerosis group received a chow diet for an additional 12-weeks, while the advanced atherosclerosis group continued the Western-type diet. The Menaquinone-7 (MK-7) and Warfarin groups received MK-7 or Warfarin supplementation during the additional 12-weeks, respectively. Control wild type mice were fed a chow diet for 24-weeks. All of the mice were scanned with Na[^{18}F]F using a small animal positron emission tomography (PET)/computed tomography (CT). The Warfarin group presented spotty calcifications on the CT in the proximal aorta. All of the spots corresponded to dense mineralisations on the von Kossa staining. After the control, the MK-7 group had the lowest Na[^{18}F]F uptake. The advanced and Warfarin groups presented the highest uptake in the aortic arch

and left ventricle. The advanced stage group did not develop spotty calcifications, however Na[^{18}F]F uptake was still observed, suggesting the presence of micro-calcifications. In a newly applied mouse model, developing spotty calcifications on CT exclusively in the proximal aorta, Na[^{18}F]F seems to efficiently monitor plaque progression and the beneficial effects of vitamin K on cardiovascular disease.

Keywords: cardiovascular diseases; positron-emission tomography; sodium fluoride; vitamin K; warfarin; vascular calcification; micro-calcification

---

1. Introduction

Medical associations around the globe, including the American Heart Association, recommend the early identification of subclinical atherosclerosis via non-invasive imaging (*i.e.*, coronary artery calcification score or carotid artery ultrasound) in order to guide preventive care [1]. Indeed, considering the recent advancements in medical imaging, these techniques can be used for patient selection and stratification [2].

Numerous imaging techniques have been proposed for the identification of vascular calcification, especially after its acknowledgment as an independent cardiovascular risk factor and as a marker for plaque vulnerability, alongside inflammation [3,4]. In a recent review, the superiority of sodium [^{18}F]Fluoride (Na[^{18}F]F) positron emission tomography (PET) over other modalities to correctly identify micro-calcified plaque has been elaborated [5]. Na[^{18}F]F is a PET tracer that binds to hydroxyapatite crystals and is therefore able to identify osseous and ectopic calcifications (including vascular calcifications). Moreover, its high specificity makes it highly valuable for the non-invasive identification of micro-calcified plaque [6]. It is also considered that Na[^{18}F]F uptake in plaque with no visible calcifications on the computed tomography (CT) is a result of actively developing micro-calcifications [7]. The smallest vascular calcification formation visible with computed tomography (CT) is termed “spotty calcification”, being less than 3 mm in diameter and having an increased attenuation compared with the surrounding tissue [8]. However, the Multi-Ethnic Study of Atherosclerosis study (*i.e.*, MESA) showed an inverse association of vascular calcification on CTs with cardiovascular risk [9]. Na[^{18}F]F PET remains the only available clinical tool that can non-invasively detect potentially vulnerable micro-calcified plaque [5,10].

Given the high sensitivity and specificity of Na[^{18}F]F for vascular calcifications, we wanted to investigate the ability of this tracer to monitor therapy and disease progression.

In a recent review paper, we also presented emerging data that suggest vitamin K—especially MK-7—as a cost-effective method for delaying the progression of vascular calcification [5]. In short, vitamin K is a crucial cofactor in the post-translational modification of various proteins, including coagulation factors and matrix γ-carboxyglutamate protein (*i.e.*, MGP), the latter of which is involved in the inhibition of ectopic calcification. Considering this mechanism of action, vitamin K has received the attention of several on-going clinical trials. Out of all vitamins that fall under the umbrella of "vitamin K", MK-7 is one of the most used in preclinical and clinical trials, thanks to its increased half-life in blood, which extends its uptake availability through extra-hepatic tissues [11]. Conversely, the vitamin K inhibitor Warfarin is able to block the post-translational modifications of the matrix γ-carboxyglutamate protein, and thus accelerates ectopic calcifications, including vascular ones. It is well known that rodents under Warfarin treatment alone develop lethal bleedings caused by inhibiting the proper hepatic synthesis of vitamin K-dependent coagulation factors. By supplementing the respective diets with Phylloquinone (*i.e.*, vitamin K1), the liver function is recovered; however, Warfarin is still able to inhibit the proper synthesis of matrix γ-carboxyglutamate protein (*i.e.*, MGP) [12–14].

In our current study, we wanted to assess the ability of Na[^{18}F]F to monitor therapy and disease progression in a unitary atherosclerotic mouse model. Hence, the ability of Na[^{18}F]F PET to detect small changes in plaque morphology was prospectively tested in atherosclerotic mice, that were given either Menaquinone-7 (MK-7) supplementation, or Warfarin or Phylloquinone supplementation, or were maintained on the atherogenic diet.

2. Materials and Methods

2.1. Mouse Strains and Care

All of the animal experiments were approved by a German competent authority (Landesamt für Natur, Umwelt und Verbraucherschutz Nordrhein-Westfalen) for compliance with the Animal Protection Act, in conjunction with the regulation for the protection of animals used for experimental and other scientific purposes (file number 81-02.04.2018.A286). Wild type (n = 5) and ApoE$^{-/-}$ (n = 20) male mice were purchased from Charles River Laboratories Italy (*i.e.*, C57BL/6J and B6.129P2-Apoe$^{tm1Unc/J}$, respectively). Upon arrival, all of the mice were kept in the Institute for Laboratory Animal Science of the University Hospital RWTH Aachen, and one week prior to the scans, they were moved to the Department of Nuclear medicine of the University Hospital RWTH Aachen for acclimatization.

The animals were housed under a 12-h-light/12-h-dark cycle and were given free access to their respective diets and to water. The room temperature and relative humidity were kept between 20–25 °C and 45–65%, respectively.

Because all of mice used had a C57BL/6 background, and in combination of the 24-weeks feeding scheme, some animals developed skin lesions suggestive of ulcerative dermatitis. Hence, a Dexpanthenol ointment (Bepanthen® from Bayer Vital GmbH, Leverkusen, Germany) was applied to ease scratching; moreover, these mice had priority on the day of scanning.

Over the course of the study, one animal was lost due to anesthesia.

2.2. Experimental Groups and Feeding Scheme

All of the mice used were male and were 6 weeks of age at the start of the trial. Upon arrival, five animals per experimental group were caged in order to ease the feeding scheme. Each mouse was fed for a total of 24 weeks prior to the measurements. The entire feeding scheme is illustrated in Figure 1.

At 6 weeks of age, all of the wild type mice ($n = 5$) started a regular chow diet (1324; Altromin, Lage, Germany), which was maintained for the entire length of the experiment (24 weeks).

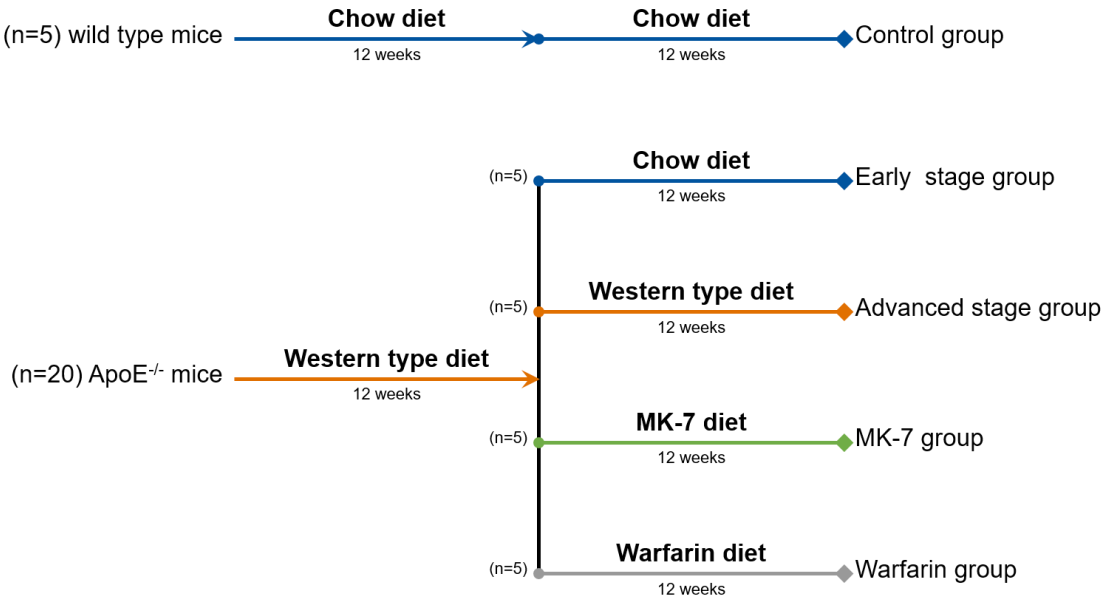

Figure 1. Feeding scheme: 20 ApoE$^{-/-}$ mice started a Western-type diet for 12 weeks, in order to develop early stage plaque. At the end of the 12 weeks, 5 mice were switched to a regular chow feed (early stage group), 5 mice continued their Western type diet for the additional 12 weeks (advanced stage group), 5 mice were switched to a vitamin K deficient chow feed supplemented with MK-7 (100 µg/g of feed; MK-7 group), and the remaining 5 mice were switched to a vitamin K deficient chow supplemented with Warfarin (3 mg/g of feed) and Phylloquinone (1.5 mg/g of feed) for an additional 12 weeks (Warfarin group).

At 6 weeks of age, ApoE$^{-/-}$ mice (n = 20) started a Western-type diet with 0.15% cholesterol and 19.5% casein (Altromin, Lage, Germany) for a minimum of 12 weeks, in order to develop early stage plaque. For the early stage plaque group, the diet was switched to a regular chow feed (1324; Altromin, Lage, Germany), in order to slow the plaque development. For the advanced plaque group, the Western-type diet was continued throughout the additional 12 weeks.

To investigate the effect of vitamin K on plaque development, an additional MK-7 (kind gift of NattoPharma, Oslo, Norway) group and Warfarin (A4571-10G; Merck KGaA, Darmstadt, Germany) group were created. In the MK-7 group, after the original 12 weeks of the Western-type diet, the feed was switched to a vitamin K deficient chow diet (C 1020; Altromin, Lage, Germany) supplemented with MK-7 (100 µg/g of feed). The Warfarin group was switched to the same vitamin K deficient chow feed (C 1020; Altromin, Lage, Germany) supplemented with Warfarin (3 mg/g of feed) and Phylloquinone (1.5 mg/g of feed, V3501-10G; Merck KGaA, Darmstadt, Germany) [14].

During the acclimatization period, all of the mice maintained their respective feeding schemes.

Over the course of the study, three mice developed skin lesions suggestive of ulcerative dermatitis and received a topical Dexpanthenol ointment (*i.e.*, one mouse from the control group, one from the MK-7 group, and one from the Warfarin group).

2.3. Na[^{18}F]F Preparation

One Na[^{18}F]F preparation was done for each scanning day.

The quaternary methyl ammonium (*i.e.*, QMA) carbonate cartridges (186004540; Waters GmbH, Eschborn, Germany) were first conditioned with a 0.9% NaCl solution, then washed with sterile water. Afterwards, crude [^{18}F]-fluoride (proton irradiated target water) was loaded onto the cartridge, washed with sterile water, and eluted with a 0.9% NaCl. This was used for the intravenous injections.

2.4. Na[^{18}F]F PET/CT Measurements

All of the mice were imaged with a small animal PET/SPECT/CT system (*i.e.*, Triumph® II, Northridge Tri-Modality Imaging, Inc., Chatsworth, USA), however only the PET and CT modalities were used for this study.

Under 1.5–2.5% isoflurane anesthesia in oxygen at 0.8 L/min, the lateral tail vein was injected with 50 µL of CT contrast agent (130-095-698; Viscover™) and 15 ± 2 MBq of Na[^{18}F]F in a maximum total volume of 125 µL. After injection, the mice were placed on the scanner bed and the CT scan was initiated. The exposure settings used were as

follows: 130 uA, 75 kVp, 230 ms exposure time, and 360° rotation with 720 views with an average of two frames for each view; the duration of the CT scans was ~15 min. A dynamic 1h PET scan was initiated at the end of the CT scan (*i.e.*, ~25 min post injection). The CT had an axial field of view of 91.1 mm and a PET one of 112 mm. During the scans, the isoflurane concentration was adapted so as to achieve a respiratory rate between 75–50 breaths per minute.

One mouse from the early stage group was lost due to anesthesia overdose during the PET scan; therefore, this data was excluded from the final image analysis. However, tissues were used for the final validation stainings.

2.5. Image Processing and Analysis

The CT images were reconstructed using a Feldkamp filtered back projection reconstruction process to a voxel size of 0.154 × 0.154 × 0.154 mm^3 in a 592 × 592 × 560 matrix. Using vendor software, the CT values were converted into Hounsfield units (HU) using the following formula

$$HU = 1000 \times ((\mu_t - \mu_w) \div \mu_w) \quad (1)$$

where μ_w is the linear attenuation coefficient of the water and μ_t is the linear attenuation coefficient of the tissue.

The PET data were reconstructed using a 3D ordered-subset expectation maximization (*i.e.*, OSEM-3D with three iterations and eight subsets) with a maximum a posteriori probability algorithm (30 iterations) into a 240 × 240 × 192 image matrix (resulting in final voxel dimensions of 0.25 × 0.25 × 0.597 mm^3). PET normalization, CT attenuation correction, and CT scatter correction were applied to all of the PET reconstructions.

The PET images were automatically aligned to the CT using a custom-made transformation in PMOD software package version 3.13 (PMOD Technologies LLC, Zürich, Switzerland) from a capillary phantom. The co-registered PET/CT images were further used for the PET quantification. To avoid bone spillover, a bone auto-contour was defined as 5% of the activity (in kBq/cc) of the hottest registered voxel of the scan (*i.e.*, ~450 kBq/cc) and was then masked. The manually drawn volumes of interest (VOIs) were placed at a distance of at least two voxels from the masked bone auto-contour. All of the VOI were placed on the axial view.

To calculate the blood pool background activity, a VOI, comprising of ~10 consecutive slices, was manually placed in the thoracic region of the inferior vena cava,

encompassing the contrast enhanced lumen. The mean activity (in kBq/cc) and the average of the top 10 hottest voxels were recorded from this VOI.

A VOI for the left ventricle was created as follows: initially, the entire left ventricle (*i.e.*, including the free ventricular wall, the interventricular septum, and the ventricular cavity) was manually isolated in a region spanning from the apex to the aortic root. Afterwards, an automatic isocontour was generated using the mean activity of the background (*i.e.*, from the inferior vena cava VOI) as the minimal threshold.

The same technique was applied for the VOIs of the aortic root and aortic arch. Upon completion of all target VOIs, the average of the top 10 hottest voxels was recorded. All VOIs were drawn by a blinded member of our team, in order to exclude analysis bias.

In order to quantify the PET data and to correct for the blood compartment contribution, the maximum target-to-background ratio (TBRmax) was calculated using the following formula:

$$\text{TBRmax} = ((\text{HotAverage}(10)_{\text{target}} - \text{HotAverage}(10)_{\text{background}}) \div \text{HotAverage}(10)_{\text{background}}) \quad (2)$$

where $\text{HotAverage}(10)_{\text{target}}$ is the average of the top 10 hottest voxels recorded in the primary volumes of interest and $\text{HotAverage}(10)_{\text{background}}$ is the average of the top 10 hottest voxels recorded in the inferior vena cava.

As only the Warfarin group presented modifications on the CT images, the data from only this group were also analyzed using PMOD software package version 3.13 (PMOD Technologies LLC, Zürich, Switzerland). The average background created by the blood pool and vessel wall was recorded by loading the aortic arch VOI that was created during the PET quantification and deleting the slices in which the radio-dense spots were visible (*i.e.*, no thresholding was applied). One VOI, which included all spotty calcifications developed by one mouse, was serially drawn by hand in the axial slices, which contained no VOI for the background. Upon completion of all of the volumes of interest, the average of all of the voxels and the value of the hottest voxel were recorded. In order to quantify the CT data, the HU values of all volumes of interest were used.

2.6. Statistical Analysis

All of the variables are presented as data dots with a line and a value indicating the mean and error bars for the standard deviation. To calculate the statistical differences between multiple groups, one-way analysis of variance (one-way ANOVA) tests were applied. Additionally, the standard deviation of all of the variables was calculated and used alongside the average in the Results section. If the differences from this test exceeded the statistical significance threshold (*i.e.*, $p < 0.05$), Tukey's honestly significant difference test was performed for a post hoc analysis. Statistically significant results are indicated in charts, with stars suggesting a p-value lower than 0.05.

2.7. Organ Harvesting and Validation Staining Protocols

At the end of the scans, the mice were sacrificed by applying an isoflurane overdose, and the heart and aortic arch were collected using a well described protocol [15].

The aortic root was considered as the heart region where aortic leaflets are present. The aortic arch was considered to be the aortic region between the emergence of the ascending aorta from the heart and the third intercostal space; this sample also included the brachiocephalic artery and the emergences of the left common carotid and left subclavian artery.

All of the organ samples were formalin-fixed, paraffin-embedded, and sectioned with a thickness of 5 µm prior to staining using standard Hematoxylin eosin (HE) and von Kossa staining protocols.

3. Results

3.1. Validation Stainings

3.1.1. HE Staining

All of the ApoE$^{-/-}$ mice (*i.e.*, the Warfarin, MK-7, advanced stage, and early stage groups) developed plaque, starting at the aortic root and then continuing along the aortic arch (Figure 2). Moreover, all of the mice from the Warfarin group presented several intense basic spots at different levels of the aortic arch—some in the aortic wall, while others in the wall of the brachiocephalic artery (Figure 2). The wild type control mice did not develop any plaque at the investigated levels (Figure 2).

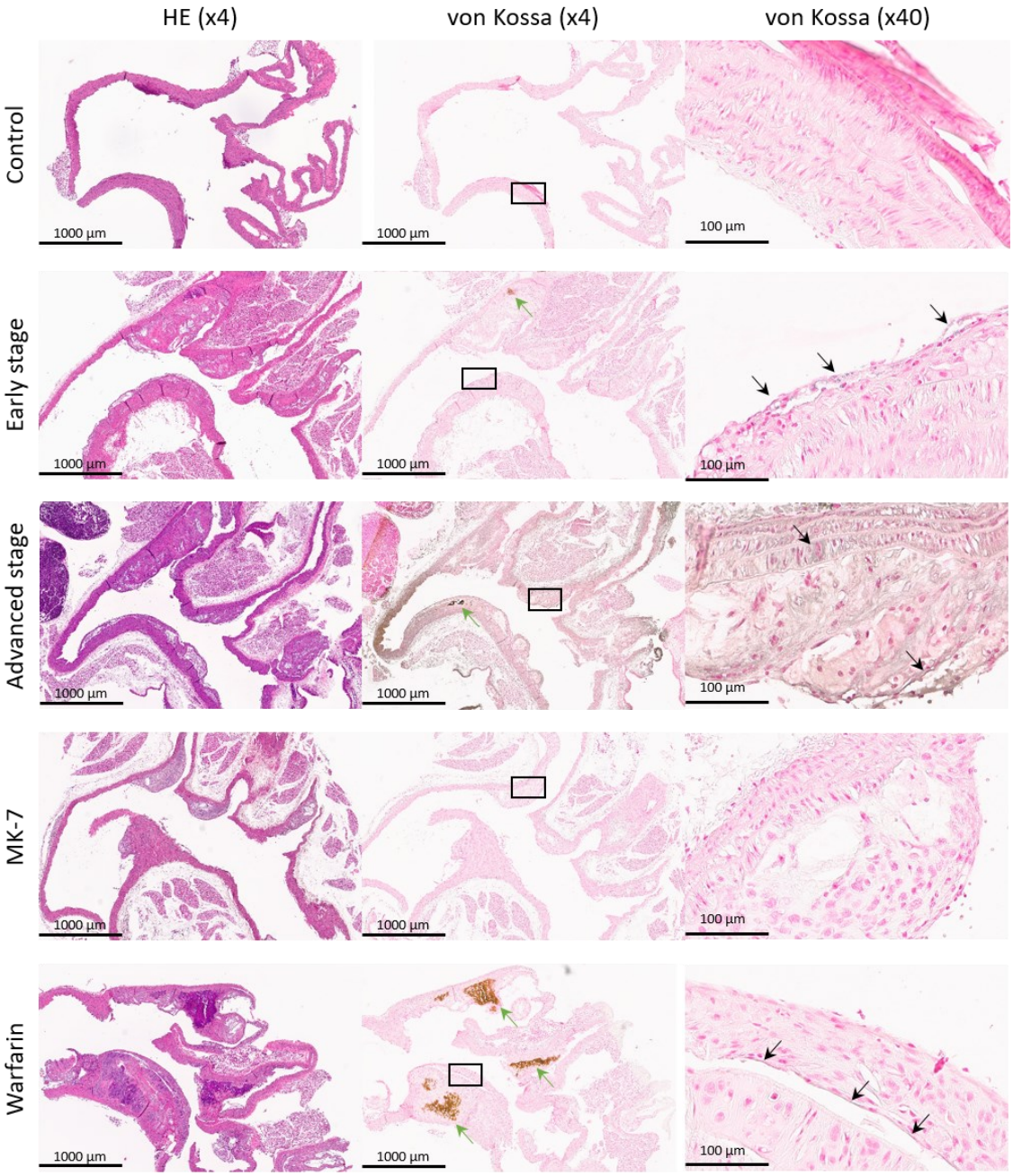

Figure 2. Validation stainings: example of an aortic arch Hematoxylin eosin (HE) and von Kossa stainings from each experimental group. The first image column is stained with HE followed by the next paraffin slice, which is stained with von Kossa (green arrows indicate calcifications larger than 50 µm). The von Kossa (×40) column contains representative enlargements with sites of microscopic calcification (black arrows indicate calcifications smaller than 50 µm).

3.1.2. Von Kossa Staining

All of the mice from the Warfarin group exclusively presented dense mineralization spots in the aortic wall and the wall of the brachiocephalic artery, which co-localized with the intense basic spots from the HE staining (Figure 2). As these spots were present inside the plaque, this is suggestive of the pro-calcification potential of Warfarin.

3.2. CT Findings

Examples of CT and PET/CT fusions of Na[^{18}F]F uptake in the heart region of all of the experimental groups are illustrated in Figure 3.

The CT data from only the Warfarin group were analyzed, as in this group, radio-dense spots suggestive of spotty calcifications were observed in the proximal aorta. Each mouse presented at least two radio-dense spots in different regions of the proximal aorta. Table 1 presents the number and anatomical regions in which these spots were observed on the CT of each mouse from the Warfarin group.

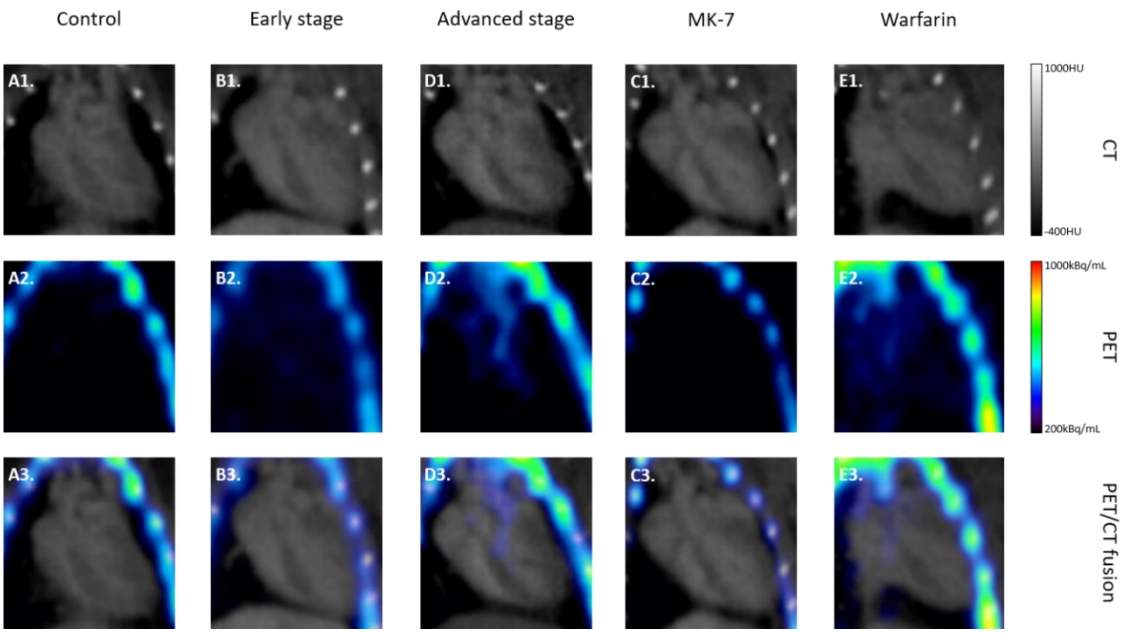

Figure 3. Na[^{18}F]F PET/CT: examples of computed tomography (CT), positron emission tomography (PET), and PET/CT fusions of Na[^{18}F]F uptake in the heart region of all of the experimental groups. Exemplary CT and PET are given in the first and second rows, respectively, while in the third row the fusions of the corresponding images are presented. All CT images are scaled between -400 HU and 1000 HU, while the PET images are between 200 kBq/mL and 1000 kBq/mL.

Table 1. Number and anatomical regions of the radio-dense spots observed in the Warfarin group.

Mouse NO.	Aortic Arch	Brachiocephalic Artery	Left Carotid Artery	Total [1]
1	2	1	0	3
2	1	1	1	3
3	0	1	1	2
4	2	1	0	3
5	2	0	0	2

[1] Total number of spotty calcifications developed by each mouse.

After a side by side comparison of the CT images with selected histological stainings (*i.e.*, HE and von Kossa), all radio-dense spots corresponded with intense basic spots and dense mineralizations (Figure 4). Compared with the background created by the contrast

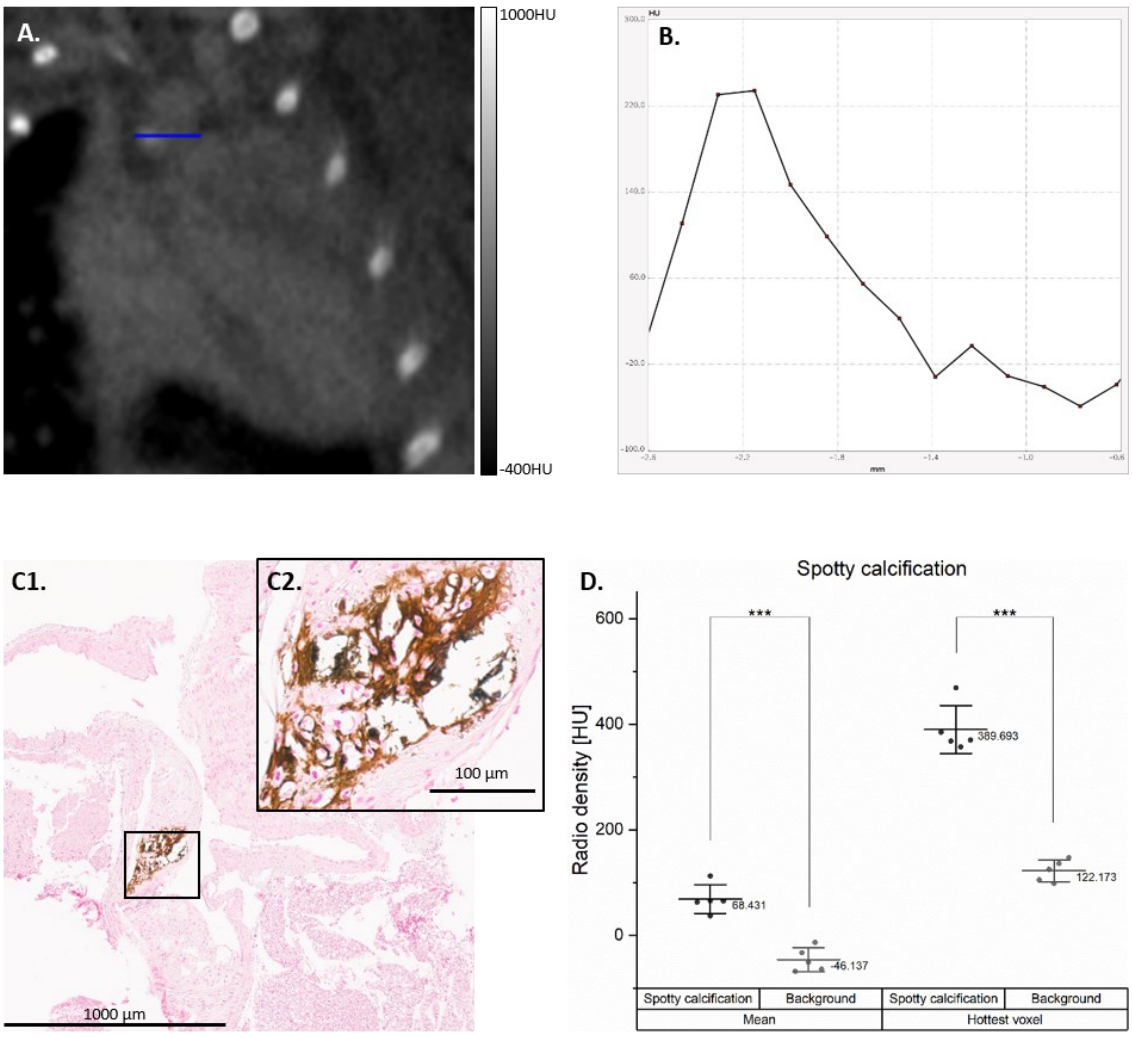

Figure 4. Spotty calcifications developed by the Warfarin group. Example of spotty calcification developed on the CT from the Warfarin group (**A**) with horizontal line profile (**B**). The spotty calcification was correlated with intense mineralization in the aortic arch in the von Koss staining (**C1**), with a x40 enlargement (**C2**). The mean Hounsfield units (HU) value (averaged) and the hottest voxel (max) of the spotty calcifications are compared to the blood pool background created by the contrast agent (**D**); *** $p < 0.001$).

agent in the blood, both the mean HU value of the calcification spots ($p < 0.001$) and the hottest voxel ($p < 0.001$) were significantly higher (Figure 4D).

3.3. Na[^{18}F]F PET Findings

Examples of the PET and PET/CT fusions of Na[^{18}F]F uptake in the heart region of all of the experimental groups are illustrated in Figure 3. Statistical analysis of all TBRmax values in the analyzed regions is presented in Figure 5. In all of the regions, the lowest TBRmax was found, as expected, in the control group followed by the MK-7 group (p = n.s.).

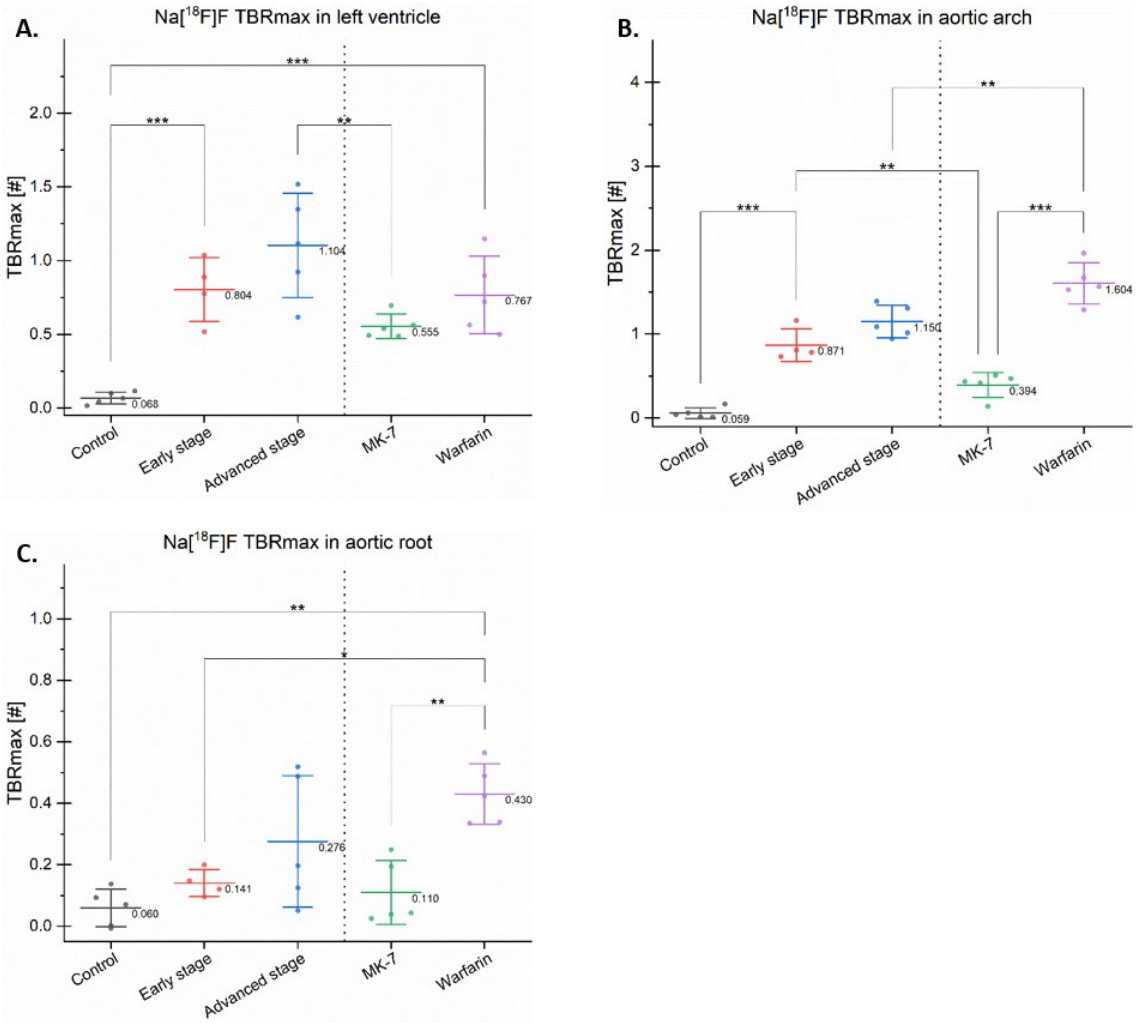

Figure 5. Maximum target-to-background ratios in different regions. The maximum target-to-background ratio (TBRmax) of Na[^{18}F]F is presented as dots with a line and a value indicating the mean and error bars for the standard deviation in the left ventricle (**A**), aortic arch (**B**), and aortic root (**C**); * $p < 0.05$, ** $p < 0.01$, *** $p < 0.001$.

Na[^{18}F]F TBRmax in all of the investigated regions seemed to reflect the duration of the Western-type diet (control *vs.* early stage *vs.* advanced stage). In the left ventricle and aortic arch, these increases reached statistical significance ($p < 0.001$), suggesting that these regions are more prone to develop micro-calcifications compared with the aortic root, which only includes the aortic leaflets.

The mice treated with MK-7 had a lower Na[^{18}F]F TBRmax in all investigated regions compared with the Warfarin group. MK-7 reduced the Na[^{18}F]F uptake, while Warfarin increased it, suggesting an analogue role in calcification.

In the aortic arch and left ventricle, the early, advanced stage, and Warfarin groups presented a high TBRmax compared with the control ($p < 0.05$), suggesting that all of the aforementioned groups developed calcifications (Figure 5A,B).

In the aortic root, significant differences were found in the control *vs.* Warfarin groups ($p < 0.01$), and in the early stage *vs.* Warfarin groups ($p < 0.05$). However, the differences between the control and both early and advanced stages were not significant.

In the aortic arch, the early stage had a significantly increased uptake compared with the MK-7 group ($p < 0.01$). Moreover, in this region, the Warfarin group had a higher TBRmax ($p < 0.05$) compared with the advanced stage group (Figure 5B). This increased uptake was due to the spotty calcifications developed by this new model, which is avid for Na[^{18}F]F.

3.4. Skin Lesions Suggestive of Ulcerative Dermatitis

The images of the skin lesions developed by the three mice are available in the Supplementary Material (Figure S1). No correlation was observed between the diet and these skin lesions, as one was from the control group, one from the MK-7 group, and one from the Warfarin group. Post hoc, the PET data of these specific mice were double-checked; however, none of the mice had outlying TBRmax values within their respective groups. Therefore, the data of these mice were included in the statistical analysis.

Moreover, there was no abnormal bleeding observed in the lesions of the mouse from the Warfarin group, when compared with the other two animals.

4. Discussion

In this study, we have shown the potential ability of Na[^{18}F]F to detect changes in diet in a uniform mouse model.

According to the maintenance phantom measurements, our small animal PET had a reconstructed resolution of ~1 mm^3, while the mean cross-sectional plaque surface developed by ApoE$^{-/-}$ mice (*i.e.*, fed for 12 weeks with a high fat diet) was ~3000 μm^2

[16]. Our targets were thus in the lower range of the PET detection; therefore, we decided to use relatively large VOIs so that multiple targets could be included. With a higher volume, the mean uptake is lowered by the blood pool activity, so we semi-quantitatively determined the uptake as a target of the background ratio of the hottest voxels (*i.e.*, TBRmax), as suggested by other research groups in the field [17].

Our data suggest that Na[^{18}F]F was able to discriminate between early and advanced stage plaque developed by ApoE$^{-/-}$ mice fed a Western-type diet for 12 and 24 weeks, respectively. This trend may be due to the increase over time of the plaque calcium load [18]. Moreover, MK-7 supplementation seemed to have the lowest tracer uptake in the aortic arch and left ventricle of all of the other groups. In fact, uptakes in the MK-7 treatment and control groups were similar in all of the investigated regions. These results suggest that Na[^{18}F]F is able to detect morphological changes induced by vitamin K treatment. One study showed that vitamin K reduced the plaque size and vascular (micro) calcification levels in ApoE$^{-/-}$ mice [16].

Recently, it has been shown that Na[^{18}F]F is sensitive enough to reflect the changes of progressive exercise on atherosclerotic calcium deposits in ApoE$^{-/-}$ mice [19], and also sustained vascular mineralization in an uremic mouse model [17]. Taken together with our data, it seems that Na[^{18}F]F is able to distinguish between different stages of atherosclerosis, thus adding to the current trend for the introduction of Na[^{18}F]F PET in clinical practice.

It was anticipated that the MK-7 group would have an increased uptake compared with the control, as these mice showed plaque in the histological analysis. However, the fact that this group had the lowest TBRmax compared with the other groups fed a Western-type diet suggests a protective role of MK-7 against micro-calcification formation, as revealed by the Na[^{18}F]F uptake, which was already linked to the plaque calcification level [20].

Additionally, Na[^{18}F]F revealed a difference between the continuation of the Western-type diet (*i.e.*, advanced group) and the switch to a normal diet supplemented with vitamin K (*i.e.*, MK-7 group). As C57BL/J mice consume on average 4 g of food per day [21], in our MK-7 group, each mouse received on average a daily supplementation of 400 μg vitamin K. This finding adds to the previously [5] described list of the beneficial effects of vitamin K for cardiovascular health, which, in combination with ongoing clinical trials, may favor the increase in the recommended daily dose of vitamin K or its introduction in clinical practice. Some clinical studies failed to observe a change in Na[^{18}F]F uptake after 6 months [22] and 18 months [23] of MK-7 supplementation. This

discrepancy between humans and mice may be explained by several changes in our preclinical study design, namely: mice have a higher metabolism, which is suggested to be 45 times faster in mice compared with humans [24]; moreover, taking into account the higher homogeneity of inbred mice, the variance is innately lower in preclinical studies compared with clinical trials.

Warfarin treatment induced the formation of calcified lesion in our mice. Previously, it was shown that when supplemented to a Western-type diet, it induced intimal plaque calcification in ApoE$^{-/-}$ mice [14]. Moreover, this compound caused changes in the plaque morphology with features suggestive of plaque vulnerability [14].

An unexpected finding was the Warfarin-induced spotty calcifications detected by the CT. ApoE$^{-/-}$ in a C57BL/6 background started to develop intra-plaque calcifications after 45 weeks of chow diet [25]. In our study, after 24 weeks of feeding, the Warfarin group developed spotty calcifications exclusively in the proximal aorta, despite extensive evaluation of all other regions. To our knowledge, this is the first detection via a small animal CT of the ectopic calcifications developed by Warfarin fed mice; moreover, the lesions developed were very similar to those observed in humans [8]. Similar lesions have been described in isolated aortas of 6-month old (*i.e.*, 24 weeks) Ldlr$^{-/-}$ mice scanned with a high resolution micro-CT suitable for small samples [26]. Other mouse models have developed vascular calcifications [27]; however, these mice require an additional mutation and they have a reduced life-span (*i.e.*, Fetuin-A knock-out). On the other hand, there is no described reduced lifespan of the ApoE$^{-/-}$ mice on Warfarin. In the present study, all of the mice from this group reached 6 months of age (*i.e.*, 24 weeks of diet) with no apparent health problems. Moreover, in some of our still unpublished studies, the mice in this group reached 9 months of age (*i.e.*, 36 weeks of diet), also with no apparent issues. To our knowledge, the only described side-effect is lethal bleeding, which may be kept in check by dietary supplementation with Phylloquinone [12].

No radio-dense spots were observed in the early and advanced stage groups, suggesting that the Western-type diet induced micro-calcified plaque, and only Warfarin supplementation induced spotty calcifications.

4.1. Limitations

The data generated by this study are mainly based on PET and CT analysis. Therefore, the assumptions that the different Na[^{18}F]F uptakes reflect changes in the calcification micro-architecture are solely based on already published works. Irkle et al. [20] previously showed that this tracer is able to specifically detect active vascular calcifications in human plaque. Meanwhile, Hu et al. [18] recently reported that a similar correlation exists in ApoE−/− mice at different ages. Therefore, in our study, no systematic qualitative assessments of plaque micro-calcification levels have been performed. As Na[^{18}F]F has been shown to be able to detect calcification sites invisible by regular histological stainings [10,20], additional investigations that have been performed for other models [14,26,28] are still required (*e.g.*, micro-autoradiography, atomic absorption-spectrometry, or energy-dispersive X-ray spectroscopy).

Another limitation of the presented study and mouse model is the extended feeding scheme, which prevented a post hoc repeat of this study. Additionally, the long feeding scheme combined with the C57BL/6 background led to some mice developing skin lesions suggestive of ulcerative dermatitis, for which a Dexpanthenol ointment (Bepanthen® from Bayer Vital GmbH, Leverkusen, Germany) was applied to ease scratching. However, there was no described influence of Dexpanthenol topical ointment on atherosclerotic development.

Lastly, it is worth mentioning that the term "spotty calcification" was used to describe the radio-dense spots in the aortic arches of the Warfarin group, however there is no clear-cut definition of this term in preclinical research [29].

4.2. Future Prospects

Na[^{18}F]F has shown its ability to target vulnerable micro-calcified plaque in many independent studies [5]. Our findings also point to its utility in monitoring treatment and disease progression. However, further clinical studies are also necessary to show its potential in human plaque, as mice develop morphologically different plaque [30]. This data opens the path for future clinical studies to be able to debate the use of Na[^{18}F]F PET in micro-calcified plaque monitoring. The same is true for our vitamin K data, which will come to the aid of future studies that want to investigate the benefits of this complex on vascular health.

As spotty calcifications detected on CTs are still used in the clinical diagnosis of vulnerable plaque, our new Warfarin model may be used to first assess the efficacy of novel therapeutic approaches in a preclinical setup. We do not expect excessive bleeding

during the surgery of these mice, as the animal with skin lesions did not present any abnormal bleeding in comparison with the other two mice with the same condition.

5. Conclusions

In this study, Na[^{18}F]F PET showed potential to monitor plaque progression and treatment. This tracer also seemed to be able to detect the beneficial effects of vitamin K on cardiovascular micro-calcification, when compared with the continuation of a Western-type diet. Additionally, we describe a novel mouse model, which spontaneously develops spotty calcifications, detected by small animal CT, exclusively in the proximal aorta, with no apparent life-span reduction.

Supplementary Materials: The following are available online at www.mdpi.com/xxx/s1: Figure S1: Ulcerative dermatitis.

Author Contributions: conceptualization, A.F., J.B., L.J.S., and F.M.M.; data curation, A.F. and O.H.W.; formal analysis, A.F. and J.P.S.; funding acquisition, J.B., L.J.S., and F.M.M.; investigation, A.F. and A.M.; methodology, A.F. and O.H.W.; project administration, F.M.M.; resources, A.F., A.M., A.V., S.S., O.H.W., and L.J.S.; supervision, F.M.M.; validation, A.F., A.M., and O.H.W.; visualization, A.F., O.H.W., J.B., L.J.S., and F.M.M.; writing—original draft, A.F.; writing—review and editing, J.P.S., A.M., A.V., S.S., O.H.W., J.B., L.J.S., and F.M.M.. All of the authors have read and agreed to the published version of the manuscript.

Funding: This research was funded by the European Union's Horizon 2020 research and innovation program under Marie Skłodowska - Curie grant (grant number 722609).

Institutional Review Board Statement: The study was conducted according to the German Animal Protection Act, in conjunction with the regulation for the protection of animals used for experimental and other scientific purposes and approved by the Ethics Committee of a German competent authority (*i.e.*, Landesamt für Natur, Umwelt und Verbraucherschutz Nordrhein-Westfalen) (file number 81-02.04.2018.A286, approved on 20.11.2018).

Informed Consent Statement: Not applicable.

Data Availability Statement: Data available in a publicly accessible repository. The data presented in this study are openly available in Zenodo at DOI:10.5281/zenodo.4478936.

Acknowledgments: Special mentions to Dr. Barbara Klinkhammer and to Prof. Dr. Peter Boor from the Department of Pathology, University Hospital RWTH Aachen, for their support with the image acquisition of our histological slides.

Conflicts of Interest: Dr. Alexandru Florea, Prof. Leon J. Schurgers, Prof. Jan Bucerius, and Prof. Felix M. Mottaghy received research funding from the ITN INTRICARE of European Union's Horizon 2020 research and innovation program under the Marie Skłodowska-Curie grant (grant number 722609). Prof. Leon J. Schurgers receives research funding from the ITN EVOluTION of European Union's Horizon 2020 research and innovation program under the Marie Skłodowska-Curie grant, (grant number 675111); from the Norwegian Research Council (grant number 241584); and from the Dutch Thrombosis Service (grant number 2014.02). Dr. Agnieszka Morgenroth and Prof. Felix M. Mottaghy receive research funding from the German Research Foundation

(DGN) in the framework of the Research Training Group for “Tumor-targeted Drug Delivery” (grant number 331065168), and for “Severity assessment in animal-based research” (grant number 321137804). Prof. Leon J. Schurgers has received institutional grants from Bayer, Boehringer Ingelheim, Daichi Sankyo, NattoPharma, and IDS. Prof. Felix M. Mottaghy is on the advisory board of Advanced Accelerator Applications GmbH and has received institutional grants from GE Healthcare, Siemens, and Nano-Map. All of the other authors declare no conflict of interest. The funders had no role in the design of the study; in the collection, analyses, or interpretation of data; in the writing of the manuscript; or in the decision to publish the results.

References

1. Benjamin, E.J.; Muntner, P.; Alonso, A.; Bittencourt, M.S.; Callaway, C.W.; Carson, A.P.; Chamberlain, A.M.; Chang, A.R.; Cheng, S.; Das, S.R.; et al. Heart Disease and Stroke Statistics—2019 Update: A Report From the American Heart Association. *Circulation* **2019**, *139*, e56–e528.
2. Kassem, M.; Florea, A.; Mottaghy, F.M.; van Oostenbrugge, R.; Kooi, M.E. Magnetic resonance imaging of carotid plaques: Current status and clinical perspectives. *Ann. Transl. Med.* **2020**, *8*, 1266–1266.
3. Budoff, M.J.; Shaw, L.J.; Liu, S.T.; Weinstein, S.R.; Tseng, P.H.; Flores, F.R.; Callister, T.Q.; Raggi, P.; Berman, D.S.; Mosler, T.P. Long-Term Prognosis Associated With Coronary Calcification. *J. Am. Coll. Cardiol.* **2007**, *49*, 1860–1870.
4. Nakahara, T.; Dweck, M.R.; Narula, N.; Pisapia, D.; Narula, J.; Strauss, H.W. Coronary Artery Calcification: From Mechanism to Molecular Imaging. *JACC Cardiovasc. Imaging* **2017**, *10*, 582–593.
5. Florea, A.; Morgenroth, A.; Bucerius, J.; Schurgers, L.J.; Mottaghy, F.M. Locking and loading the bullet against micro-calcification. *Eur. J. Prev. Cardiol.* **2020**, doi:10.1177/2047487320911138.
6. Bucerius, J.; Dijkgraaf, I.; Mottaghy, F.M.; Schurgers, L.J. Target identification for the diagnosis and intervention of vulnerable atherosclerotic plaques beyond 18F-fluorodeoxyglucose positron emission tomography imaging: Promising tracers on the horizon. *Eur. J. Nucl. Med. Mol. Imaging* **2019**, *46*, 251–265.
7. Creager, M.D.; Hohl, T.; Hutcheson, J.D.; Moss, A.J.; Schlotter, F.; Blaser, M.C.; Park, M.-A.; Lee, L.H.; Singh, S.A.; Alcaide-Corral, C.J.; et al. 18 F-Fluoride Signal

Amplification Identifies Microcalcifications Associated With Atherosclerotic Plaque Instability in Positron Emission Tomography/Computed Tomography Images. *Circ. Cardiovasc. Imaging* **2019**, *12*, 7835.

8. Obaid, D.R.; Calvert, P.A.; Brown, A.; Gopalan, D.; West, N.E.J.; Rudd, J.H.F.; Bennett, M.R. Coronary CT angiography features of ruptured and high-risk atherosclerotic plaques: Correlation with intra-vascular ultrasound. *J. Cardiovasc. Comput. Tomogr.* **2017**, *11*, 455–461.
9. Criqui, M.H.; Knox, J.B.; Denenberg, J.O.; Forbang, N.I.; McClelland, R.L.; Novotny, T.E.; Sandfort, V.; Waalen, J.; Blaha, M.J.; Allison, M.A. Coronary Artery Calcium Volume and Density: Potential Interactions and Overall Predictive Value: The Multi-Ethnic Study of Atherosclerosis. *JACC Cardiovasc. Imaging* **2017**, *10*, 845–854.
10. Dweck, M.R.; Aikawa, E.; Newby, D.E.; Tarkin, J.M.; Rudd, J.H.F.; Narula, J.; Fayad, Z.A. Noninvasive Molecular Imaging of Disease Activity in Atherosclerosis. *Circ. Res.* **2016**, *119*, 330–340.
11. Schurgers, L.J.; Teunissen, K.J.F.; Hamulyak, K.; Knapen, M.H.J.; Vik, H.; Vermeer, C. Vitamin K-containing dietary supplements: Comparison of synthetic vitamin K1 and natto-derived menaquinone-7. *Blood* **2007**, *109*, 3279–3283.
12. Price, P.A.; Faus, S.A.; Williamson, M.K. Warfarin Causes Rapid Calcification of the Elastic Lamellae in Rat Arteries and Heart Valves. *Arterioscler. Thromb. Vasc. Biol.* **1998**, *18*, 1400–1407.
13. Krüger, T.; Oelenberg, S.; Kaesler, N.; Schurgers, L.J.; van de Sandt, A.M.; Boor, P.; Schlieper, G.; Brandenburg, V.M.; Fekete, B.C.; Veulemans, V.; et al. Warfarin Induces Cardiovascular Damage in Mice. *Arterioscler. Thromb. Vasc. Biol.* **2013**, *33*, 2618–2624.
14. Schurgers, L.J.; Joosen, I.A.; Laufer, E.M.; Chatrou, M.L.L.; Herfs, M.; Winkens, M.H.M.; Westenfeld, R.; Veulemans, V.; Krueger, T.; Shanahan, C.M.; et al. Vitamin K-Antagonists Accelerate Atherosclerotic Calcification and Induce a Vulnerable Plaque Phenotype. *PLoS One* **2012**, *7*, e43229.
15. Mohanta, S.; Yin, C.; Weber, C.; Hu, D.; Habenicht, A.J. Aorta Atherosclerosis Lesion Analysis in Hyperlipidemic Mice. *Bio-protocol* **2016**, *6*.

16. Wang, Z.; Wang, Z.; Zhu, J.; Long, X.; Yan, J. Vitamin K2 can suppress the expression of Toll-like receptor 2 (TLR2) and TLR4, and inhibit calcification of aortic intima in ApoE −/− mice as well as smooth muscle cells. *Vascular* **2018**, *26*, 18–26.

17. Rucher, G.; Cameliere, L.; Fendri, J.; Anfray, A.; Abbas, A.; Kamel, S.; Dupas, Q.; Delcroix, N.; Berger, L.; Manrique, A. Molecular imaging of endothelial activation and mineralization in a mouse model of accelerated atherosclerosis. *EJNMMI Res.* **2019**, *9*.

18. Hu, Y.; Hu, P.; Hu, B.; Chen, W.; Cheng, D.; Shi, H. Dynamic monitoring of active calcification in atherosclerosis by 18F–NaF PET imaging. *Int. J. Cardiovasc. Imaging* **2020**, 1–9.

19. Hsu, J.J.; Fong, F.; Patel, R.; Qiao, R.; Lo, K.; Soundia, A.; Chang, C.C.; Le, V.; Tseng, C.H.; Demer, L.L.; et al. Changes in microarchitecture of atherosclerotic calcification assessed by 18F-NaF PET and CT after a progressive exercise regimen in hyperlipidemic mice. *J. Nucl. Cardiol.* **2020**, 1–8.

20. Irkle, A.; Vesey, A.T.; Lewis, D.Y.; Skepper, J.N.; Bird, J.L.E.; Dweck, M.R.; Joshi, F.R.; Gallagher, F.A.; Warburton, E.A.; Bennett, M.R.; et al. Identifying active vascular microcalcification by 18F-sodium fluoride positron emission tomography. *Nat. Commun.* **2015**, *6*, 7495.

21. Bachmanov, A.A.; Reed, D.R.; Beauchamp, G.K.; Tordoff, M.G. Food intake, water intake, and drinking spout side preference of 28 mouse strains. *Behav. Genet.* **2002**, *32*, 435–443.

22. Zwakenberg, S.R.; de Jong, P.A.; Bartstra, J.W.; van Asperen, R.; Westerink, J.; de Valk, H.; Slart, R.H.J.A.; Luurtsema, G.; Wolterink, J.M.; de Borst, G.J.; et al. The effect of menaquinone-7 supplementation on vascular calcification in patients with diabetes: A randomized, double-blind, placebo-controlled trial. *Am. J. Clin. Nutr.* **2019**, *110*, 883–890.

23. de Vriese, A.S.; Caluwé, R.; Pyfferoen, L.; de Bacquer, D.; de Boeck, K.; Delanote, J.; de Surgeloose, D.; van Hoenacker, P.; van Vlem, B.; Verbeke, F. Multicenter randomized controlled trial of Vitamin K antagonist replacement by rivaroxaban with or without vitamin K2 in hemodialysis patients with atrial fibrillation: The Valkyrie study. *J. Am. Soc. Nephrol.* **2020**, *31*, 186–196.

24. Flurkey, K.; Currer, J.; Harrison, D. Mouse Models in Aging Research. In *The Mouse in Biomedical Research*; Fox, J., Barthold, S., Davisson, M., Newcomer, C., Quimby, F., Smith, A., Eds.; Elsevier: New York, 2007; Vol. 3, pp. 637–72 ISBN 9780080555287.

25. Rattazzi, M.; Bennett, B.J.; Bea, F.; Kirk, E.A.; Ricks, J.L.; Speer, M.; Schwartz, S.M.; Giachelli, C.M.; Rosenfeld, M.E. Calcification of advanced atherosclerotic lesions in the innominate arteries of ApoE-deficient mice: Potential role of chondrocyte-like cells. *Arterioscler. Thromb. Vasc. Biol.* **2005**, *25*, 1420–1425.

26. Awan, Z.; Denis, M.; Bailey, D.; Giaid, A.; Prat, A.; Goltzman, D.; Seidah, N.G.; Genest, J. The LDLR deficient mouse as a model for aortic calcification and quantification by micro-computed tomography. *Atherosclerosis* **2011**, *219*, 455–462.

27. Jahnen-Dechent, W.; Heiss, A.; Schäfer, C.; Ketteler, M. Fetuin-A Regulation of Calcified Matrix Metabolism. *Circ. Res.* **2011**, *108*, 1494–1509.

28. Roijers, R.B.; Debernardi, N.; Cleutjens, J.P.M.; Schurgers, L.J.; Mutsaers, P.H.A.; van der Vusse, G.J. Microcalcifications in Early Intimal Lesions of Atherosclerotic Human Coronary Arteries. *Am. J. Pathol.* **2011**, *178*, 2879–2887.

29. Wang, Y.; Osborne, M.T.; Tung, B.; Li, M.; Li, Y. Imaging Cardiovascular Calcification. *J. Am. Heart Assoc.* **2018**, *7*.

30. Jackson, C.L.; Bennett, M.R.; Biessen, E.A.L.; Johnson, J.L.; Krams, R. Assessment of Unstable Atherosclerosis in Mice. *Arterioscler. Thromb. Vasc. Biol.* **2007**, *27*, 714–720.

Chapter IV: Clinical study protocol

Effects of combined Vitamin K2 and Vitamin D3 supplementation on Na[^{18}F]F PET/MRI in patients with carotid artery disease: the INTRICATE rationale and trial design

Alexandru Florea, M. Eline Kooi, Werner Mess, Leon J. Schurgers, Jan Bucerius, and Felix M. Mottaghy

This work was published in *Nutrients* on 19 March 2021

doi: 10.3390/nu13030994

Article

Effects of Combined Vitamin K2 and Vitamin D3 Supplementation on Na[^{18}F]F PET/MRI in Patients with Carotid Artery Disease: The INTRICATE Rationale and Trial Design

Alexandru Florea [1,2,3], M. Eline Kooi [2,3], Werner Mess [4], Leon J. Schurgers [3,5,6], Jan Bucerius [2,3,7,†] and Felix M. Mottaghy [1,2,3,*,†]

[1] Department of Nuclear Medicine, University Hospital RWTH Aachen, 52074 Aachen, Germany; aflorea@ukaachen.de

[2] Department of Radiology and Nuclear Medicine, Maastricht University Medical Center, 6229HX Maastricht, The Netherlands; eline.kooi@mumc.nl (M.E.K.)

[3] School for Cardiovascular Diseases (CARIM), Maastricht University, 6229HX Maastricht, The Netherlands; l.schurgers@maastrichtuniversity.nl

[4] Department of Clinical Neurophysiology, Maastricht University Medical Center, 6229HX Maastricht, The Netherlands; werner.mess@mumc.nl

[5] Department of Biochemistry, Maastricht University, 6229HX Maastricht, The Netherlands

[6] Institute of Experimental Medicine and Systems Biology, RWTH Aachen University, 52074 Aachen, Germany

[7] Department of Nuclear Medicine, University of Göttingen, 37075 Göttingen, Germany; jan.bucerius@med.uni-goettingen.de (J.B.)

* Correspondence: fmottaghy@ukaachen.de; Tel.: +49-241-80-88741

† These authors have contributed equally to this work.

Abstract

INTRICATE is a prospective double-blind placebo-controlled feasibility study, assessing the influence of combined vitamin K2 and vitamin D3 supplementation on micro-calcification in carotid artery disease as imaged by hybrid Sodium [^{18}F]Fluoride (Na[^{18}F]F) positron emission tomography (PET)/ magnetic resonance imaging (MRI). Arterial calcification is an actively regulated process and results from the imbalance between calcification promoting and inhibiting factors. Considering the recent advancements in medical imaging, ultrasound (US), PET/MRI, and computed tomography (CT) can be used for the selection and stratification of patients with atherosclerosis. Fifty-two subjects with asymptomatic carotid artery disease on at least one side of the neck will be included in the study. At baseline, an Na[^{18}F]F PET/MRI and CT examination will be performed. Afterwards, subjects will be randomized (1:1) to a

vitamin K (400 µg MK-7/day) and vitamin D3 (80 µg/day) or to placebo. At the 3-month follow-up, subjects will undergo a second Na[^{18}F]F PET/MRI and CT scan. The primary endpoint is the change in Na[^{18}F]F PET/MRI (baseline *vs.* after 3 months) in the treatment group as compared to the placebo arm. Secondary endpoints are changes in plaque composition and in blood-biomarkers. The INTRICATE trial bears the potential to open novel avenues for future large scale randomized controlled trials to intervene in the plaque development and micro-calcification progression.

Keywords: cardiovascular diseases; positron emission tomography; magnetic resonance imaging; sodium fluoride; vitamin K; vitamin D; vascular calcification; micro-calcification

---

1. Introduction

Arterial calcification is an active process and results from the imbalance between calcification promoting and inhibiting factors [1]. Extracellular matrix calcification is initiated by matrix vesicles, secreted by osteoblasts or osteoblast-like cells (*i.e.*, vascular smooth muscle cells that acquired the pathological osteogenic phenotype [2]), inducing the nucleation of calcium phosphate crystals (*i.e.*, hydroxyapatite) [3]. Accumulation of calcium and phosphate ions into vesicles will initiate crystal formation [3]. Next, hydroxyapatite crystals will elongate radially, penetrate the vesicle membrane, and will form calcifying nodules with neighboring matrix vesicles [3]. The subsequent growth of the calcifying nodule seems to be regulated by the availability of organic compounds (*e.g.*, matrix Gla protein, MGP) [3].

Considering the recent advancements in medical imaging, ultrasound (US), magnetic resonance imaging (MRI), computed tomography (CT), as well as positron emission tomography (PET) with different (new) PET-tracers can be used for the selection and stratification of patients with atherosclerosis [4–7]. In a recent review, the superiority of sodium [^{18}F]Fluoride (Na[^{18}F]F) PET over other modalities to correctly identify micro-calcified plaques has been elaborated [8]. Na[^{18}F]F PET is considered to be the only available clinical tool that can non-invasively detect (potentially) vulnerable micro-calcified plaques more sensitively than CT [8,9].

In the last two decades, a series of proteins that can bind calcium ions have been discovered and most of them share a common feature, the γ-carboxyglutamic acid (Gla) rich domain. As a result that Gla-residues are biologically converted from protein-bound

glutamic acid residues by an enzyme which uses vitamin K as a cofactor, all these proteins are called vitamin K dependent proteins. MGP [10] is one of the most studied vitamin K dependent proteins that has proven to have a role in the protection against ectopic calcification [11,12].

MGP is able to avidly bind the calcium from hydroxyapatite crystals [13] and therefore to block the growth of calcifying nodules. In order to become biologically active, MGP requires two post-translational modifications: γ-carboxylation and phosphorylation.

MGP can be found in the blood stream and there are numerous human and animal studies in which MGP has been used as a marker for different inflammatory diseases that also involve calcification (*e.g.*, coronary artery disease, type 2 diabetes, chronic kidney disease) [14–16]. High plasma levels of dephosphorylated uncarboxylated MGP (dp-ucMGP) correlate with an increased cardiovascular risk in type 2 diabetes patients [17]. Moreover, dp-ucMGP inversely correlates with vascular calcification levels of patients suffering from coronary artery disease [18], type 2 diabetes [19], and end stage kidney disease [20]. One study did not measure the inactive form, but the total concentration of MGP and found a significant reduction in MGP synthesis in patients with aortic valve calcification [21] and chronic kidney disease [22]. Moreover, low plasma levels of dp-ucMGP are associated with an increased all-cause and cardiovascular mortality in the general European population [23].

Therefore, dp-ucMGP might be used as a marker for vitamin K status and in extension for vascular health.

In a recent review paper, we have presented emerging data, which suggests vitamin K—especially Menaquinone-7 (MK-7)—as a cost-effective method of delaying progression of vascular calcification [8]. Although these studies support the idea that MK-7 protects against vascular calcification, there have been no controlled trials in humans assessing the effects of MK-7 supplementation on arterial calcification in the context of atherosclerosis.

Experimental studies suggest positive effects of vitamin D on vitamin K-dependent metabolism [24–27]. In mice, a diet high in active vitamin D for 20 weeks induced higher amounts of uncarboxylated (inactive) MGP, reflecting low vitamin K status and renal calcification [24]. Indeed, large randomized clinical trials failed to show a positive effect of vitamin D3 supplementation in the prevention of cardiovascular disease [28,29]. Vitamin K supplementation can overcome this untoward effect of excess vitamin D on calcification as demonstrated by lower calcium and phosphorus content in aorta and

kidney [27]. The MGP-gene promoter contains a vitamin D response element, capable of a two to threefold enhanced MGP expression after vitamin D binding [25,30]. The upregulation of MGP due to vitamin D needs vitamin K to ensure full activation of MGP for optimal functioning. This implies that the combination of both vitamin K and vitamin D could provide enhanced protection against progressive vascular calcification, cardiovascular disease, and mortality [31].

It is for these above-mentioned reasons that we intend to use Na[^{18}F]F PET/MRI in the proposed feasibility study, which will assess the influence of MK-7 and vitamin D3 supplementation on the development of arterial micro-calcification in the context of atherosclerosis. The primary objective of this study is to assess the combination of vitamin K and vitamin D on the pathophysiological process of arterial micro-calcification in carotid artery disease via hybrid Na[^{18}F]F PET/MRI. Furthermore, the longitudinal change of micro-calcifications under MK-7 and D3 supplementation in the coronary arteries will be assessed by means of a coronary artery calcification (CAC) scan. The aforementioned scans will be compared between baseline and end of the study in a group receiving the vitamin supplementation as compared to placebo. In addition, dp-ucMGP will be measured in order to determine whether this biomarker can be used to assess the degree of calcification in the arterial wall of patients with coronary and carotid artery disease.

2. Study Design

The INTRICATE trial (acronym for the "Effects of combined vitamin K2 and vitamin D3 supplementation on Na[^{18}F]F PET/MRI in patients with carotid artery disease" trial) is a double-blind randomized, placebo-controlled feasibility study, performed at the Maastricht University Medical Center, with an end of the study visit after 3 months. The research file of this trial, including the study protocol, was approved by the accredited local Medical Ethics Committee of the Academic Hospital Maastricht and University of Maastricht in the Netherlands (*i.e.*, METC azM/UM) under the file number NL69450.068.19/METC300103 and is being conducted according to the principles of the Declaration of Helsinki. The INTRICATE trial is also registered at clinicaltrials.gov under NCT04010578. All subjects give their written informed consent for inclusion before they participate in the study. The informed consent is being received in writing, in the native language of the subjects (*i.e.*, Dutch) and is available in the Supplementary Materials.

Subjects with asymptomatic carotid artery disease (*i.e.*, on the common or the internal carotid) on at least one side with a degree of stenosis >25% (according to ECST criteria) as detected by means of B-mode US and who meet the inclusion criteria will be recruited. After providing informed consent, they will be randomized in two groups:

1. the first group will receive a daily dose of 400 µg MK-7 and 80 µg D3 and
2. the second (*i.e.*, control) group will receive a placebo.

Both, the investigators as well as the patients will be blinded regarding the treatment used.

At baseline, a Na[^{18}F]F PET/MRI, a CAC scan, and an US examination of the neck vessels will be performed; moreover, samples of venous blood will be taken. Subjects will be asked for a follow-up evaluation after 3 months of supplementation, when Na[^{18}F]F PET/MRI, CAC scan, and US scan will be repeated, in order to measure the degree of vascular calcifications and the changes in time of atherosclerosis. Additionally, venous blood samples will be obtained by standard venous puncture for routine biochemical, hematological, and serum biomarker assessments.

3. Study Population

Patients with asymptomatic carotid artery disease on one side, who meet the inclusion criteria and who provide a signed informed consent are being invited in this study.

3.1. Inclusion Criteria

In order to be eligible to participate in this study, a subject must meet all following criteria:

- Asymptomatic carotid artery disease on at least one side with a degree of stenosis > 25 % (according to the ECST criteria). If the patient has a symptomatic carotid artery disease on the contra-lateral side, he/she will still be included in the study, if intensified medical treatment for this symptomatic stenosis (*e.g.*, statins, antiplatelet medication) was started ≥ 6 month before inclusion of the patient. This protocol was chosen in order to assure a stable situation on the plaque(s), which avoids an overspill from this medication on the assumed effects of the supplementation.
- Age older than 18 years.
- Signed informed consent provided.

3.2. Exclusion Criteria

A potential subject who meets any of the following criteria will be excluded from participation in this study:

- Antiplatelet or cholesterol lowering medication started within the past 6 months.
- Chronic or paroxysmal atrial fibrillation.
- Already performed or scheduled coronary or carotid revascularization procedure (*e.g.*, stent implantation, coronary artery bypass graft, balloon-dilatation, endarterectomy, angioplasty).
- History of myocardial infarction or stroke.
- Malignant disease (except for treated basal-cell or squamous cell carcinoma).
- Use of vitamin K antagonists treatment.
- A life-expectancy < 1 year.
- Claustrophobia.
- Presence of a pacemaker, intra-cardiac defibrillator, or metallic implant (*e.g.*, vascular clip, neuro-stimulator, cochlear implant, metal splinter in the eye).
- Body weight > 130 kg or body habitus that does not fit into the gantry.
- Pregnancy or wish to become pregnant in the near future.
- Breast feeding.
- (History of) metabolic or gastrointestinal disease.
- Use of vitamin K or D containing supplements or vitamin K-rich foods (*e.g.*, fermented soya).
- Chronic inflammatory disease.
- Systemic treatment or topical treatment likely to interfere with evaluation of the study parameters.
- Corticoid treatment.
- Participation in a clinical study within one month before enrolment in the current study.

4. Study Objectives and Statistical Analyses Plan

The objective of this study is to assess the influence of MK-7 and vitamin D3 on the pathophysiological process of arterial micro-calcification in carotid artery disease as assessed by hybrid Na[^{18}F]F PET/MRI. Furthermore, the longitudinal change of micro-calcifications and plaque composition and volume under this supplementation in coronary artery disease patients will be assessed by means of MRI and CAC scan. The aforementioned scans will be compared between baseline and the end of the study visit

in a group receiving vitamin K supplementation as compared to the placebo group. In addition, dp-ucMGP will be measured, in order to determine whether this biomarker can be used to assess the degree of calcification in the arterial wall of patients with coronary and carotid artery disease. Finally, blood samples will be stored in the Biobank, creating the opportunity to investigate new biomarkers regarding vitamins K and D status in the future (*e.g.*, their influence on osteocalcin or alkaline phosphatase).

4.1. Primary Objective

We investigated whether MK-7 and vitamin D3 supplementation can diminish, halt, or even reverse the development of arterial micro-calcification in the carotid arteries in the context of atherosclerosis as detected by Na[^{18}F]F PET/MRI compared to placebo after 3 months.

4.2. Secondary Objectives

Secondary objectives of the trial include assessing whether:

- the vitamin supplementation can diminish, halt, or even reverse the development of arterial micro-calcification in the coronary arteries in the context of atherosclerosis as detected by CAC score compared to placebo after 3 months;
- the primary parameter correlates or is able to predict the results of the CAC score;
- the vitamin supplementation can influence MRI parameters such as normalized wall index (*i.e.*, measurement of plaque burden), intra-plaque hemorrhage volume, lipid-rich necrotic core volume, and fibrous cap status;
- the vitamin supplementation can influence US after 3 months of supplementation;
- Na[^{18}F]F uptake in the carotids is associated with US at the end of the study visit;
- the vitamin supplementation is influencing plasma levels of dp-ucMGP after 3 months, in comparison with a placebo, in order to select a possible peripheral marker for vitamin K-status;
- baseline plasma levels of dp-ucMGP can be reliable biomarkers of plaque vulnerability and of its calcified state;
- there is a correlation between serum MK-7 concentrations and the values of the prothrombin time (PT) or the international normalized ratio (INR).

4.3. Statistical Analyses Plan

Our null hypotheses states that MK-7 and vitamin D3 do not influence the change (*i.e.*, progression) of micro-calcifications in 3 months of supplementation when compared

to a placebo; there will be no difference in the degree of calcification between the MK7+D3 group *vs.* the placebo at the end of the study. Our alternative hypothesis states that MK-7 and vitamin D3 have a greater effect on the change of micro-calcification in 3 months of supplementation compared to placebo.

The descriptive statistics for each variable at baseline will be presented for both groups combined and individually (*i.e.*, MK7+D3 and placebo) for each of the following parameters: mean, standard deviation of the variable, standard error of the mean, range (minimum-maximum), median, quartiles, and confidence intervals where necessary. Descriptive statistics for variables at the end of the study will be presented separate for both groups (*i.e.*, MK7+D3 and placebo).

Both intention-to-treat and per protocol analysis will be performed. For the intention-to-treat analysis, all randomized subjects (with data available from the end of the study visit) will be included. In the per protocol analysis, only subjects who fully complied with the prescribed supplementation will be included.

The main outcome parameter (*i.e.*, the longitudinal change time of micro-calcification as measured by the Na[^{18}F]F uptake via hybrid PET/MRI) will be presented as a continuous variable. It will be expressed as a mean difference (*i.e.*, the standard uptake value and target-to-background radio of Na[^{18}F]F at the end of the study visit minus Na[^{18}F]F maximal uptake at baseline). To investigate the existence of significant predictor(s) for the main outcome parameter (*i.e.*, the longitudinal change of micro-calcification), univariate analysis will be used. If the significance level (*i.e.*, α) will be between 5 % and 25 % at the univariate *t*-test hypothesis testing (*i.e.*, $p > 0.05$ and $p < 0.25$), a multivariate analysis will be used, in order to investigate a possible association or interaction between variables.

In order to decide to either reject or accept our null hypothesis, a two-sided confidence interval using 95% confidence will be calculated and reported. A two-sided hypothesis test using a significance level (*i.e.*, α) of 5% will also be reported.

The CAC score and the US data will be presented as continuous variables. Their longitudinal change will be also expressed as a mean difference (*i.e.*, value at the end of the study visit minus value at baseline) and will be presented as continuous variables.

For the continuous data including age, blood pressure, body-mass index, lipid-rich necrotic volume, normalized wall index, dp-ucMGP, and other laboratory tests, the distribution of variables will be analyzed (verification of normality of distribution for all subjects) by histograms. To investigate the existence of significant predictor(s) for the secondary outcome parameters, univariate analysis will be used. If the significance level

(*i.e.*, α) will be between 5% and 25% at the univariate t-test hypothesis testing (*i.e.*, $p > 0.05$ and $p < 0.25$), a multivariate analysis will be used, in order to investigate a possible association or interaction between variables. If variables display no normal distribution, data will be transformed using appropriate transformations. If transformation is not possible, this data is analyzed by non-parametric statistical tests (*i.e.*, Chi-square test).

Baseline parameters will be presented: sex, age, bodyweight, length, body-mass index, medical history, medication, family history, and cardiovascular risk factors.

Health status and use/changes of medication will be verified during the baseline visit and at the end of the study visit.

5. Study Procedures

An outline in chronological order, with all the procedures that will be received by the subjects, is available in Table 1.

Table 1. Outline of visit procedures.

Study Procedure	Recruitment ($t \approx -7$ Days)	Baseline Visit ($t = 0$)	End of the Study Visit ($t \approx 3$ Months)
Informed consent	X [1]		
Hospital visit	X	X [1]	X [1]
• demographic factors	X		
• medical history	X		
• current medication	X	X [1]	X [1]
• physical examination	X	X [1]	X [1]
• blood pressure	X		X
• ECG	X		X
Blood sampling and laboratory assessments		X [1]	X [1]
US examination		X [1]	X [1]
Na[^{18}F]F PET/MRI		X [1]	X [1]
CAC scan		X [1]	X [1]
Randomization		X [1]	
Drug distribution		X [1]	
Drug count			X [1]

[1] Different from routine clinical care.

5.1. Hospital Visit

At baseline visit, a complete medical interview and physical examination will be performed with emphasis on the detection of signs of cardiovascular disease (*i.e.*, coronary and carotid artery disease). Furthermore, the height, weight, and waist-hip circumference will be measured.

Both at baseline and end of the study visits arterial blood pressure will be measured on both arms with an electronic blood-pressure measurement device. Before measurement, the subject will be seated for at least 5 min. Moreover, an ECG will be acquired.

5.2. Na[^{18}F]F PET/MRI

The PET/MRI will be performed using a hybrid PET/MRI scanner (Siemens Biograph mMR, Siemens, Forchheim, Germany). During the PET scan (on hybrid PET/MRI scanner), MRI images will be concomitantly acquired to the PET images. A dedicated coil will be used for imaging of the carotid bifurcation. This coil allows for sub-millimeter resolution imaging of the lumen, vessel walls, and atherosclerotic plaques.

As Na[^{18}F]F is eliminated by the kidneys, it will accumulate in the urinary bladder. In order to reduce the radiation exposure to the entire urinary tract, subjects will be asked to drink 0.5 L water in the hour before arrival at the hospital; for Na[^{18}F]F, there is no fasting required. Upon arrival, study participants will be asked to drink an additional 0.5 L water and the procedure will be explained once more. Afterwards, 185 MBq of Na[^{18}F]F will be injected via a venipuncture of the arm. Subjects will be asked to empty their bladder right before the start of the scan (*i.e.*, 1 h post injection). The patient will be in supine position during scanning. The total scanning procedure will take about 1 h.

First, the carotid bifurcation will be identified by means of MR angiography without contrast agent enhancement. Subsequently, transverse images will be obtained around the carotid bifurcation, so that the complete plaque will be imaged for all patients. A multi-sequence MRI protocol will be used, including a dark blood T1 and a bright blood sequence to assess the juxtaluminal calcifications, a hyper T1 weighted sequence for intra-plaque hemorrhage, and a post-contrast dark blood T1 weighted sequence to assess the lipid-rich necrotic core and fibrous cap status. Concomitantly with the MRI, a static PET scan will be performed. The total PET/MRI examination time will take approximately 1 h.

Images derived from the PET/MRI will be used to determine the uptake of Na[^{18}F]F, which is well known to sensitively reflect the degree of vascular calcification. Secondly, the MRI images will serve for evaluation of the carotid artery morphology. For this purpose, a contrast agent (*i.e.*, Gadobutrol) is injected (dose 0.1 mmol/kg of body weight). This MRI contrast agent will be injected according to the standard medical practice of the Maastricht University Medical Center as described within the respective ODIN protocol.

5.2.1. PET Image Evaluation

A certified nuclear medicine physician will evaluate all the PET images, which are corrected for attenuation based on the MRI data, unaware of all clinical information, outcome of the extensive MRI analysis. A dedicated fusion software (Syngovia, Siemens) will be used to analyze the PET images. Mean and maximum standard uptake values (*i.e.*, SUVs) will be normalized for blood tracer activity by dividing them by the mean standard uptake value of blood as measured in the internal jugular vein, the superior vena cava, or the right atrium depending on the vessel wall of interest.

5.2.2. MRI Evaluation

The MRI reader will be trained using an independent training set. This training set is developed to be able to identify all different plaque characteristics, which are scored during this study. The reader will have to independently score images in this independent training set that has been previously scored by a highly experienced reader, to determine the inter-observer agreement. If the inter-observer agreement is not good or not very good, then the reader will be further trained until he performs excellent reading of the training set (*i.e.*, good or very good inter-observer agreement with the highly experienced reader). The MRI reader, blinded to the results from the other modalities and clinical data, will independently score carotid plaque characteristics on the MR Images (vessel wall and lumen area, size of lipid-rich necrotic core, and size of calcifications, fibrous cap status, and size of intra-plaque hemorrhage). All data will be entered in a common database and analyzed by the investigator, supervised by a statistician.

5.3. CAC Scan

Non-contrast enhanced CT (Somatom FORCE, Siemens Healthcare), which will determine the CAC score, will be obtained at baseline and at the end of the study visits. The scans will be made using standard procedure.

The patient will be in supine position with his/her arms raised above his/her head during scanning. In addition, he/she is required to hold his/her breath for several seconds. The total procedure will take about 2–3 min. The procedure described above is the standard scanning-method in this hospital. The CAC score will be determined by performing a non-contrast enhanced high pitch scan.

All images will be assessed in consensus between an experienced radiologist and cardiologist. In case of disagreement, consensus will be reached by reviewing findings jointly.

As with the PET and MRI images, all CT images will also be examined by dedicated radiologists for incidental findings, which then will be reported to the general practitioner of the patients. Patients who do not want to be informed about additional findings are not able to participate in this study.

5.4. US Examination

The US examination is performed with the Art-Lab system (Esaote/Pie Medical, Maastricht, The Netherlands). With the subject lying supine, both common carotid arteries are identified on a longitudinal US image. On both walls of the common carotid

arteries, a double line pattern can be observed, consisting of the edges of the lumen-intima-transition and media-adventitia-transition. On the far wall of the common carotid artery, the intima-media thickness is measured as the distance between these two lines in micrometers.

Additionally, the following parameters are measured:

- gray-scale median of the intima-media thickness;
- gray-scale median of the plaque;
- adventitia-adventitia diameter;
- intima-intima diameter;
- plaque echolucency.

The total duration of this investigation is approximately 15 min.

5.5. Laboratory Assessments

At baseline and at the end of the study visits, blood-samples (after an overnight fast) will be obtained for the measurement of several different cardiovascular parameters and markers of calcification and vitamin K status. In addition, 7 mL will be stored for future research. In total, almost 25 mL of blood will be obtained per study-visit for blood analysis. Therefore, almost 50 mL per subject for the entire project.

Blood samples will be processed by the Biobank Maastricht within 1 h and stored at -80 °C until analysis. We will investigate whether an association between biomarkers and calcification exists in an experimental setting. Therefore, we do not intend to inform the subjects of the blood results.

The routine assessments will be:

- total cholesterol;
- LDL-cholesterol;
- HDL-cholesterol;
- triglycerides;
- creatinine;
- glucose;
- albumin;
- parathyroid hormone;
- calcium;
- phosphate;
- coagulation function (*e.g.*, PT, INR).

Specific laboratory assessments will consist in measuring the dp-ucMGP blood level.

6. Randomization, Blinding, and Treatment Allocation

A custom-made software with minimization as a randomization method (*i.e.*, operated by the researcher) will randomize consecutive patients in the two arms, using the carotid stenosis as a stratification factor. The software will stratify the subjects according to the initial carotid stenosis into one of the following groups: stenosis 25—50 % or stenosis > 50 %. This software will assign subjects with a specific randomization number. This randomization number will be used by NattoPharma (Oslo, Norway) for coding and labelling of the capsule bottles. The list with all the randomization number will be stored in a secure location and will not be accessible for the investigators during this study.

The study code will be de-blinded if a serious adverse event occurs in an individual subject.

7. Investigational Product

Subjects in the intervention-group will receive a daily dose of 400 µg MK-7 and 80 µg vitamin D3. Each intervention capsule contains Cholecalciferol (per capsule: 1.6 mg of 1,000,000 UI/g; 1 UI of vitamin D = 0.025 µg) and MenaQ7 K2 oil (per capsule: 133.33 mg of 1500 ppm vitamin K).

MenaQ7 K2 oil is a synthetic MK-7 oil produced by NattoPharma (Oslo, Norway). Euro-Pharma Alliance Sp. zo.o. (Rzeplin, Poland) uses this oil to manufacture the capsules, which are later marketed by TG Montgomery AS (Oslo, Norway). TG Montgomery AS also distributes them as a food supplement on the Norwegian over-the-counter market. MenaQ7 is Generally Recognized as Safe (*i.e.*, GRAS) by the U.S. Food and Drug Administration (*i.e.*, FDA).

Both MK-7 and vitamin D3 are registered as food-supplements. MK-7 is well tolerated and does not cause a state of hypercoagulability [32]. There are no reported negative side effects associated with the use of MK-7 or vitamin D3, at the concentrations used in this study.

Subjects in the placebo-group will receive a capsule that is identical to the MK7+D3 one, but that does not contain any active substances. In all other aspects (*e.g.*, shape, taste, weight, additives), this capsule is similar to the MK7+D3 one. The shell of both type of capsules is the same and compared to the MK-7+D3 ones, the placebos only contain bulking agent (the same one, *i.e.*, linseed oil) in a higher amount, so that both capsules

have the same weight. There are no reported negative side effects with the use of this placebo.

Both capsules are provided by TG Montgomery as a complete end-product ready to use and packaged separately for each participant in bottles. They are stored according to the manufacturer recommendation, which has already tested the shelf life and recommended a maximum storage time. This information will also be given to the subjects and they may request at any time a bottle replacement, in case of improper storage or passing the recommended maximum storage time.

8. Discussion

Both Phylloquinone (*i.e.*, vitamin K1) and Menaquinones (*i.e.*, vitamin K2) consist of a naphthoquinone-ring structure and an aliphatic sidechain [33]. The bioactive part of vitamin K is the naphthoquinone-ring structure [33]. MK-4 has already been proposed for the treatment of osteoporosis in Japan [34]; however, the same supplementation failed to show positive effects on coronary artery calcification and on vascular stiffness [35]. The selection of MK-7 over other types of vitamin K was done based on its already proven positive effects on arterial stiffness and on the risk of coronary heart disease [36,37].

The INTRICATE trial is a proof-of-concept study, in which the effects of MK-7 and vitamin D3 on vascular calcification will be assessed via Na[^{18}F]F PET. In a randomized double-blind placebo-controlled trial of 340 adults, vitamin D3 alone showed a reduction in pulse wave velocity, an indirect marked of arterial stiffness [38].

However, there are also other vitamins (*i.e.*, B12, C, and E) being studied in the context of vascular calcification, which showed promising results [39]. In another randomized controlled trial, co-administration of intravenous vitamin B12 and oral folate in hemodialysis patients showed improved effects on arterial stiffness compared to folate single treatment [40]. On the other hand, vitamin A failed in several clinical trials to show a protection against cardiovascular diseases [39,41].

There are many other intervention treatments which may be assessed with Na[^{18}F]F PET. Taking into consideration the burden of the subjects, who will be included in the INTRICATE trial, a safe and cost-effective treatment was used to show the treatment monitorization potential of this imaging technique in cardiovascular diseases [8].

9. Summary

The INTRICATE study is a proof-of-concept trial that will provide us with information on micro-calcification development in the context of atherosclerosis in the carotid arteries and the potential effect of supplementation with vitamin K (*i.e.*, MK-7) and vitamin D3. This trial bears the potential to open novel avenues for future large scale randomized controlled trials to intervene in the plaque development and micro-calcification progression.

Supplementary Materials: The following are available online at www.mdpi.com/xxx/s1, Text S1: Informed consent.

Author Contributions: Conceptualization, A.F., M.E.K., W.M., L.J.S., J.B., and F.M.M.; funding acquisition, M.E.K., L.J.S., J.B., and F.M.M.; methodology, M.E.K. and W.M.; supervision, J.B. and F.M.M.; visualization, A.F., M.E.K., W.M., L.J.S., J.B., and F.M.M.; writing—original draft, A.F.; writing—review and editing, M.E.K., W.M., L.J.S., J.B., and F.M.M. All authors have read and agreed to the published version of the manuscript.

Funding: This research is funded by the European Union's Horizon 2020 research and innovation program under the Marie Skłodowska Curie, grant number 722609.

Institutional Review Board Statement: The study is conducted according to the guidelines of the Declaration of Helsinki and approved by the accredited local Medical Ethics Committee of the Academic Hospital Maastricht and University of Maastricht in the Netherlands (*i.e.*, METC azM/UM) (file number NL69450.068.19/METC300103, approved on 18.12.2019).

Informed Consent Statement: Informed consent is obtained from all subjects involved in the study.

Data Availability Statement: Data sharing is not applicable. No new data were created or analyzed in this study.

Conflicts of Interest: Leon J. Schurgers received institutional grants from Bayer, Boehringer Ingelheim, NattoPharma, and IDS. Felix M. Mottaghy is on the advisory board of Advanced Accelerator Applications GmbH and received institutional grants from GE Healthcare, Siemens, and Nano-Mab. All other authors declare no conflict of interest. The funders had no role in the design of the study; in the collection, analyses, or interpretation of data; in the writing of the manuscript, or in the decision to publish the results.

References

1. Johnson, R.C.; Leopold, J.A.; Loscalzo, J. Vascular Calcification. *Circ. Res.* **2006**, *99*, 1044–1059.

2. Vattikuti, R.; Towler, D.A. Osteogenic regulation of vascular calcification: An early perspective. *Am. J. Physiol. Metab.* **2004**, *286*, E686–E696.

3. Hasegawa, T. Ultrastructure and biological function of matrix vesicles in bone mineralization. *Histochem. Cell Biol.* **2018**, *149*, 289–304.

4. Boulos, N.M.; Gardin, J.M.; Malik, S.; Postley, J.; Wong, N.D. Carotid Plaque Characterization, Stenosis, and Intima-Media Thickness According to Age and Gender in a Large Registry Cohort. *Am. J. Cardiol.* **2016**, *117*, 1185–1191.

5. Saba, L.; Yuan, C.; Hatsukami, T.S.; Balu, N.; Qiao, Y.; DeMarco, J.K.; Saam, T.; Moody, A.R.; Li, D.; Matouk, C.C.; et al. Carotid Artery Wall Imaging: Perspective and Guidelines from the ASNR Vessel Wall Imaging Study Group and Expert Consensus Recommendations of the American Society of Neuroradiology. *Am. J. Neuroradiol.* **2018**, *39*, E9–E31.

6. Bucerius, J.; Dijkgraaf, I.; Mottaghy, F.M.; Schurgers, L.J. Target identification for the diagnosis and intervention of vulnerable atherosclerotic plaques beyond 18F-fluorodeoxyglucose positron emission tomography imaging: Promising tracers on the horizon. *Eur. J. Nucl. Med. Mol. Imaging* **2019**, *46*, 251–265.

7. Kassem, M.; Florea, A.; Mottaghy, F.M.; van Oostenbrugge, R.; Kooi, M.E. Magnetic resonance imaging of carotid plaques: Current status and clinical perspectives. *Ann. Transl. Med.* **2020**, *8*, 1266–1266.

8. Florea, A.; Morgenroth, A.; Bucerius, J.; Schurgers, L.J.; Mottaghy, F.M. Locking and loading the bullet against micro-calcification. *Eur. J. Prev. Cardiol.* **2020**, doi:10.1177/2047487320911138.

9. Dweck, M.R.; Aikawa, E.; Newby, D.E.; Tarkin, J.M.; Rudd, J.H.F.; Narula, J.; Fayad, Z.A. Noninvasive Molecular Imaging of Disease Activity in Atherosclerosis. *Circ. Res.* **2016**, *119*, 330–340.

10. Price, P.A.; Urist, M.R.; Otawara, Y. Matrix Gla protein, a new γ-carboxyglutamic acid-containing protein which is associated with the organic matrix of bone. *Biochem. Biophys. Res. Commun.* **1983**, *117*, 765–771.

11. Luo, G.; Ducy, P.; McKee, M.D.; Pinero, G.J.; Loyer, E.; Behringer, R.R.; Karsenty, G. Spontaneous calcification of arteries and cartilage in mice lacking matrix GLA protein. *Nature* **1997**, *386*, 78–81.

12. Schurgers, L.J.; Uitto, J.; Reutelingsperger, C.P. Vitamin K-dependent carboxylation of matrix Gla-protein: A crucial switch to control ectopic mineralization. *Trends Mol. Med.* **2013**, *19*, 217–226.

13. Price, P.A.; Otsuka, A.A.; Poser, J.W.; Kristaponis, J.; Raman, N. Characterization of a gamma-carboxyglutamic acid-containing protein from bone. *Proc. Natl. Acad. Sci. USA* **1976**, *73*, 1447–1451.

14. Cranenburg, E.C.M.; Vermeer, C.; Koos, R.; Boumans, M.L.; Hackeng, T.M.; Bouwman, F.G.; Kwaijtaal, M.; Brandenburg, V.M.; Ketteler, M.; Schurgers, L.J. The circulating inactive form of matrix Gla protein (ucMGP) as a biomarker for cardiovascular calcification. *J. Vasc. Res.* **2008**, *45*, 427–436.

15. Ueland, T.; Gullestad, L.; Dahl, C.P.; Aukrust, P.; Aakhus, S.; Solberg, O.G.; Vermeer, C.; Schurgers, L.J. Undercarboxylated matrix Gla protein is associated with indices of heart failure and mortality in symptomatic aortic stenosis. *J. Intern. Med.* **2010**, *268*, 483–492.

16. Parker, B.D.; Schurgers, L.J.; Brandenburg, V.M.; Christenson, R.H.; Vermeer, C.; Ketteler, M.; Shlipak, M.G.; Whooley, M.A.; Ix, J.H. The associations of fibroblast growth factor 23 and uncarboxylated matrix Gla protein with mortality in coronary artery disease: The heart and soul study. *Ann. Intern. Med.* **2010**, *152*, 640–648.

17. Dalmeijer, G.W.; van der Schouw, Y.T.; Magdeleyns, E.J.; Vermeer, C.; Verschuren, W.M.M.; Boer, J.M.A.; Beulens, J.W.J. Matrix Gla Protein Species and Risk of Cardiovascular Events in Type 2 Diabetic Patients. *Diabetes Care* **2013**, *36*, 3766–3771.

18. Dalmeijer, G.W.; van der Schouw, Y.T.; Vermeer, C.; Magdeleyns, E.J.; Schurgers, L.J.; Beulens, J.W.J. Circulating matrix Gla protein is associated with coronary artery calcification and vitamin K status in healthy women. *J. Nutr. Biochem.* **2013**, *24*, 624–628.

19. Liabeuf, S.; Olivier, B.; Vemeer, C.; Theuwissen, E.; Magdeleyns, E.; Aubert, C.; Brazier, M.; Mentaverri, R.; Hartemann, A.; Massy, Z.A. Vascular calcification in patients with type 2 diabetes: The involvement of matrix Gla protein. *Cardiovasc. Diabetol.* **2014**, *13*, 85.

20. Delanaye, P.; Krzesinski, J.-M.; Warling, X.; Moonen, M.; Smelten, N.; Médart, L.; Pottel, H.; Cavalier, E. Dephosphorylated-uncarboxylated Matrix Gla protein concentration is predictive of vitamin K status and is correlated with vascular calcification in a cohort of hemodialysis patients. *BMC Nephrol.* **2014**, *15*, 145.

21. Venardos, N.; Bennett, D.; Weyant, M.J.; Reece, T.B.; Meng, X.; Fullerton, D.A. Matrix Gla protein regulates calcification of the aortic valve. *J. Surg. Res.* **2015**, *199*, 1–6.

22. Wei, F.-F.; Drummen, N.E.A.; Schutte, A.E.; Thijs, L.; Jacobs, L.; Petit, T.; Yang, W.-Y.; Smith, W.; Zhang, Z.-Y.; Gu, Y.-M.; et al. Vitamin K Dependent Protection of Renal Function in Multi-ethnic Population Studies. *EBioMedicine* **2016**, *4*, 162–169.

23. Riphagen, I.; Keyzer, C.; Drummen, N.; de Borst, M.; Beulens, J.; Gansevoort, R.; Geleijnse, J.; Muskiet, F.; Navis, G.; Visser, S.; et al. Prevalence and Effects of Functional Vitamin K Insufficiency: The PREVEND Study. *Nutrients* **2017**, *9*, 1334.

24. Fu, X.; Wang, X.-D.; Mernitz, H.; Wallin, R.; Shea, M.K.; Booth, S.L. 9-Cis Retinoic Acid Reduces 1α,25-Dihydroxycholecalciferol-Induced Renal Calcification by Altering Vitamin K-Dependent γ-Carboxylation of Matrix γ-Carboxyglutamic Acid Protein in A/J Male Mice. *J. Nutr.* **2008**, *138*, 2337–2341.

25. Fraser, J.D.; Price, P.A. Induction of matrix gla protein synthesis during prolonged 1,25-Dihydroxyvitamin D3 treatment of osteosarcoma cells. *Calcif. Tissue Int.* **1990**, *46*, 270–279.

26. Miyake, N.; Hoshi, K.; Sano, Y.; Kikuchi, K.; Tadano, K.; Koshihara, Y. 1,25-Dihydroxyvitamin D 3 Promotes Vitamin K 2 Metabolism in Human Osteoblasts. *Osteoporos. Int.* **2001**, *12*, 680–687.

27. Seyama, Y.; Horiuch, M.; Hayashi, M.; Kanke, Y. Effect of vitamin K2 on experimental calcinosis induced by vitamin D2 in rat soft tissue. *Int. J. Vitam. Nutr. Res.* **1996**, *66*, 36–38.

28. Scragg, R.; Stewart, A.W.; Waayer, D.; Lawes, C.M.M.; Toop, L.; Sluyter, J.; Murphy, J.; Khaw, K.-T.; Camargo, C.A. Effect of Monthly High-Dose Vitamin D Supplementation on Cardiovascular Disease in the Vitamin D Assessment Study. *JAMA Cardiol.* **2017**, *2*, 608.

29. Manson, J.E.; Cook, N.R.; Lee, I.-M.; Christen, W.; Bassuk, S.S.; Mora, S.; Gibson, H.; Gordon, D.; Copeland, T.; D'Agostino, D.; et al. Vitamin D Supplements and Prevention of Cancer and Cardiovascular Disease. *N. Engl. J. Med.* **2019**, *380*, 33–44.

30. Arbour, N.C.; Darwish, H.M.; DeLuca, H.F. Transcriptional control of the osteocalcin gene by 1,25-dihydroxyvitamin D-2 and its 24-epimer in rat osteosarcoma cells. *Biochim. Biophys. Acta Gene Struct. Expr.* **1995**, *1263*, 147–153.

31. van Ballegooijen, A.J.; Beulens, J.W.J.; Kieneker, L.M.; de Borst, M.H.; Gansevoort, R.T.; Kema, I.P.; Schurgers, L.J.; Vervloet, M.G.; Bakker, S.J.L. Combined low vitamin D and K status amplifies mortality risk: A prospective study. *Eur. J. Nutr.* **2020**, doi:10.1007/s00394-020-02352-8.

32. Asakura, H.; Myou, S.; Ontachi, Y.; Kato, M.; Saito, M.; Yamazaki, M.; Nakao, S.; Mizutani, T.; Morishita, E. Vitamin K Administration to Elderly Patients with Osteoporosis Induces No Hemostatic Activation, Even in Those with Suspected Vitamin K Deficiency. *Osteoporos. Int.* **2001**, *12*, 996–1000.

33. Halder, M.; Petsophonsakul, P.; Akbulut, A.C.; Pavlic, A.; Bohan, F.; Anderson, E.; Maresz, K.; Kramann, R.; Schurgers, L. Vitamin K: Double bonds beyond coagulation insights into differences between vitamin K1 and K2 in health and disease. *Int. J. Mol. Sci.* **2019**, *20*, 896.

34. Asakura, H.; Myou, S.; Ontachi, Y.; Mizutani, T.; Kato, M.; Saito, M.; Morishita, E.; Yamazaki, M.; Nakao, S. Vitamin K administration to elderly patients with osteoporosis induces no hemostatic activation, even in those with suspected vitamin K deficiency. *Osteoporos. Int.* **2001**, *12*, 996–1000.

35. Ikari, Y.; Torii, S.; Shioi, A.; Okano, T. Impact of menaquinone-4 supplementation on coronary artery calcification and arterial stiffness: An open label single arm study. *Nutr. J.* **2016**, *15*, 1–6.

36. Mansour, A.G.; Hariri, E.; Daaboul, Y.; Korjian, S.; El Alam, A.; Protogerou, A.D.; Kilany, H.; Karam, A.; Stephan, A.; Bahous, S.A. Vitamin K2 supplementation and arterial stiffness among renal transplant recipients—a single-arm, single-center clinical trial. *J. Am. Soc. Hypertens.* **2017**, *11*, 589–597.

37. Gast, G.C.M.; de Roos, N.M.; Sluijs, I.; Bots, M.L.; Beulens, J.W.J.; Geleijnse, J.M.; Witteman, J.C.; Grobbee, D.E.; Peeters, P.H.M.; van der Schouw, Y.T. A high

menaquinone intake reduces the incidence of coronary heart disease. *Nutr. Metab. Cardiovasc. Dis.* **2009**, *19*, 504–510.

38. Forouhi, N.G.; Menon, R.K.; Sharp, S.J.; Mannan, N.; Timms, P.M.; Martineau, A.R.; Rickard, A.P.; Boucher, B.J.; Chowdhury, T.A.; Griffiths, C.J.; et al. Effects of vitamin D2 or D3 supplementation on glycaemic control and cardiometabolic risk among people at risk of type 2 diabetes: Results of a randomized double-blind placebo-controlled trial. *Diabetes, Obes. Metab.* **2016**, *18*, 392–400.

39. Mozos, I.; Stoian, D.; Luca, C.T. Crosstalk between Vitamins A, B12, D, K, C, and e Status and Arterial Stiffness. *Dis. Markers* **2017**, *2017*, doi:10.1155/2017/8784971.

40. Koyama, K.; Ito, A.; Yamamoto, J.; Nishio, T.; Kajikuri, J.; Dohi, Y.; Ohte, N.; Sano, A.; Nakamura, H.; Kumagai, H.; et al. Randomized Controlled Trial of the Effect of Short-term Coadministration of Methylcobalamin and Folate on Serum ADMA Concentration in Patients Receiving Long-term Hemodialysis. *Am. J. Kidney Dis.* **2010**, *55*, 1069–1078.

41. Omenn, G.S.; Goodman, G.E.; Thornquist, M.D.; Balmes, J.; Cullen, M.R.; Glass, A.; Keogh, J.P.; Meyskens, F.L.; Valanis, B.; Williams, J.H.; et al. Effects of a Combination of Beta Carotene and Vitamin A on Lung Cancer and Cardiovascular Disease. *N. Engl. J. Med.* **1996**, *334*, 1150–1155.

An introduction into Chapter V for chemokines, cytokines, and CXCR-4

Cytokines are a broad and loose category of small proteins important in cell signalling. Among the ones implicated in leukocyte recruitment during inflammation, the family of chemotactic peptides, known as chemokines, are the most significant (Edgington, 1993). Chemokines are 8-12 kDa proteins that mediate cell chemotaxis and arrest by binding to their respective receptors on the cell surface (Blanchet et al., 2012). Chemokine synthesis has been long known to induce an inflammatory response against immunological stimuli, and their presence is detected locally in many diseases like atherosclerosis and stroke (Gupta et al., 1999).

Chemokines are defined by their primary amino acid sequence and the arrangement of specific structurally important cysteine residues within the mature protein. These form disulphide bonds that maintain the structure of the chemokine monomer, which consists of a central three stranded β-sheet, an overlying C-terminal α-helix, and a short unstructured N-terminus that plays a critical role in receptor activation (Miller & Mayo, 2017). Variation in the precise configuration of the two cysteines closest to the N-terminus allows chemokines to be split into four sub-families: CC, CXC, CX_3C, and XC. In CC chemokines, these cysteines are directly juxtaposed, while CXC chemokines have a single variable amino acid between them. Although chemokines were originally named according to specific functions, a systematic nomenclature was introduced in 2000 that includes a subfamily designation (*i.e.,* CC, CXC, CX_3C, or XC), followed by the letter L (denoting 'ligand'), and then a number according to when the gene was first isolated (Hughes & Nibbs, 2018).

Most CXC chemokines, like interleukin-8, target neutrophils and appear to be important during acute inflammation. On the other hand, CC chemokines like monocyte chemoattractant protein-1 (*i.e.*, MCP-1 or CCL-2), macrophage inflammatory protein-1α (*i.e.*, MIP-1α or CCL-3), and RANTES (*i.e.*,CCL-5) mainly target monocytes and T cells (Gupta et al., 1999).

The chemokine receptor CXCR-4 and its ligand CXCL-12 are attractive therapeutic targets in the treatment of cancer, as they support migration, proliferation, and survival of cancer cells, but also CXCR-4 has become intensively studied in different autoimmune and inflammatory diseases (Döring et al., 2014; Teicher & Fricker, 2010). In pioneering studies, the CXCR-4/CXCL-12 axis has been found to be essential in various autoimmune diseases, such as rheumatoid arthritis (Firestein, 2003), or systemic lupus erythematosus (Wang et al., 2010). CXCR-4 also accumulates progressively during atherosclerotic

plaque development by modulating neutrophil migration, as well as specifically co-localizing with macrophage infiltration (Hyafil et al., 2017).

References

Blanchet X., Langer M., Weber C., Koenen R., von Hundelshausen P.: Touch of chemokines. Front Immunol (2012) 3:

Döring Y., Pawig L., Weber C., Noels H.: The CXCL12/CXCR4 chemokine ligand/receptor axis in cardiovascular disease. Front Physiol (2014) 5:

Edgington S. M.: Chemokines in Cardiovascular Disease. Bio/Technology 1993 11:6 (1993) 11:676–681

Firestein G. S.: Evolving concepts of rheumatoid arthritis. Nature 2003 423:6937 (2003) 423:356–361

Gupta S. K., Pillarisetti K., Lysko P. G.: Modulation of CXCR4 expression and SDF-1alpha functional activity during differentiation of human monocytes and macrophages. J Leukoc Biol (1999) 66:135–143

Hughes C. E., Nibbs R. J. B.: A guide to chemokines and their receptors. The FEBS Journal (2018) 285:2944–2971

Hyafil F., Pelisek J., Laitinen I., Schottelius M., Mohring M., Döring Y., … Schwaiger M.: Imaging the Cytokine Receptor CXCR4 in Atherosclerotic Plaques with the Radiotracer 68 Ga-Pentixafor for PET. Journal of Nuclear Medicine (2017) 58:499–506

Miller M. C., Mayo K. H.: Chemokines from a Structural Perspective. Int J Mol Sci (2017) 18:

Teicher B. A., Fricker S. P.: CXCL12 (SDF-1)/CXCR4 pathway in cancer. Clinical Cancer Research (2010) 16:2927–2931

Wang A., Guilpain P., Chong B. F., Chouzenoux S., Guillevin L., Du Y., … Mohan C.: Dysregulated expression of CXCR4/CXCL12 in subsets of patients with systemic lupus erythematosus. Arthritis & Rheumatism (2010) 62:3436–3446

Chapter V: [^{68}Ga]Ga-Pentixafor preclinical study

[^{68}Ga]Ga-Pentixafor uptake increases during atherosclerotic plaque development

Alexandru Florea, Sabri Sahnoun, Pardes Habib, Agnieszka Morgenroth, Andreas Vogg, Oliver H. Winz, Jan Bucerius, Leon J. Schurgers, and Felix M. Mottaghy

Submitted

[^{68}Ga]Ga-Pentixafor uptake increases during atherosclerotic plaque development

Alexandru Florea[1,2,3], Sabri Sahnoun[1], Pardes Habib[4,5], Agnieszka Morgenroth[1], Andreas Vogg[1], Oliver H. Winz[1], Jan Bucerius[2,3,6], Leon J. Schurgers[3,7,8], and Felix M. Mottaghy[1,2,3,*]

1. *Department of Nuclear Medicine, University Hospital RWTH Aachen, Aachen, Germany*
2. *Department of Radiology and Nuclear Medicine, Maastricht University Medical Centre, Maastricht, Netherlands*
3. *School for Cardiovascular Diseases (CARIM), Maastricht University Medical Centre, Maastricht, the Netherlands*
4. *Department of Neurology, University Hospital RWTH Aachen, Aachen, Germany*
5. *Department of Neurosurgery, Stanford University, Stanford, USA*
6. *Department of Nuclear Medicine, University of Göttingen, Göttingen, Germany*
7. *Department of Biochemistry, Maastricht University Medical Centre, Maastricht, Netherlands*
8. *Institute of Experimental Medicine and Systems Biology, RWTH Aachen University, Aachen, Germany*

* *Correspondence: fmottaghy@ukaachen.de; Tel.: +49-241-80-88741*

Abstract

Aims

Inflammation is an established hallmark of atherosclerotic plaque development. Given the high affinity of [^{68}Ga]Ga-Pentixafor for the inflammatory marker CXCR-4, the aim of this study is to assess the ability of [^{68}Ga]Ga-Pentixafor to determine different stages of inflammation during atherosclerotic plaque development in an already published atherosclerotic mouse model.

Methods and Results

ApoE$^{-/-}$ mice were placed on a Western-type diet for 12-weeks and then split into two groups. The early-stage atherosclerosis group received a chow diet for an additional 12-weeks, while the advanced atherosclerosis group continued the Western-type diet. Control wild type mice were fed a chow diet for 24-weeks. All mice were scanned with [^{68}Ga]Ga-Pentixafor using a small animal PET/CT. There was no uptake visible in the control group. The early and advanced stage groups presented an uptake proportional to the duration of the Western-type diet. The highest difference in the uptake was detected in the aortic arch, suggesting a maintained inflammatory response in this region. In the left ventricle and aortic root, only the advanced stage showed a difference to the control, suggesting that these regions are less prone to develop inflamed plaques during the early stage.

Conclusion

In this study, [^{68}Ga]Ga-Pentixafor PET showed potential to monitor the progression of atherosclerotic plaques from early to advanced stages.

Keywords

Inflammation · Cardiovascular disease · Atherosclerosis · CXCR-4 · [^{68}Ga]Ga-Pentixafor

Introduction

Inflammation is a well-known hallmark of atherosclerosis (Ross, 1999), which may lead to unstable plaque formation (Libby et al., 2011; Zhu et al., 2018). Formation of an atherosclerotic lesion is initiated by endothelial dysfunction, followed by chronic accumulation of lipids, triggering a chemotaxis-orchestrated migration of atherogenic, pro-inflammatory immune cells to the lesion (Gargiulo et al., 2016; Stary et al., 1995).

Leukocyte recruitment to the injured endothelium and subsequent plaque formation is an important step throughout the progression of atherosclerosis, which is mainly regulated by chemokines (Zernecke & Weber, 2010). Within this process the CXC receptor 4 (CXCR-4) seems to play an important role for the proinflammatory progression in atherosclerotic plaques (Koenen & Weber, 2011). CXCR-4 is a transmembrane G-protein-coupled receptor that plays a pivotal role in recruitment of immune and progenitor cells to injured and inflamed tissue *via* interaction with its ligand CXCL-12 (Derlin et al., 2018). In atherosclerosis, the CXCL-12/CXCR-4 axis exerts atherogenic, prothrombotic, and plaque-destabilizing effects (Swirski & Nahrendorf, 2013). CXCR-4 is highly expressed by monocytes, differentiated macrophages and lymphocytes migrating into arterial lesions (Gupta et al., 1999), and by platelets (von Hundelshausen & Schmitt, 2014). Furthermore, CXCR-4 is also expressed by different cell types including smooth muscle cell progenitors and endothelial progenitor cells which contribute to plaque evolution (Döring et al., 2014). Accordingly, CXCR-4 may be a useful target for non-invasive molecular imaging, to determine the degree of inflammation, likelihood of lesion progression or repair, and the effect of potential targeted therapies in injured atherosclerotic plaques (Weiberg et al., 2018).

To this end, combined PET/CT has emerged as a well-characterized imaging technique to assess plaque biology *via* mechanisms such as increased metabolism and micro-calcification (Derlin et al., 2011; Florea, Morgenroth, et al., 2021; Kwiecinski et al., 2020). A couple of years ago, a promising CXCR-4 specific ligand (*i.e.*, Pentixafor), coupled with the radioisotope Gallium-68 has been introduced for clinical molecular imaging of CXCR-4 expression (Demmer et al., 2011). [^{68}Ga]Ga-Pentixafor, with its high affinity for CXCR-4 (Gourni et al., 2011), is able to identify a regional inflammatory response in mice (Thackeray et al., 2015) and in patients (Reiter et al., 2018) post-myocardial infarction. Moreover, a first clinical study supports its use to determine vessel wall CXCR-4 expression (Weiberg et al., 2018). Indeed, this tracer was able to detect

CXCR-4 expression of CD68-positive macrophages present in atherosclerotic plaques (Hyafil et al., 2017).

In our current study, we wanted to assess the ability of [^{68}Ga]Ga-Pentixafor to monitor atherosclerotic plaque progression in an already evaluated mouse model (Florea, et al., 2021). Hence, the ability of [^{68}Ga]Ga-Pentixafor to detect changes in the inflammatory status of the plaque during an already tested feeding scheme, which develops early and advanced stage disease.

Materials and methods

Mouse strains and care

All animal experiments were approved by a German competent authority (Landesamt für Natur, Umwelt und Verbraucherschutz Nordrhein-Westfalen) for compliance with the Animal Protection Act, in conjunction with the regulation for the protection of animals used for experimental and other scientific purposes (file number 81-02.04.2018.A286). Wild type (n = 5) and ApoE$^{-/-}$ (n = 10) male mice were purchased from Charles River Laboratories Italy (*i.e.*, C57BL/6J and B6.129P2-Apoe$^{tm1Unc/J}$, respectively). Upon arrival, all mice were kept in the Institute for Laboratory Animal Science of the University Hospital RWTH Aachen, and one week prior to the scans, they were moved to the Department of Nuclear medicine of the University Hospital RWTH Aachen for acclimatization.

The animals were housed under a 12-h-light/12-h-dark cycle and were given free access to their respective diets and to water. The room temperature and relative humidity were kept between 20–25 °C and 45–65%, respectively.

Because all of mice used had a C57BL/6 background, and in combination of the 24-weeks feeding scheme, some animals developed skin lesions suggestive of ulcerative dermatitis. Hence, a Dexpanthenol ointment (Bepanthen® from Bayer Vital GmbH, Leverkusen, Germany) was applied to ease scratching; moreover, these mice had priority on the day of scanning.

Experimental groups and feeding scheme

All animals were 6 weeks of age at the start of the trial. Upon arrival, five animals per experimental group were caged to ease the feeding scheme. Each mouse was fed for a

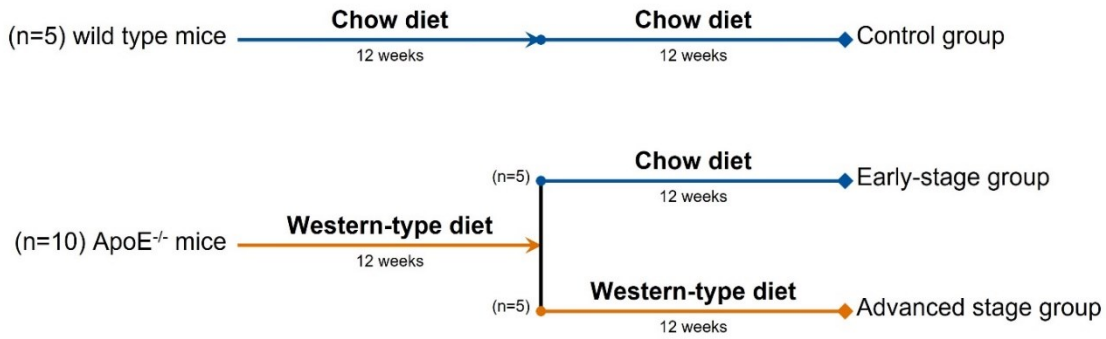

Figure 5: Feeding scheme: 10 ApoE$^{-/-}$ mice started a Western-type diet for 12 weeks, to develop early-stage plaque. At the end of the 12 weeks, 5 mice were switched to a regular chow feed (early-stage group), while the other 5 continued their Western-type diet for the additional 12 weeks (advanced stage group). For control, 5 C57BL/6 animals were kept on a regular chow diet for 24 weeks (control group).

total of 24 weeks prior to the measurements. The entire feeding scheme is illustrated in Figure 1.

At 6 weeks of age, all wild type mice (n = 5) started a regular chow diet (1324; Altromin, Lage, Germany), which was maintained for the entire length of the experiment (24 weeks).

At 6 weeks of age, ApoE$^{-/-}$ mice (n = 20) started a Western-type diet with 0.15% cholesterol and 19.5% casein (Altromin, Lage, Germany) for a minimum of 12 weeks, in order to develop early-stage plaque (Florea, et al., 2021). For the early-stage plaque group, the diet was switched to a regular chow feed (1324; Altromin, Lage, Germany), to slow the plaque development. For the advanced plaque group, the Western-type diet was continued throughout the additional 12 weeks.

Over the course of the study, one control animal developed skin lesions suggestive of ulcerative dermatitis and received a topical Dexpanthenol ointment.

[^{68}Ga]Ga-Pentixafor synthesis

One synthesis was required for every 3 animals scanned; therefore, two synthesis per scanning day were required and, in each day, to scan one experimental group.

The tracer was produced by a routine procedure, primarily used for patient care. For this purpose, a cassette synthesizer type GRP 3 V (Scintomics, Germany) with SC-01 cassettes (ABX, Germany) was used with HEPES buffer during labelling. Briefly, 10 mL of $^{68}GaCl_3$ containing 0.6 M HCl generator eluate (iThemba, South Africa) was diluted with water and trapped on a cation exchange SPE cartridge, eluted with 5 M NaCl, and added to the reactor containing 50 µl of an aqueous (0.25 mg/mL) DOTA functionalized Pentixafor derivative (Scintomics Molecular ATT, Germany) and HEPES. After a labelling reaction at 120 °C for 10 min, HEPES was removed by reversed phase SPE

extraction. The product was eluted from a C8 cartridge by 0.1 mL aqueous ethanol (80 %) followed by formulation with 0.9 mL PBS. Radiochemical yield was for all synthesis > 98 %.

The final product was then used for the intravenous injections.

[^{68}Ga]Ga-Pentixafor PET/CT measurements

All animals were imaged with a small animal PET/SPECT/CT system (*i.e.*, Triumph® II, Northridge Tri-Modality Imaging, Inc., Chatsworth, USA), however only the PET and CT modalities were used for this study.

Under 1.5–2.5% isoflurane anaesthesia in oxygen at 0.8 L/min, the lateral tail vein was injected with 50 µL of CT contrast agent (130-095-698; Viscover™) and 15 ± 2 MBq of [^{68}Ga]Ga-Pentixafor in a maximum total volume of 125 µL. After injection, the mice were placed on the scanner bed and the CT scan was initiated. The exposure settings used were as follows: 130 µA, 75 kVp, 230 ms exposure time, and 360° rotation with 720 views with an average of two frames for each view; the duration of the CT scans was ~15 min. A dynamic 45min PET scan was initiated at the end of the CT scan (*i.e.*, ~25 min post injection). The CT had an axial field of view of 91.1 mm and the PET one of 112 mm. During the scans, the isoflurane concentration was adapted to achieve a respiratory rate between 75–50 breaths per minute.

Image processing and analysis

The CT images were reconstructed using a Feldkamp filtered back projection reconstruction process to a voxel size of 0.154 × 0.154 × 0.154 mm^3 in a 592 × 592 × 560 matrix. Using vendor software, the CT values were converted into Hounsfield units (HU) using the following formula:

$$HU = 1000 \times ((\mu_t - \mu_w) \div \mu_w)$$

where μ_w is the linear attenuation coefficient of the water and μ_t is the linear attenuation coefficient of the tissue.

The PET data were reconstructed using a 3D ordered-subset expectation maximization (*i.e.*, OSEM-3D with three iterations and eight subsets) with a maximum a posteriori probability algorithm (30 iterations) into a 240 × 240 × 192 image matrix (resulting in final voxel dimensions of 0.25 × 0.25 × 0.597 mm^3). PET normalization, CT attenuation correction, and CT scatter correction were applied to all PET reconstructions.

The PET images were automatically aligned to the CT using a custom-made transformation in PMOD software package version 3.13 (PMOD Technologies LLC, Zürich, Switzerland) from a capillary phantom. The co-registered PET/CT images were further used for the PET quantification.

To calculate the blood pool background activity, a volume of interest (VOI), comprising of 10 consecutive slices, was manually placed in the thoracic region of the inferior vena cava, encompassing the contrast enhanced lumen. The 50^{th} percentile, mean activity (in kBq/cc) and average of the top 10 hottest voxels were recorded from this VOI.

An additional VOI was created for the left ventricle as follows: initially, the entire left ventricle (*i.e.*, including the free ventricular wall, the interventricular septum, and the ventricular cavity) was manually masked in a region spanning from the apex to the aortic root. Afterwards, an automatic isocontour was generated using the 50^{th} percentile of the background (*i.e.*, from the inferior vena cava VOI) as the minimal threshold.

The same technique was applied for the VOIs of the aortic root and aortic arch. The mask of the aortic root was created in the first 10 slices following the left ventricle mask and included the aortic bulb and intracardiac aorta. The mask for the aortic arch included the ascending aorta, the arch itself, the brachiocephalic trunk, the emergence of the left common carotid artery, the emergence of the left subclavian artery, and the descending aorta until the initial slice of this VOI.

Upon completion of all target VOIs, the average of the top 10 hottest voxels was recorded. All VOIs were drawn by a blinded member of our team, to exclude analysis bias.

To quantify the PET data and to correct for the blood compartment contribution, the maximum target-to-background ratio (TBRmax) was calculated using the following formula:

$$\text{TBRmax} = \text{HotAverage}(10)_{\text{target}} \div \text{Average}_{\text{background}}$$

where $\text{HotAverage}(10)_{\text{target}}$ is the mean of the top 10 hottest voxels recorded in the target VOI (*i.e.*, left ventricle, aortic root, or aortic arch) and $\text{Average}_{\text{background}}$ is the mean activity recorded in the background (*i.e.*, inferior vena cava).

Statistical analysis

All statistical analysis was performed using GraphPad Prism version 9 (GraphPad Software LLC, San Diego, CA, USA). Initially, all experimental data sets were tested for outliers using the ROUT method. To calculate the statistical differences between multiple

groups, non-parametric one-way analysis of variance (*i.e.*, Kruskal-Wallis test) tests were applied. Additionally, the standard deviation of all variables was calculated and used alongside the average in the Results section. If the differences from this test exceeded the statistical significance threshold (*i.e.*, $P < 0.05$), Dunn's correction for multiple comparisons was performed for a post hoc analysis. Statistically significant results are indicated in charts, with stars indicate a P value lower than 0.05.

All variables are presented as data dots with a line indicating the mean and error bars for the standard deviation.

Organ harvesting and validation staining protocols

At the end of the scans, the mice were sacrificed by applying an isoflurane overdose, and the heart and aortic arch were collected using a well described protocol (Mohanta et al., 2016).

The aortic root was considered as the heart region where aortic leaflets are present. The aortic arch was considered to be the aortic region between the emergence of the ascending aorta from the heart and the third intercostal space; this sample also included the brachiocephalic artery and the emergences of the left common carotid and left subclavian artery.

All organ samples were formalin-fixed, paraffin-embedded, and sectioned with a thickness of 5 µm prior to staining using standard and CXCR-4 immunostaining and Haematoxylin Eosin (HE) protocols. To be able to discriminate between the CXCR-4 positive cells and non-specific binding, a co-staining for the cell nucleus using 4′,6-diamidino-2-phenylindole (*i.e.*, DAPI) was performed.

Results

Validation stainings

Both the early stage and the advanced stage groups developed plaque, starting at the aortic root, and continuing along the aortic arch (Figure 2). On the other hand, the control mice did not develop any plaque at the investigated levels (data not shown). Additionally, within the plaque region of the two groups, CXCR-4 positive cells were identified.

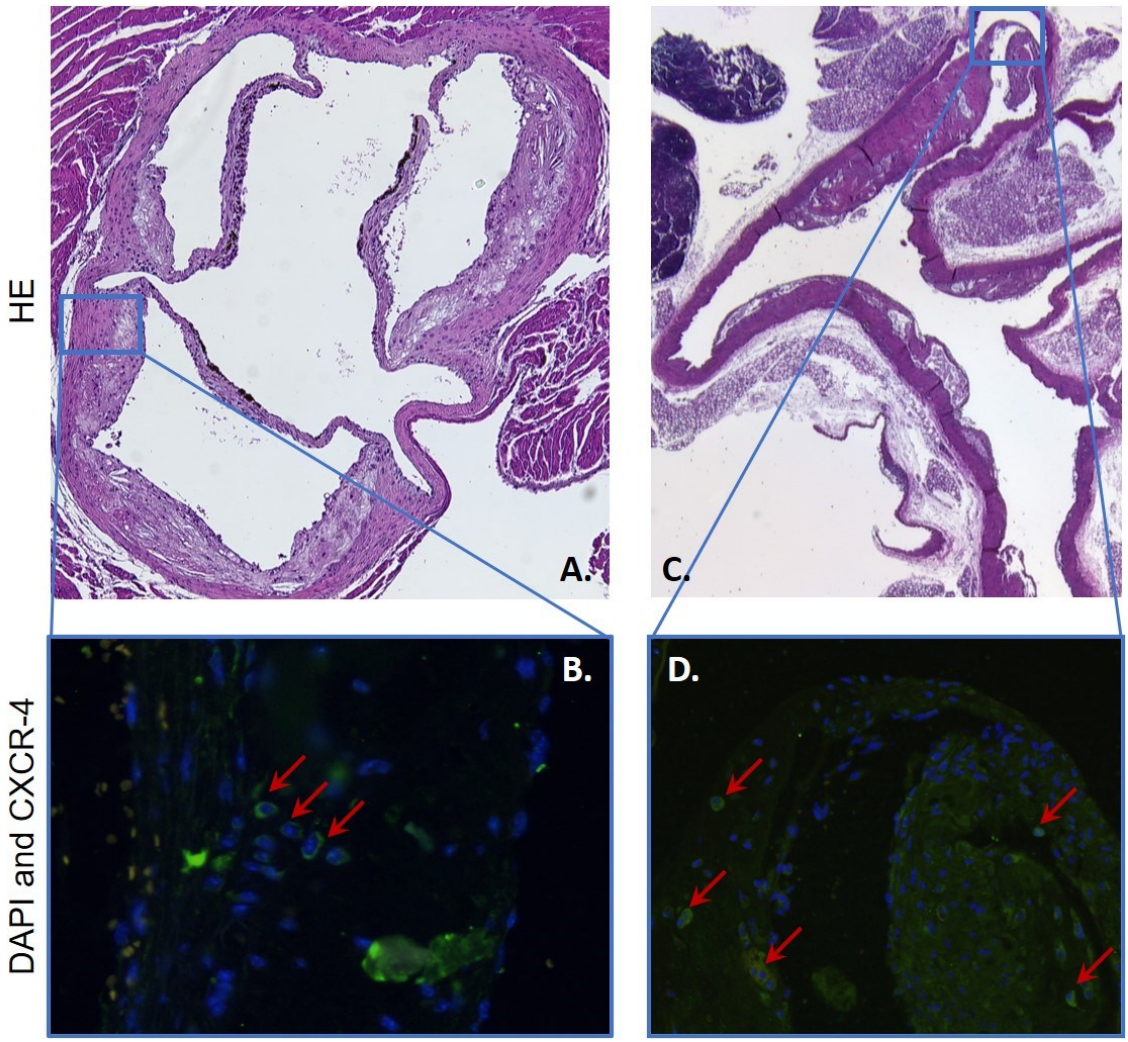

Figure 6: Validation stainings: example of an aortic root and aortic arch Haematoxylin eosin (HE) and CXCR-4 stainings from the advanced stage group. The first image row (A and C) is stained with HE, while the enlarges (B and D) represent the next paraffin slice co-immuno-stained with DAPI (blue) and CXCR-4 (green) and imaged at a higher magnification (×40). The red arrows indicate CXCR-4 positive cells present in the plaque visible on HE.

[^{68}Ga]Ga-Pentixafor PET findings

Examples of the PET/CT fusions of [^{68}Ga]Ga-Pentixafor uptake in the heart region of all experimental groups are illustrated in Figure 3. Statistical analysis of all TBRmax values in the analysed regions is presented in Figure 4. In all regions, the lowest TBRmax was found, as expected, in the control group (TBRmax in the left ventricle, aortic root, and aortic arch were 1.15±0.11, 1.11±0.05, and 1.07±0.05 respectively).

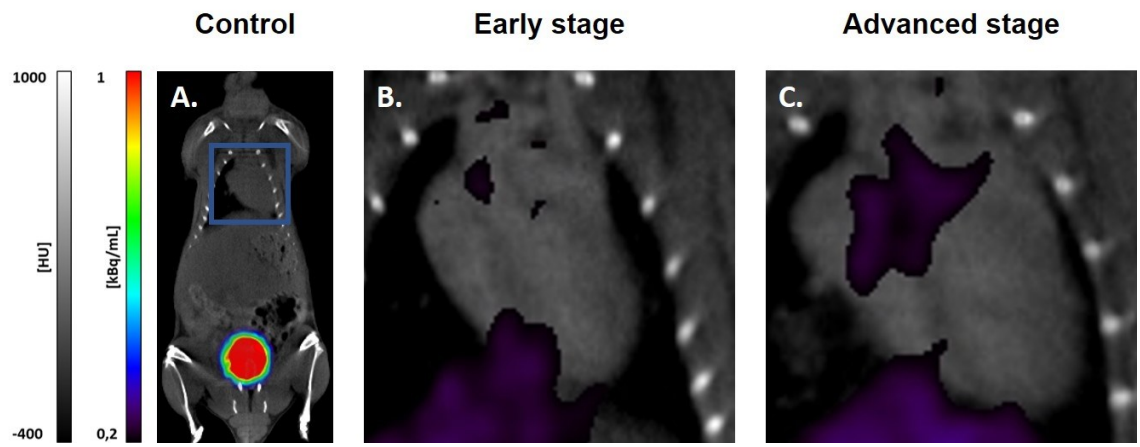

Figure 7: [^{68}Ga]Ga-Pentixafor PET/CT: examples of computed tomography (CT)/positron emission tomography (PET) fusions of [^{68}Ga]Ga-Pentixafor uptake in the heart region of all experimental groups. For the control group (A) the whole-body PET/CT image is shown to illustrate the normal biodistribution of the tracer (*i.e.*, no specific uptake, except for the renal excretion). The enlargements for the early and advanced stage groups show the specific [^{68}Ga]Ga-Pentixafor uptake in the aortic arch; additionally, for the advanced stage image, a ventricular wall uptake is visible. All CT images are scaled between -400 HU and 1000 HU, while the PET images are between 0,2 MBq/mL and 1 MBq/mL.

[^{68}Ga]Ga-Pentixafor TBRmax in all investigated regions seemed to reflect the duration of the Western-type diet (control *vs.* early stage *vs.* advanced stage). The highest difference was detected in the aortic arch, where both the early and advanced stages showed statistical significance differences compared to the control group ($P < 0.05$), suggesting a maintained inflammatory response in this region. On the other hand, in the left ventricle and aortic root, only the difference between the advanced stage and control group reached statistical significance ($P < 0.05$ and $P < 0.01$ respectively), suggesting that these regions are less prone to develop inflamed plaques during the early stage.

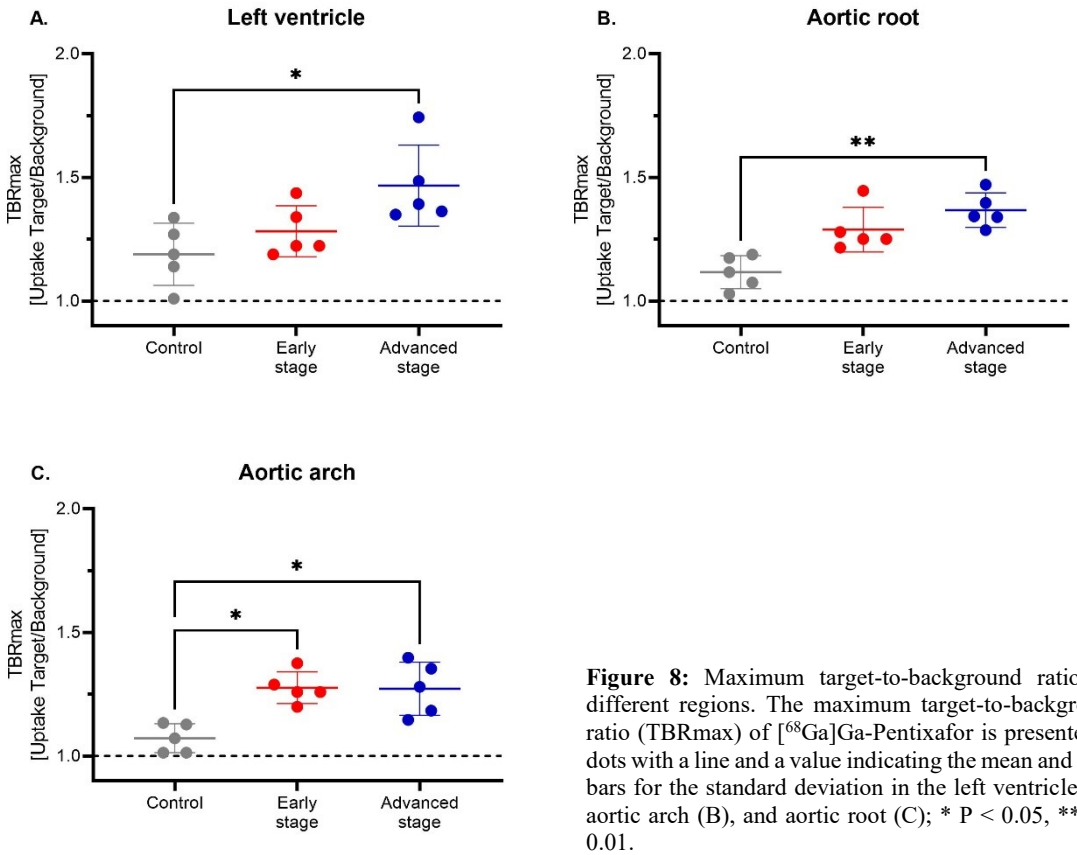

Figure 8: Maximum target-to-background ratios in different regions. The maximum target-to-background ratio (TBRmax) of [^{68}Ga]Ga-Pentixafor is presented as dots with a line and a value indicating the mean and error bars for the standard deviation in the left ventricle (A), aortic arch (B), and aortic root (C); * $P < 0.05$, ** $P < 0.01$.

Discussion

In this study, we have shown the ability of [^{68}Ga]Ga-Pentixafor to detect different stages of the atherosclerotic plaque development.

As is the case with molecular imaging of atherosclerotic mouse models, the regions of interest (*i.e.*, the plaques themselves) reach the limit of the spatial resolution of current available scanners (Florea, et al., 2021). Therefore, as in our previous studies, we semi-quantitatively determined the uptake as a target of the background ratio of the hottest voxels (*i.e.*, TBRmax).

Our data suggests that the vessel wall [^{68}Ga]Ga-Pentixafor uptake increases with the length of the period that animals are on the atherogenic diet (*i.e.*, western-type diet). The control animals showed a TBRmax close to 1.0 in all investigated regions, showing no increased uptake compared to the blood pool from the inferior vena cava, which was taken as background. On the other hand, the animals form the early-stage group showed an increased TBRmax, with a further increase in the animals from the advanced stage group, suggesting that [^{68}Ga]Ga-Pentixafor is able to monitor disease progression. Indeed, the same tracer was shown to detect elevated CXCR-4 expression post-myocardial infarction both in a murine model as well as in a small patient group (Thackeray et al., 2015).

The CXCR-4 plays a major role in atherosclerosis and arterial injury (Döring et al., 2014; Weiberg et al., 2018). Previous immunohistochemical analyses of CXCR-4 expression revealed a progressive accumulation of CXCR4-positive cells during plaque evolution, and CXCR4-positive leukocytes have been detected in unstable plaques (Naruko et al., 2002). In human advanced plaques, the macrophage density is suggestive of the atherothrombotic risk as macrophages release matrix metalloproteases, which degrade the fibrous cap, and promote intralesional inflammation (Joseph & Tawakol, 2016). Therefore, CXCR-4 expression is associated with unstable plaques and holds promise for identification of vulnerable plaque (Weiberg et al., 2018).

Conclusion

In this study, [^{68}Ga]Ga-Pentixafor PET showed potential to monitor the progression of atherosclerotic plaques from healthy individuals to early-stage plaques and to more advanced stages.

Funding

This research was funded by the European Union's Horizon 2020 research and innovation program under Marie Skłodowska - Curie grant (grant number 722609).

Institutional Review Board Statement

The study was conducted according to the German Animal Protection Act, in conjunction with the regulation for the protection of animals used for experimental and other scientific purposes and approved by the Ethics Committee of a German competent authority (*i.e.*, Landesamt für Natur, Umwelt und Verbraucherschutz Nordrhein-Westfalen) (file number 81-02.04.2018.A286, approved on 20.11.2018).

Informed Consent Statement

Not applicable.

Data Availability Statement

All datasets to this article are available upon request from the corresponding author.

Acknowledgments

Special mentions to Dr. Barbara Klinkhammer and to Prof. Dr. Peter Boor from the Department of Pathology, University Hospital RWTH Aachen, for their support with the image acquisition of our histological slides.

Conflicts of Interest

Dr. Alexandru Florea, Prof. Leon J. Schurgers, Prof. Jan Bucerius, and Prof. Felix M. Mottaghy received research funding from the ITN INTRICARE of European Union's Horizon 2020 research and innovation program under the Marie Skłodowska-Curie grant (grant number 722609). Prof. Leon J. Schurgers receives research funding from the ITN EVOluTION of European Union's Horizon 2020 research and innovation program under the Marie Skłodowska-Curie grant, (grant number 675111); from the Norwegian Research Council (grant number 241584); and from the Dutch Thrombosis Service (grant number 2014.02). Dr. Agnieszka Morgenroth and Prof. Felix M. Mottaghy receive research funding from the German Research Foundation (DGN) in the framework of the Research Training Group for "Tumor-targeted Drug Delivery" (grant number 331065168), and for "Severity assessment in animal-based research" (grant number 321137804). Prof. Leon J. Schurgers has received institutional grants from Bayer, Boehringer Ingelheim, Daichi Sankyo, NattoPharma, and IDS. Prof. Felix M. Mottaghy is on the advisory board of Advanced Accelerator Applications GmbH and has received

institutional grants from GE Healthcare, Siemens, and Nano-Map. All of the other authors declare no conflict of interest. The funders had no role in the design of the study; in the collection, analyses, or interpretation of data; in the writing of the manuscript; or in the decision to publish the results.

References

Demmer O., Gourni E., Schumacher U., Kessler H., Wester H.-J.: PET Imaging of CXCR4 Receptors in Cancer by a New Optimized Ligand. ChemMedChem (2011) 6:1789–1791

Derlin T., Sedding D. G., Dutzmann J., Haghikia A., König T., Napp L. C., … Bengel F. M.: Imaging of chemokine receptor CXCR4 expression in culprit and nonculprit coronary atherosclerotic plaque using motion-corrected [68Ga]pentixafor PET/CT. European Journal of Nuclear Medicine and Molecular Imaging (2018) 45:1934–1944

Derlin T., Toth Z., Papp L., Wisotzki C., Apostolova I., Habermann C. R., … Klutmann S.: Correlation of Inflammation Assessed by 18F-FDG PET, Active Mineral Deposition Assessed by 18F-Fluoride PET, and Vascular Calcification in Atherosclerotic Plaque: A Dual-Tracer PET/CT Study. Journal of Nuclear Medicine (2011) 52:1020–1027

Döring Y., Pawig L., Weber C., Noels H.: The CXCL12/CXCR4 chemokine ligand/receptor axis in cardiovascular disease. Front Physiol (2014) 5:

Florea A., Morgenroth A., Bucerius J., Schurgers L. J., Mottaghy F. M.: Locking and loading the bullet against micro-calcification. European Journal of Preventive Cardiology (2021) 28:1370–1375

Florea A., Sigl J. P., Morgenroth A., Vogg A., Sahnoun S., Winz O. H., … Mottaghy F. M.: Sodium [18F]Fluoride PET Can Efficiently Monitor In Vivo Atherosclerotic Plaque Calcification Progression and Treatment. Cells (2021) 10:275

Gargiulo S., Gramanzini M., Mancini M.: Molecular Imaging of Vulnerable Atherosclerotic Plaques in Animal Models. International Journal of Molecular Sciences (2016) 17:1511

Gourni E., Demmer O., Schottelius M., D'Alessandria C., Schulz S., Dijkgraaf I., … Wester H. J.: PET of CXCR4 Expression by a 68Ga-Labeled Highly Specific Targeted Contrast Agent. Journal of Nuclear Medicine (2011) 52:1803–1810

Gupta S. K., Pillarisetti K., Lysko P. G.: Modulation of CXCR4 expression and SDF-1alpha functional activity during differentiation of human monocytes and macrophages. J Leukoc Biol (1999) 66:135–143

Hyafil F., Pelisek J., Laitinen I., Schottelius M., Mohring M., Döring Y., … Schwaiger M.: Imaging the Cytokine Receptor CXCR4 in Atherosclerotic Plaques with the

Radiotracer 68 Ga-Pentixafor for PET. Journal of Nuclear Medicine (2017) 58:499–506

Joseph P., Tawakol A.: Imaging atherosclerosis with positron emission tomography. European Heart Journal (2016) 37:2974–2980

Koenen R. R., Weber C.: Chemokines: established and novel targets in atherosclerosis. EMBO Mol Med (2011) 3:713–725

Kwiecinski J., Slomka P. J., Dweck M. R., Newby D. E., Berman D. S.: Vulnerable plaque imaging using 18 F-sodium fluoride positron emission tomography. The British Journal of Radiology (2020) 93:20190797

Libby P., Ridker P. M., Hansson G. K.: Progress and challenges in translating the biology of atherosclerosis. Nature 2011 473:7347 (2011) 473:317–325

Mohanta S., Yin C., Weber C., Hu D., Habenicht A. Jr.: Aorta Atherosclerosis Lesion Analysis in Hyperlipidemic Mice. Bio Protoc (2016) 6:

Naruko T., Ueda M., Haze K., van der Wal A. C., van der Loos C. M., Itoh A., … Becker A. E.: Neutrophil infiltration of culprit lesions in acute coronary syndromes. Circulation (2002) 106:2894–2900

Reiter T., Kircher M., Schirbel A., Werner R. A., Kropf S., Ertl G., … Lapa C.: Imaging of C-X-C Motif Chemokine Receptor CXCR4 Expression After Myocardial Infarction With [68Ga]Pentixafor-PET/CT in Correlation With Cardiac MRI. JACC: Cardiovascular Imaging (2018) 11:1541–1543

Ross R.: Atherosclerosis — An Inflammatory Disease. New England Journal of Medicine (1999) 340:115–126

Stary H. C., Chandler A. B., Dinsmore R. E., Fuster V., Glagov S., Insull W., … Wissler R. W.: A definition of advanced types of atherosclerotic lesions and a histological classification of atherosclerosis. A report from the Committee on Vascular Lesions of the Council on Arteriosclerosis, American Heart Association. Circulation (1995) 92:1355–1374

Swirski F. K., Nahrendorf M.: Leukocyte behavior in atherosclerosis, myocardial infarction, and heart failure. Science (2013) 339:161–166

Thackeray J. T., Derlin T., Haghikia A., Napp L. C., Wang Y., Ross T. L., … Bengel F. M.: Molecular Imaging of the Chemokine Receptor CXCR4 After Acute Myocardial Infarction. JACC: Cardiovascular Imaging (2015) 8:1417–1426

von Hundelshausen P., Schmitt M. M. N.: Platelets and their chemokines in atherosclerosis-clinical applications. Frontiers in Physiology (2014) 5 AUG:294

Weiberg D., Thackeray J. T., Daum G., Sohns J. M., Kropf S., Wester H.-J., … Derlin T.: Clinical Molecular Imaging of Chemokine Receptor CXCR4 Expression in Atherosclerotic Plaque Using 68 Ga-Pentixafor PET: Correlation with Cardiovascular Risk Factors and Calcified Plaque Burden. Journal of Nuclear Medicine (2018) 59:266–272

Zernecke A., Weber C.: Chemokines in the vascular inflammatory response of atherosclerosis. Cardiovasc Res (2010) 86:192–201

Zhu Y., Xian X., Wang Z., Bi Y., Chen Q., Han X., … Chen R.: Research Progress on the Relationship between Atherosclerosis and Inflammation. Biomolecules 2018, Vol. 8, Page 80 (2018) 8:80

Chapter VI: General discussion

An estimate of 17.9 million people died in 2019 from cardiovascular diseases, representing 32% of all global deaths; these numbers are expected to have risen in the last years. Therefore, early detection and subsequent treatment of atherosclerosis would prove to be an exceptional gain in human life and reducing the burden of cardiovascular disease on healthcare in general. In this thesis both a tool for the detection of vulnerable plaques (*i.e.*, Na[^{18}F]F and [^{68}Ga]Ga-Pentixafor) and a safe mean to treat it (*i.e.*, vitamin K) were investigated.

Na[^{18}F]F for imaging atherosclerotic plaques

As mentioned in Chapter 2, micro-calcification is now considered a hallmark of vulnerable plaque (Nakahara et al., 2017). Moreover, Na[^{18}F]F has shown its ability to target micro-calcified plaques in many independent studies. The findings presented in Chapter 3 reinforce the utility of this simple tracer to monitor treatment and disease progression. However, future clinical studies would be necessary to convince the medical community of its potential. This is since mice develop morphologically different plaques compared to humans (Jackson et al., 2007). Our data opens the path for future clinical studies to be able to argue on the use of Na[^{18}F]F PET in micro-calcified plaque monitoring. The preclinical data presented in Chapter III suggests the feasibility and need for future prospective clinical trials to assess the predictive value of Na[^{18}F]F for ischemic events.

As spotty calcifications as seen on CT are still used in the clinical diagnosis of vulnerable plaques, our new Warfarin model may be used to predict the site of calcification with Na[^{18}F]F. In this model mice are first placed on a western-type diet and later switched to a Warfarin supplemented diet to start developing vascular calcifications. As in our hand the animals developed the spotty calcifications on the CT after 12 weeks of Warfarin, we suggest for Na[^{18}F]F PET to be performed at an earlier time point to predict the exact site where the animal will develop the spotty calcification by the 12th week. Additionally, this model may serve to assess the efficacy of novel therapeutic approaches in a preclinical setup. The constant development of spotty calcifications in the aortic arch and brachiocephalic artery makes this model easily accessible by catheters for stent implantation. We do not expect excessive bleeding during surgery of these mice, as the animal with skin lesions did not present any abnormal bleeding in comparison with the other two mice with the same condition.

Na[^{18}F]F has an affinity for micro-calcifications because of the high surface-to-volume ratio of hydroxyapatite in the form of nanocrystals (Dweck et al., 2016). In large deposits, the inner crystals of hydroxyapatite are no longer available for binding and thus Na[^{18}F]F uptake is only observed at the periphery (Dweck et al., 2016). In these cases, the CT can show a more accurate depiction of spotty calcifications (Irkle et al., 2015). However, since the density of vascular calcification on CT showed an inverse association with cardiovascular risk in the MESA study (Criqui et al., 2017), Na[18F]F is the only available clinical imaging approach that can non-invasively detect vascular micro-calcification (Dweck et al., 2016; Florea, Morgenroth, et al., 2021).

Vitamin K supplementation in atherosclerosis

In Chapter 2, emerging data arguing for vitamin K - especially MK-7 - as a cost-effective method of delaying the progression of vascular calcification is described. Shortly, vitamin K is a crucial cofactor in the post-translational modifications of various proteins, including coagulation factors and matrix γ-carboxyglutamate protein (*i.e.,* MGP), the latter of which is involved in the inhibition of ectopic calcification. Considering this mechanism of action, vitamin K has received the attention of several on-going clinical trials. Out of all vitamins that fall under the umbrella of "vitamin K", MK-7 is one of the most used in preclinical and clinical trials thanks to its increased half-life in blood, which extends its uptake availability by extra-hepatic tissues (Schurgers et al., 2007).

Vitamin K supplementation does not induce or increase a state of hypercoagulability (Asakura et al., 2001). Thus, a higher intake of vitamin K cannot be associated with any negative reaction on the coagulation side; because a couple of extra-hepatic VKDPs have anti-calcification properties, we consider the effects on the calcification side as positive. Moreover, it seems that plasma levels of vitamin K and of uncarboxylated osteocalcin, another example of an extra-hepatic VKDP, rapidly change after modifying the intake of Phylloquinone regardless of age and sex (Truong et al., 2012).

The focus of most research trials is on the naturally occurring vitamers (*i.e.,* Phylloquinone and MKs). However, it is worth putting together the possible health benefits of supplementation with vitamins K3, K4, or K5. Even though they have never been tested in clinical studies, all synthetic vitamins K have been shown to possess anti-neoplastic effects. Vitamin K3 alongside K5 has been proven to activate caspase-dependent apoptosis in colorectal carcinoma cells (Ogawa et al., 2007), while K4 seems to also induce mitochondrial dysfunction in osteosarcoma patients (Di et al., 2017).

Vitamin K5 is also known to mimic insulin and to determine the downregulation of insulin receptors (Maegawa et al., 1985). Moreover, it has been found to also possess anti-microbial activity against various bacteria and fungi (Merrifield & Yang, 1965a, 1965b). For these reasons and because it has a low toxicity, vitamin K5 has already been proposed as a food preservative (Merrifield & Yang, 1965a). To emphasise even more the feasibility of this idea, several clinical trials that assess vitamin K5 supplementation in ectopic calcification are needed.

Preclinical studies

VKAs induce ectopic calcification

The vitamin K inhibitor Warfarin blocks the post-translational modifications of the matrix γ-carboxyglutamate protein and thus accelerates ectopic calcifications, including vascular ones. It is well known that rodents under Warfarin treatment alone develop lethal bleedings caused by inhibiting the proper hepatic synthesis of vitamin K dependent coagulation factors. By supplementing the respective diet with Phylloquinone (*i.e.,* vitamin K1), the liver function is recovered, however Warfarin is still able to inhibit the proper synthesis of matrix γ-carboxyglutamate protein (Krüger et al., 2013; Price et al., 1998).

One of the most used animal models that develops vascular calcification is the co-treatment with Warfarin and Phylloquinone. Because mice and rats usually develop lethal bleedings during treatment with VKAs, it was found out that, by supplementing with Phylloquinone, the animals still develop extra-hepatic calcifications, but they are saved from the bleedings (Price et al., 1998). This mechanism has already been applied in Sprague-Dawley rats and ApoE-knockout and DBA/2 mice (Howe & Webster, 2001; Krüger et al., 2013; Schurgers et al., 2012). With the help of those animal models, it was found that VKAs seem to have detrimental effect on the arterial wall (Price et al., 1998).

Warfarin treatment induces the formation of calcified lesions in the mice as described in Chapter 3. Previously it was shown that its supplementation to a western-type diet induces intimal plaque calcification in ApoE-knockout mice (Schurgers et al., 2012). Moreover, this compound causes changes in plaque morphology with features suggestive of plaque vulnerability (Schurgers et al., 2012).

An unexpected finding was the warfarin-induced spotty calcifications detected by the CT. In this study, the spotty calcifications were developed exclusively in the proximal aorta (*i.e.*, aortic arch, brachiocephalic artery, and left common carotid artery), despite

extensive evaluation of all other regions of interest. This is one of the very few mouse models that spontaneously develops constant ectopic calcifications exclusively in the aortic arch; moreover, the lesions developed by our model, are very similar to those observed in humans (Obaid et al., 2017).

There are indeed other mouse models, which develop vascular calcifications (Jahnen-Dechent et al., 2011), however these mice require an additional mutation, and they have a reduced lifespan. On the other hand, there is no described reduced lifespan of the ApoE-knockout mice on Warfarin. In Chapter 3, all mice from this group reached 6 months of age (*i.e.,* 24 weeks of diet) with no apparent health problems. Moreover, in some of our yet unpublished studies, mice in this group also reached 9 months of age (*i.e.,* 36 weeks of diet) also with no apparent issues. To my knowledge, the only described side-effect is the lethal bleedings, which may be kept in check by dietary supplementation with Phylloquinone (Price et al., 1998).

Vitamin K inhibits ectopic calcification

A preclinical study showed that Phylloquinone supplementation improves the glycaemic status and lowers the degree of vascular inflammation in type 2 diabetic mice, while reducing the plasma-level of uncarboxylated MGP (Dihingia et al., 2018). Moreover, as it is known that bone morphogenetic proteins promote the inflammation in atherogenic conditions (Simões Sato et al., 2014), vitamin K supplementation may also improve vascular health by directly activating MGP, the natural inhibitor of the pro-apoptotic bone morphogenetic protein 2 (Wallin et al., 2000).

Most studies regarding the mechanisms behind vitamin K absorption and bio-distribution have assessed Phylloquinone, therefore much less is known about MKs and even less about the synthetic vitamins K. Unlike other lipid soluble vitamins like A and D, which have specific plasma carriers, vitamin K is transported mainly by lipoproteins: nascent chylomicrons (ApoA, ApoB-48, ApoC, and ApoE), chylomicron remnants (ApoB-48 and ApoE), VLDL (ApoB-100, ApoC, and ApoE), IDL (ApoB-100 and ApoE), and LDL (ApoB-100).

Despite the emphasis on importance of ApoE during the uptake of vitamin K (Cooper, 1997), our data is in line with the other independent groups that have fed it to ApoE-knockout mice and had statically significant results. ApoE-knockout mice put on a Warfarin and Phylloquinone supplemented diet revealed the negative effects of VKAs in intimal and medial arterial calcification (Schurgers et al., 2012). Furthermore Wang *et al.*

showed that by supplementing MK (*i.e.*, the exact MK is not specified) to a high fat diet, ApoE-knockout mice reduce their plaque size (Wang et al., 2018). Therefore, vitamin K is still able to enter the cells without the help of ApoE mediated endocytosis by a yet unknown mechanism.

In the absence of ApoE, the cellular uptake of vitamin K may be achieved *via* LDL-mediated endocytosis. Another explanation of the protective effect of vitamin K in ApoE-knockout mice is the modulation of the plaque inflammatory response *via* a reduced VSMCs expression of Toll-like receptors (Wang et al., 2018). Yet, an open question remains: how is the hepatic uptake (which is based on a predominance of ApoE on chylomicron remnants (Cooper, 1997)) possible in this model?

Phylloquinone supplementation also improves the glycaemic status and lowers the degree of vascular inflammation in type 2 diabetic mice, while reducing the plasma-level of uncarboxylated MGP (Dihingia et al., 2018). Moreover, as it is known that bone morphogenetic proteins promote the inflammation in atherogenic conditions (Simões Sato et al., 2014), vitamin K supplementation may also improve vascular health by directly activating MGP, the natural inhibitor of the pro-apoptotic bone morphogenetic protein 2 (Wallin et al., 2000).

Translation into the clinic

Mice age 45 times faster than humans

In Chapter 3 it is presented how Na[^{18}F]F can discriminate between early and advanced stage plaques developed by ApoE-knockout mice fed a western-type diet for 12 and 24 weeks, respectively. Moreover, ApoE-knockout mice on a MK-7 supplemented diet seemed to have the lowest tracer uptake in the aortic arch and left ventricle of all atherosclerotic groups. In fact, there was no significant difference between the uptake between the MK-7 treatment and control in all investigated regions. Hence, Na[^{18}F]F can detect the morphological changes induced by vitamin K treatment in ApoE-knockout mice; these changes include reduction of plaque size and of vascular (micro-)calcification (Wang et al., 2018). Moreover, Na[^{18}F]F can distinguish between early and advanced stage atherosclerosis (Florea, Sigl, et al., 2021).

The 24-week long preclinical study presented in Chapter 3 has ramifications for clinical translation. Here 6-week-old animals were placed on a western-type diet for 12 weeks, while the intervention lasted for an additionally 12 weeks. Mice between 1-6 months, which fit the age of our animals, age 45 times faster than humans (Flurkey et al., 2007);

this would translate into a ~10 yearlong intervention. Moreover, as the mice used in Chapter 3 consume on average 4g of food per day (Bachmanov et al., 2002), each mouse received a 400µg daily supplementation of vitamin K, while the current recommended nutrient intake (*i.e.*, RNI) recommended by the WHO is of 1µg a day of vitamin K for each kilogram of body weight (World Health Organization, 2005). This finding adds to the list of the beneficial effects of vitamin K on cardiovascular health described in Chapter 2 and may serve as an argument for the increase in the recommended daily dose of vitamin K. Moreover, if the clinical trial described in Chapter 4 also provides positive results on the protective role of vitamin K, this may even favour its introduction in clinical practice. Some clinical studies failed to observe a change in Na[^{18}F]F uptake after a 6-month MK-7 supplementation (Zwakenberg et al., 2019). However, this discrepancy may be explained by several changes in our study design: our mice received the supplementation for a human equivalent of 10 years (Flurkey et al., 2007). Moreover, considering the higher homogeneity of inbred mice, the variance is innately lower in preclinical studies compared to clinical trials.

Clinical studies

Vitamin K improves vascular health

The detrimental effect of VKAs on cardiovascular and renal systems have already been established (Böhm et al., 2015). Moreover, a considerable number of emerging data from the last two decades associate vitamin K supplementation with several positive outcomes in bone and vascular health. Interestingly, a polish group found that there may be a link between coronary artery calcification and bone metabolism (Bentkowski et al., 2013).

As far as bone metabolism is concerned, even after 3 years Phylloquinone alone has no effect in subjects with osteoarthritis (Neogi et al., 2008). However, several studies show that supplementation with calcium and vitamin D, alongside Phylloquinone, improves bone matrix density in the ultradistal radius in 2 years and in the femoral neck in 3 years, while the percentage of uncarboxylated OC from total OC decreases considerably (Bolton-Smith et al., 2007; L. A. J. L. M. Braam et al., 2003). The same supplementation showed beneficial effects on the arterial elasticity after a follow-up of 3 years (L. Braam et al., 2004).

On the other hand, vitamin K supplementation alone seems to have beneficial effects on vascular health and calcification. Poor vitamin K status is correlated with extreme coronary artery calcification in hypertensive patients even under medication (Shea et al.,

2013). Meanwhile, a 3-year Phylloquinone supplementation reduces the already existing coronary artery calcification score in healthy volunteers (Shea et al., 2009).

There is one study that did not see any improvement in older patients with known vascular disease after 6 months of MK-7 supplementation (Fulton et al., 2016). However, it is worth pointing out that the subjects received a lower dose (*i.e.,* 100µg/day) than in other studies. One trial links the increased consumption of MK with a reduced relative risk of coronary heart disease mortality (Geleijnse et al., 2004). A more in-depth study also observed an inverse association between MK intake (but not for Phylloquinone intake) and the risk of coronary heart disease; this association was mainly due to subtypes MK-7, MK-8, and MK-9 (Gast et al., 2009). Indeed, MK-7 supplementation was also associated with improved MGP and OC levels in chronic kidney disease patients (n=53 with 45, 135, or 360µg/day (Westenfeld et al., 2012), n=200 with 360, 720, or 1080µg/3days (Caluwe et al., 2014), and n=50 with 360µg/day (Aoun et al., 2017)) and with decreased arterial stiffness in healthy postmenopausal women (n=244 with 180µg/day (Knapen et al., 2015)). Moreover, MK-7 supplementation (360µg/day) showed a beneficial effect on arterial stiffness in renal transplant recipients with stable graft function (Mansour et al., 2017).

Because of the frequent use with positive results of the 360µg/day MK-7 dose and of the negative results of 100µg/day, it is wise to keep the 360µg/day as a minimal supplementation dose.

A take home message

In this thesis, Na[^{18}F]F PET showed potential to monitor plaque micro calcification progression and treatment. This tracer also seemed to be able to detect the beneficial effects of vitamin K on cardiovascular micro-calcification in a robust preclinical trial. This now serves as the testing hypothesis of the larger INTRICATE clinical study, which will provide information on micro-calcification development in the context of atherosclerosis in the human situation and the potential beneficial effect of supplementation with vitamin K. This trial bears the potential to open novel avenues for future large scale randomized controlled trials to intervene in the plaque development and micro-calcification progression. Additionally, here a novel mouse model is described, which spontaneously develops spotty calcifications, detected by small animal CT, exclusively in the proximal aorta, with no apparent life-span reduction. Lastly, the

feasibility of [^{68}Ga]Ga-Pentixafor to detect inflammatory changes in plaque morphology was suggested revealed.

All in all, this thesis shows the feasibility of both Na[^{18}F]F and [^{68}Ga]Ga-Pentixafor PET to monitor atherosclerotic plaque progression and treatment. Additionally, it serves as an argument for the increase in the recommended daily dose of vitamin K.

Summary in English

Aims: Despite recent medical advances, cardiovascular disease remains the leading cause of death worldwide. Given the high sensitivity and specificity of Na[^{18}F]F and [^{68}Ga]Ga-Pentixafor for cardiovascular calcifications and inflammation respectively and positive emerging data of vitamin K on vascular health, the aim of this thesis was to assess the ability of both tracers to monitor disease progression and therapy with vitamin K.

Materials and methods: Chapter I provided a general introduction. Chapter II identified Na[^{18}F]F PET as the most suitable technique for detecting micro-calcification, after a structured PubMed search. Presenting the pros and cons of available treatments, vitamin K supplementation emerged as a possible safe and cost-effective option to inhibit vascular (micro)-calcification. In Chapter III, a unitary atherosclerotic mouse trial was designed to assess the ability of Na[^{18}F]F PET/CT to monitor therapy and disease progression and of vitamin K to inhibit vascular calcification. In Chapter IV, a prospective double-blind placebo-controlled feasibility study was created to investigate the practicability of the results from the animal study in the human situation, using a hybrid PET/MRI. In Chapter V, the feasibility of monitoring plaque inflammatory status using [^{68}Ga]Ga-Pentixafor was preclinically assessed.

Results and discussion: After selecting Na[^{18}F]F PET as a mean to image vascular (micro-)calcifications and Vitamin K to treat it, the preclinical trial was started. Here mice treated with Warfarin (*i.e.,* a Vitamin K inhibitor) presented spotty calcifications on the CT in the proximal aorta. All the spots corresponded to dense mineralisations on the von Kossa staining. Mice with an advanced atherosclerosis did not develop spotty calcifications, however Na[^{18}F]F uptake was still observed, suggesting the presence of micro-calcifications. After the control, the Vitamin K treated animals had the lowest Na[^{18}F]F uptake, suggestion its protective role. The results of the preclinical study will be tested in the INTRICATE clinical trial, where the primary endpoint is the temporal change of Na[^{18}F]F uptake in human carotid artery atherosclerosis of the treatment arm (*i.e.*, with vitamin K) and the placebo arm. [^{68}Ga]Ga-Pentixafor seems to be able to correctly detect inflammatory changes in the atherosclerotic plaque morphology.

Conclusion: This thesis argues for the practicability of Na[^{18}F]F and [^{68}Ga]Ga-Pentixafor PET to monitor atherosclerotic plaque progression and treatment, while serving as an argument for the increase in the recommended daily dose of vitamin K.

Summary in German (Zusammenfassung auf Deutsch)

Ziel: Trotz der neuesten medizinischen Fortschritte bleiben Herz-Kreislauf-Erkrankungen weltweit die häufigste Todesursache. Angesichts der hohen Sensitivität und Spezifität von Na[^{18}F] und [^{68}Ga]Ga-Pentixafor für kardiovaskuläre Verkalkungen bzw. Entzündungen und der positiver neuer Daten zu Vitamin K auf die vaskuläre Gesundheit war es das Ziel dieser Arbeit, die Fähigkeit beider Tracer zur Überwachung des Krankheitsverlaufs und der Vitamin-K-Therapie zu bewerten.

Methodik: Kapitel I enthielt eine allgemeine Einführung. Kapitel II identifizierte nach einer strukturierten PubMed-Recherche Na[^{18}F]F PET als die geeignetste Technik zum Nachweis von Mikroverkalkung. Nach Darstellung der Vor- und Nachteile verfügbarer Behandlungen erwies sich die Vitamin-K-Supplementierung als mögliche, sichere und kosteneffektive Option zur Hemmung der Gefäß(mikro)verkalkung. In Kapitel III wurde eine unitäre Studie an atherosklerotischen Mäusen durchgeführt, um die Fähigkeit von Na[^{18}F]F PET/CT zur Überwachung der Therapie und des Krankheitsverlaufs sowie von Vitamin K zur Hemmung der Gefäßverkalkung zu bewerten. In Kapitel IV wurde eine prospektive, doppelblinde, Placebo kontrollierte Machbarkeitsstudie erstellt, um die Übertragbarkeit der Ergebnisse aus der Tierstudie auf den Menschen zu untersuchen, wobei ein PET/MRT-Hybrid verwendet wurde. In Kapitel V wurde die Durchführbarkeit der Überwachung des Plaque-Entzündungsstatus mit [^{68}Ga]Ga-Pentixafor präklinisch untersucht.

Ergebnisse: Nach der Auswahl von Na[^{18}F]F PET als Mittel zur gezielten Untersuchung von Gefäßverkalkungen und Vitamin K zur Behandlung wurde der präklinische Versuch gestartet. Bei Mäusen, die mit Warfarin (d. h. einem Vitamin-K-Hemmer) behandelt wurden, zeigten sich auf dem CT punktuelle Verkalkungen in der proximalen Aorta. Alle Punkte entsprachen dichten Mineralisierungen in der von-Kossa-Färbung. Bei Mäusen mit fortgeschrittener Atherosklerose traten keine punktuelle Verkalkungen auf, jedoch wurde weiterhin eine Na[^{18}F]F-Aufnahme festgestellt, was auf das Vorhandensein von Mikroverkalkungen hindeutet. Nach der Kontrollgruppe wiesen die mit Vitamin K behandelten Tiere die geringste Na[^{18}F]F-Aufnahme auf, was auf die schützende Wirkung von Vitamin K hindeutet. Die Ergebnisse der präklinischen Studie werden in der klinischen Studie INTRICATE getestet, deren primärer Zeil die zeitliche Veränderung der Na[^{18}F]F-Aufnahme in der humanen Halsschlagader-Atherosklerose in der Behandlungsgruppe (d. h. mit Vitamin K) und in der Placebo-Gruppe ist.

[^{68}Ga]Ga-Pentixafor scheint in der Lage zu sein, entzündliche Veränderungen in der Morphologie der atherosklerotischen Plaques korrekt zu erkennen.

Schlussfolgerungen: Diese These spricht für die Anwendbarkeit von Na[^{18}F]F- und [^{68}Ga]Ga-Pentixafor-PET-Untersuchung zur Überwachung des Verlaufs und der Behandlung atherosklerotischer Plaques und dient gleichzeitig als Argument für die Erhöhung der empfohlenen Tagesdosis von Vitamin K.

Valorisation

According to the most recent data of the World health organisation (*i.e.*, WHO), cardiovascular disease (CVDs) is the leading cause of death globally. An estimated 17.9 million people died from CVDs in 2019, representing 32% of all global deaths; as a comparison, in 2020 all types of cancer combined accounted for nearly 10 million deaths. Out of the 17 million premature deaths (*i.e.*, under the age of 70) due to non-communicable diseases in 2019, 38% were caused by CVD (World Health Organization, 2021).

Almost 90% of CVDs are caused by the formation of atherosclerotic plaques (Planer et al., 2014), which may become vulnerable, thus having an increased risk of rupture. If one of these plaques rupture, it becomes complicated and forms a blood clot, which lead to tissue ischemia either at the site of the plaque (*e.g.*, myocardial infarction, peripheral artery disease) or at another site *via* embolism (*e.g.*, stroke). Almost 85% of CVD deaths are due to one of these two mechanisms. Inflammation and micro-calcification are established hallmarks of vulnerable atherosclerotic plaque development; therefore, the identification and the subsequent early on treatment of these processes would help ease the burden and load CVD have on the medical system and society as a whole.

The aim of this thesis was twofold: (1) to try to assess novel methods for early identification of micro-calcification and later also of inflammation and (2) to test the feasibility of combating micro-calcification with vitamin K.

The knowledge gained from the experiments performed here are of general interest for every single one of us, as, because of our western diet, we all shall develop atherosclerotic plaques at some point. Detecting vulnerable plaques would first enable invasive resection therapy (*i.e.*, endarterectomy) to be directed against plaques, which may cause harm, instead of only resecting plaques, which cause a certain lumen reduction. Moreover, the findings form the vitamin K efficiency, if also reflected in humans as in mice, would help reduce the overall number of premature deaths and of deaths caused by CVD. The early detection and the subsequent treatment of atherosclerosis suggested by this thesis would prove to be an exceptional gain in human life and realising the burden of cardiovascular disease on healthcare in general.

These results of this thesis may also be of interest for several targeted groups. First, clinicians involved in the patient care may take advantage of these findings. Currently, there is no effective way to detect vulnerable plaques; they are identified with the help of

several imagistic methods, which are all based more or less on determining the degree of luminal stenosis the plaque causes on the artery. However, this is rather a poor indicator, because, as shown in Chapters I and II, plaque size is not a vulnerability feature. The promise of the two imaging techniques assessed in Chapters III and V, is to improve patient stratification, by identifying patients at risk. This would mean that the treatment and its intensity may be tailored for each patient around the degree of vulnerability of the plaques developed. This would also improve the healthcare of patient with asymptomatic CVD, as they rarely receive any treatment, only before it's too late. Second, an important target group would be the food industry and healthcare departments. As show in Chapter II and tested in Chapter III, vitamin K seems to protect against the development of micro-calcification (*i.e.*, a known marker for vulnerability); therefore, increasing the daily recommended dose or providing specific vitamin K2 (*i.e.*, more exactly MK-7) supplements in a high enough dose, would help combat micro-calcification and therefore vulnerable plaque formation at the level of general population. Here it is also worth mentioning that there is no evidence for overdose of vitamin K and also no risk associated with increasing the recommended dose for this specific type of vitamin.

The ultimate goal of this project and therefore also of this thesis was set to improve knowledge on micro-calcification and inflammation during atherosclerotic plaque development and to investigate how vitamin K influences this process. The generated data was presented at national and international conferences and published in peer-reviewed open access journals. At the end of the project, we have shown the potential of two tracers to reliably detect micro-calcification and inflammation respectively, and that vitamin K holds the potential to inhibit vascular micro-calcification within the atherosclerotic plaque. This research will serve as a steppingstone for further and more accurate detection of vulnerable plaque features and for a better treatment and prevention of CVD.

References

Aoun, M., Makki, M., Azar, H., Matta, H., & Chelala, D. N. (2017). High Dephosphorylated-Uncarboxylated MGP in Hemodialysis patients: risk factors and response to vitamin K2, A pre-post intervention clinical trial. *BMC Nephrology*, *18*(1), 191

Asakura, H., Myou, S., Ontachi, Y., Mizutani, T., Kato, M., Saito, M., Morishita, E., Yamazaki, M., Nakao, S., Mizutani, T., & Morishita, E. (2001). Vitamin K Administration to Elderly Patients with Osteoporosis Induces No Hemostatic Activation, Even in Those with Suspected Vitamin K Deficiency. *Osteoporosis International*, *12*(12), 996–1000

Bachmanov, A. A., Reed, D. R., Beauchamp, G. K., & Tordoff, M. G. (2002). Food intake, water intake, and drinking spout side preference of 28 mouse strains. *Behavior Genetics*, *32*(6), 435–443

Bentkowski, W., Kuźniewski, M., Fedak, D., Dumnicka, P., Kuśnierz-Cabala, B., Janda, K., & Sułowicz, W. (2013). [Undercarboxylated osteocalcin (Glu-OC) bone metabolism and vascular calcification in hemodialyzed patients]. *Przeglad Lekarski*, *70*(9), 703–706

Böhm, M., Ezekowitz, M. D., Connolly, S. J., Eikelboom, J. W., Hohnloser, S. H., Reilly, P. A., Schumacher, H., Brueckmann, M., Schirmer, S. H., Kratz, M. T., Yusuf, S., Diener, H.-C., Hijazi, Z., & Wallentin, L. (2015). Changes in Renal Function in Patients With Atrial Fibrillation. *Journal of the American College of Cardiology*, *65*(23), 2481–2493

Bolton-Smith, C., McMurdo, M. E., Paterson, C. R., Mole, P. A., Harvey, J. M., Fenton, S. T., Prynne, C. J., Mishra, G. D., & Shearer, M. J. (2007). Two-Year Randomized Controlled Trial of Vitamin K1 (Phylloquinone) and Vitamin D3 Plus Calcium on the Bone Health of Older Women. *Journal of Bone and Mineral Research*, *22*(4), 509–519

Braam, L. A. J. L. M., Knapen, M. H. J., Geusens, P., Brouns, F., Hamulyák, K., Gerichhausen, M. J. W., & Vermeer, C. (2003). Vitamin K1 supplementation retards bone loss in postmenopausal women between 50 and 60 years of age. *Calcified Tissue International*, *73*(1), 21–26

Braam, L., Hoeks, A., Brouns, F., Hamulyák, K., Gerichhausen, M., & Vermeer, C. (2004). Beneficial effects of vitamins D and K on the elastic properties of the vessel wall in postmenopausal women: a follow-up study. *Thrombosis and Haemostasis*, *91*(2), 373–380

Caluwe, R., Vandecasteele, S., Van Vlem, B., Vermeer, C., & De Vriese, A. S. (2014). Vitamin K2 supplementation in haemodialysis patients: a randomized dose-finding study. *Nephrology Dialysis Transplantation*, *29*(7), 1385–1390

Cooper, A. D. (1997). Hepatic uptake of chylomicron remnants. *Journal of Lipid Research*, *38*(11), 2173–2192

Criqui, M. H., Knox, J. B., Denenberg, J. O., Forbang, N. I., McClelland, R. L., Novotny, T. E., Sandfort, V., Waalen, J., Blaha, M. J., & Allison, M. A. (2017). Coronary Artery Calcium Volume and Density: Potential Interactions and Overall Predictive Value: The Multi-Ethnic Study of Atherosclerosis. *JACC: Cardiovascular Imaging*, *10*(8), 845–854

Di, W., Khan, M., Gao, Y., Cui, J., Wang, D., Qu, M., Feng, L., Maryam, A., & Gao, H. (2017). Vitamin K4 inhibits the proliferation and induces apoptosis of U2OS osteosarcoma cells via mitochondrial dysfunction. *Molecular Medicine Reports*, *15*(1), 277–284

Dihingia, A., Ozah, D., Baruah, P. K., Kalita, J., & Manna, P. (2018). Prophylactic role of vitamin K supplementation on vascular inflammation in type 2 diabetes by regulating the NF-κB/Nrf2 pathway via activating Gla proteins. *Food & Function*, *9*(1), 450–462

Dweck, M. R., Aikawa, E., Newby, D. E., Tarkin, J. M., Rudd, J. H. F., Narula, J., & Fayad, Z. A. (2016). Noninvasive Molecular Imaging of Disease Activity in Atherosclerosis. *Circulation Research*, *119*(2), 330–340

Florea, A., Morgenroth, A., Bucerius, J., Schurgers, L. J., & Mottaghy, F. M. (2021). Locking and loading the bullet against micro-calcification. *European Journal of Preventive Cardiology*, *28*(12), 1370–1375

Florea, A., Sigl, J. P., Morgenroth, A., Vogg, A., Sahnoun, S., Winz, O. H., Bucerius, J., Schurgers, L. J., & Mottaghy, F. M. (2021). Sodium [18F]Fluoride PET Can Efficiently Monitor In Vivo Atherosclerotic Plaque Calcification Progression and Treatment. *Cells*, *10*(2), 275

Flurkey, K., Currer, J., & Harrison, D. (2007). Mouse Models in Aging Research. In J. Fox, S. Barthold, M. Davisson, C. Newcomer, F. Quimby, & A. Smith (Eds.), *The Mouse in Biomedical Research* (2nd ed., Vol. 3, pp. 637–672). Elsevier

Fulton, R. L., McMurdo, M. E. T., Hill, A., Abboud, R. J., Arnold, G. P., Struthers, A. D., Khan, F., Vermeer, C., Knapen, M. H. J., Drummen, N. E. A., & Witham, M. D. (2016). Effect of vitamin K on vascular health and physical function in older people with vascular

disease–a randomised controlled trial. *The Journal of Nutrition, Health & Aging*, *20*(3), 325–333

Gast, G. C. M., de Roos, N. M., Sluijs, I., Bots, M. L., Beulens, J. W. J., Geleijnse, J. M., Witteman, J. C., Grobbee, D. E., Peeters, P. H. M., & van der Schouw, Y. T. (2009). A high menaquinone intake reduces the incidence of coronary heart disease. *Nutrition, Metabolism and Cardiovascular Diseases*, *19*(7), 504–510

Geleijnse, J. M., Vermeer, C., Grobbee, D. E., Schurgers, L. J., Knapen, M. H. J., van der Meer, I. M., Hofman, A., & Witteman, J. C. M. (2004). Dietary Intake of Menaquinone Is Associated with a Reduced Risk of Coronary Heart Disease: The Rotterdam Study. *The Journal of Nutrition*, *134*(11), 3100–3105

Howe, & Webster. (2001). Warfarin exposure and calcification of the arterial system in the rat. *International Journal of Experimental Pathology*, *81*(1), 51–56

Irkle, A., Vesey, A. T., Lewis, D. Y., Skepper, J. N., Bird, J. L. E., Dweck, M. R., Joshi, F. R., Gallagher, F. A., Warburton, E. A., Bennett, M. R., Brindle, K. M., Newby, D. E., Rudd, J. H., & Davenport, A. P. (2015). Identifying active vascular microcalcification by 18F-sodium fluoride positron emission tomography. *Nature Communications*, *6*(1), 7495

Jackson, C. L., Bennett, M. R., Biessen, E. A. L., Johnson, J. L., & Krams, R. (2007). Assessment of Unstable Atherosclerosis in Mice. *Arteriosclerosis, Thrombosis, and Vascular Biology*, *27*(4), 714–720

Jahnen-Dechent, W., Heiss, A., Schäfer, C., & Ketteler, M. (2011). Fetuin-A Regulation of Calcified Matrix Metabolism. *Circulation Research*, *108*(12), 1494–1509

Knapen, M. H. J., Braam, L. A. J. L. M., Drummen, N. E., Bekers, O., Hoeks, A. P. G., & Vermeer, C. (2015). Menaquinone-7 supplementation improves arterial stiffness in healthy postmenopausal women. *Thrombosis and Haemostasis*, *113*(5), 1135–1144

Krüger, T., Oelenberg, S., Kaesler, N., Schurgers, L. J., van de Sandt, A. M., Boor, P., Schlieper, G., Brandenburg, V. M., Fekete, B. C., Veulemans, V., Ketteler, M., Vermeer, C., Jahnen-Dechent, W., Floege, J., & Westenfeld, R. (2013). Warfarin Induces Cardiovascular Damage in Mice. *Arteriosclerosis, Thrombosis, and Vascular Biology*, *33*(11), 2618–2624

Maegawa, H., Kobayashi, M., Watanabe, N., Ishibashi, O., Takata, Y., & Shigeta, Y. (1985). Inhibition of down regulation by chloroquine in cultured lymphocytes (RPMI-1788 line). *Diabetes Research and Clinical Practice*, *1*(3), 145–153

Mansour, A. G., Hariri, E., Daaboul, Y., Korjian, S., El Alam, A., Protogerou, A. D., Kilany, H., Karam, A., Stephan, A., & Bahous, S. A. (2017). Vitamin K2 supplementation and arterial stiffness among renal transplant recipients—a single-arm, single-center clinical trial. *Journal of the American Society of Hypertension*, *11*(9), 589–597

Merrifield, L. S., & Yang, H. Y. (1965a). Factors affecting the antimicrobial activity of vitamin K5. *Applied Microbiology*, *13*(5), 766–770

Merrifield, L. S., & Yang, H. Y. (1965b). Vitamin K5 as a fungistatic agent. *Applied Microbiology*, *13*(5), 660–662

Nakahara, T., Dweck, M. R., Narula, N., Pisapia, D., Narula, J., & Strauss, H. W. (2017). Coronary Artery Calcification: From Mechanism to Molecular Imaging. *JACC: Cardiovascular Imaging*, *10*(5), 582–593

Neogi, T., Felson, D. T., Sarno, R., & Booth, S. L. (2008). Vitamin K in hand osteoarthritis: results from a randomised clinical trial. *Annals of the Rheumatic Diseases*, *67*(11), 1570–1573

Obaid, D. R., Calvert, P. A., Brown, A., Gopalan, D., West, N. E. J., Rudd, J. H. F., & Bennett, M. R. (2017). Coronary CT angiography features of ruptured and high-risk atherosclerotic plaques: Correlation with intra-vascular ultrasound. *Journal of Cardiovascular Computed Tomography*, *11*(6), 455–461

Ogawa, M., Nakai, S., Deguchi, A., Nonomura, T., Masaki, T., Uchida, N., Yoshiji, H., & Kuriyama, S. (2007). Vitamins K2, K3 and K5 exert antitumor effects on established colorectal cancer in mice by inducing apoptotic death of tumor cells. *International Journal of Oncology*, *31*(2), 323–331

Planer, D., Mehran, R., Ohman, E. M., White, H. D., Newman, J. D., Xu, K., & Stone, G. W. (2014). Prognosis of Patients With Non–ST-Segment–Elevation Myocardial Infarction and Nonobstructive Coronary Artery Disease. *Circulation: Cardiovascular Interventions*, *7*(3), 285–293

Price, P. A., Faus, S. A., & Williamson, M. K. (1998). Warfarin Causes Rapid Calcification of the Elastic Lamellae in Rat Arteries and Heart Valves. *Arteriosclerosis, Thrombosis, and Vascular Biology*, *18*(9), 1400–1407

Schurgers, L. J., Joosen, I. A., Laufer, E. M., Chatrou, M. L. L., Herfs, M., Winkens, M. H. M., Westenfeld, R., Veulemans, V., Krueger, T., Shanahan, C. M., Jahnen-Dechent, W., Biessen, E., Narula, J., Vermeer, C., Hofstra, L., & Reutelingsperger, C. P. (2012).

Vitamin K-Antagonists Accelerate Atherosclerotic Calcification and Induce a Vulnerable Plaque Phenotype. *PLoS ONE*, *7*(8), e43229

Schurgers, L. J., Teunissen, K. J. F., Hamulyak, K., Knapen, M. H. J., Vik, H., & Vermeer, C. (2007). Vitamin K-containing dietary supplements: comparison of synthetic vitamin K1 and natto-derived menaquinone-7. *Blood*, *109*(8), 3279–3283

Shea, M. K., Booth, S. L., Miller, M. E., Burke, G. L., Chen, H., Cushman, M., Tracy, R. P., & Kritchevsky, S. B. (2013). Association between circulating vitamin K1 and coronary calcium progression in community-dwelling adults: the Multi-Ethnic Study of Atherosclerosis. *The American Journal of Clinical Nutrition*, *98*(1), 197–208

Shea, M. K., O'Donnell, C. J., Hoffmann, U., Dallal, G. E., Dawson-Hughes, B., Ordovas, J. M., Price, P. A., Williamson, M. K., & Booth, S. L. (2009). Vitamin K supplementation and progression of coronary artery calcium in older men and women. *The American Journal of Clinical Nutrition*, *89*(6), 1799–1807

Simões Sato, A. Y., Bub, G. L., & Campos, A. H. (2014). BMP-2 and -4 produced by vascular smooth muscle cells from atherosclerotic lesions induce monocyte chemotaxis through direct BMPRII activation. *Atherosclerosis*, *235*(1), 45–55

Truong, J. T., Fu, X., Saltzman, E., Al Rajabi, A., Dallal, G. E., Gundberg, C. M., & Booth, S. L. (2012). Age Group and Sex Do Not Influence Responses of Vitamin K Biomarkers to Changes in Dietary Vitamin K. *The Journal of Nutrition*, *142*(5), 936–941

Wallin, R., Cain, D., Hutson, S. M., Sane, D. C., & Loeser, R. (2000). Modulation of the binding of matrix Gla protein (MGP) to bone morphogenetic protein-2 (BMP-2). *Thrombosis and Haemostasis*, *84*(6), 1039–1044

Wang, Z., Wang, Z., Zhu, J., Long, X., & Yan, J. (2018). Vitamin K2 can suppress the expression of Toll-like receptor 2 (TLR2) and TLR4, and inhibit calcification of aortic intima in ApoE -/- mice as well as smooth muscle cells. *Vascular*, *26*(1), 18–26

Westenfeld, R., Krueger, T., Schlieper, G., Cranenburg, E. C. M., Magdeleyns, E. J., Heidenreich, S., Holzmann, S., Vermeer, C., Jahnen-Dechent, W., Ketteler, M., Floege, J., & Schurgers, L. J. (2012). Effect of Vitamin K2 Supplementation on Functional Vitamin K Deficiency in Hemodialysis Patients: A Randomized Trial. *American Journal of Kidney Diseases*, *59*(2), 186–195

World Health Organization. (2005). *Vitamin and mineral requirements in human nutrition* (2nd ed.). World Health Organization

World Health Organization. (2021). *WHO | Cardiovascular diseases (CVDs)*. WHO; World Health Organization. https://www.who.int/news-room/fact-sheets/detail/cardiovascular-diseases-(cvds)

Zwakenberg, S. R., de Jong, P. A., Bartstra, J. W., van Asperen, R., Westerink, J., de Valk, H., Slart, R. H. J. A., Luurtsema, G., Wolterink, J. M., de Borst, G. J., van Herwaarden, J. A., van de Ree, M. A., Schurgers, L. J., van der Schouw, Y. T., & Beulens, J. W. J. (2019). The effect of menaquinone-7 supplementation on vascular calcification in patients with diabetes: a randomized, double-blind, placebo-controlled trial. *The American Journal of Clinical Nutrition*, *110*(4), 883–890

Back matter

List of publications

1. Florea, A., Morgenroth, A., Bucerius, J., Schurgers, L. J., Mottaghy, F. M. (2021). Locking and loading the bullet against micro-calcification. *European Journal of Preventive Cardiology*, *28*(12):1370–75.
2. Kassem, M., Florea, A., Mottaghy, F. M., van Oostenbrugge, R., Kooi, M. E. (2020). Magnetic resonance imaging of carotid plaques: current status and clinical perspectives. *Annals of Translational Medicine*, *8*(19):1266.
3. Florea, A., Sigl, J. P., Morgenroth, A., Vogg, A., Sahnoun, S., Winz, O. H., Bucerius, J., Schurgers, L. J., Mottaghy, F. M. (2021). Sodium [^{18}F]Fluoride PET Can Efficiently Monitor In Vivo Atherosclerotic Plaque Calcification Progression and Treatment. *Cells*, *10*(2):275.
4. Florea, A., Kooi, M. E., Mess, W., Schurgers, L. J., Bucerius, J., Mottaghy, F. M. (2021). Effects of Combined Vitamin K2 and Vitamin D3 Supplementation on Na[^{18}F]F PET/MRI in Patients with Carotid Artery Disease: The INTRICATE Rationale and Trial Design. *Nutrients*, *13*(3):994.
5. Florea, A., Mottaghy, F. M., Bauwens, M. (2021). Molecular Imaging of Angiogenesis in Oncology: Current Preclinical and Clinical Status. *International Journal of Molecular Sciences*, *22*(11):5544.
6. Desai, P., Rimal, R., Florea, A., Gumerov, R. A., Santi, M., Sorokina, A. S., Sahnoun, S. E. M., Fischer, T., Mottaghy, F. M., Morgenroth, A., Mourran, A., Potemkin, I. I., Möller, M., Singh, S. (2022). Tuning the Elasticity of Nanogels Improves Their Circulation Time by Evading Immune Cells. *Angewandte Chemie International Edition, 61*(20):e202116653.
7. Sankaranarayanan, R. A., Florea, A., Allekotte, S., Vogg, A. T. J., Maurer, J., Schäfer, L., Bolm, J., Terhorst, S., Classen, A., Bauwens, M., Morgenroth, A., Mottaghy, F. M. (2022). PARP targeted Auger emitter therapy with [^{125}I]PARPi-01 for triple negative breast cancer. *Eur J Nucl Med Mol Imaging, 12*(1):1–12.
8. Craveiro, R. B., Florea, A., Niederau, C., Brenji, S., Kiessling, F., Sahnoun, S. E. M., Morgenroth, A., Mottaghy, F. M., Wolf, M. (2022). [^{68}Ga]Ga-Pentixafor and Sodium [^{18}F]Fluoride PET can non-invasively identify and monitor the dynamics of orthodontic tooth movement in mouse model. *Cells*, *11*(19):2949.

Acknowledgements

This thesis would not have been possible without the help and support of different people from different backgrounds and cities. So here, I would like to thank all those wonderful people and to express my gratitude for helping me in achieving a highly important title in my professional carrier.

Before anyone else, I would like to thank Prof. Dr. Felix M. Mottaghy, Prof. Dr. M. Eline Kooi, Prof. Dr. Leon J. Schurgers, and Prof. Dr. Jan Bucerius for giving me the opportunity to complete my work and to graduate under their supervision.

Prof. Mottaghy: Thank you for helping and encouraging me every step of the way, for giving me the freedom and guidance required to learn how to become a better researcher. You have not hesitated to send me to courses for further education (the German "Weiterbildung") and trusted me with complex and delicate tasks and in the end giving me the opportunity to lead several animal experiments in your department. I highly value the expertise I have learn from you on how to assess and manage internal and cooperation project. You have also given me the opportunity to supervise a couple of students and to coordinate most animal experiments, which have given me the confidence required to create my own team. Lastly, you have trusted me to operate and later be responsible for our preclinical imagine modalities (*i.e.*, the TriFoil and the Molecubes), which combined costed more then 2M €; initially the responsibility was high, but with time I came to trust myself, become responsible of my actions, and be able to operate and solve issues in complex equipment.

Prof. Kooi: Thank you for always being there for me and for including me in your research group, giving me the opportunity to meet different people from different backgrounds also in Maastricht. You were always there, ready to help me, telling me directly who to contact and how to approach them; in any way possible and you were for me my main advisor in Maastricht.

Prof. Schurgers: Thank you for always helping me with information and supplies on how to conduct my animal experiments. Thank you also for helping me improving my scientific writing, your corrections to my initial drafts of my first paper were invaluable for me; the suggestions you had back then, I am still applying them now and suggestion them further to younger students.

Prof. Bucerius: Thank you for being my mentor on what represents clinical trials. You helped me with advice and connections to set up a complex trial. Your move from

Maastricht to Göttingen, to start there your new leading position, did not affect in any way, not even in your first days there, the communication between us. Together we planned further the human study and assessed the data from the mouse experiments. Thank you for teaching me how to write project proposals and to tackle the rather difficult question of the medical-ethical committee.

Further I would like to thank Dr. Agnieszka Morgenroth for teaching me everything I know about animal handling and animal experiments. Agnieszka, with your help, I was able to make a solid foundation for my preclinical research skill, which I will carry with me forever. Also, I would like to thank you for entrusting me with all your duties and naming me as your temporary replacement while you were on parental leave. This, together with the trust from Prof. Mottaghy definitely helped build up my character as a future PI.

To Dr. Andreas Vogg I would like to thank for his support throughout my PhD. Dear Andreas, you were always there to help me with any chemistry and radio-chemistry question I had. You together with the entire radiochemistry group also helped me and supported my experiments, by establishing the required protocols for my tracer synthesis. P.S.: I could also always rely on you that in between the experiments at exactly 11:30, I would have at least one person to go to lunch with.

To the entire radiochemistry group, I would like to show my deepest gratitude for synthesising the tracers I needed, whenever I needed them, with a to-the-clock delivery. Without you, I would have researched the effect of water on plaques; for your support, I will always be thankful.

Dr. Oliver Winz helped, learned, and trained me how to operate and analyse one of the most complex and inter-disciplinary filed of all: PET and SPECT. Oli, thank you for always being there when I had an issuer with any of the machines and for teaching me how to analyse the complex data given by these scanners.

To Prof. Alexander Heinzel I would like to thank for giving me the opportunity to learn about *in ovo* experiments and for putting me in contact, with what I think is my very first collaboration (with Dr. Carina Stegmayr). Prof. Heinzel, I would like to thank you for giving me the opportunity to show and teach students about the research we are doing. Teaching has always been one of my favourite things to do; I would like to thank you for the leap of faith you took with me.

Bernward Oedekoven helped me navigate the completely new to me at the time German and RWTH University system with a pin-point precision. Bernd, we may have worked together for roughly only one year, however, for all you help with all German institutions within that year, I would like to thank you from my heart; I have tried to help our next students with all the information I got from you, after you retired, however your absence was truly missed.

Dr. Berthold Müller and his successor Dr. Andreas Goedicke never hesitated to come to my help whenever I needed difficult radiation dose calculations and other mathematical models that are outside my expertise. Berthold and Andreas, I would like to thank you both to your ever-swift reaction and response.

The backbone of the department Andreas Keuhlartz, Natasha Dümont, and Susanne Allekotte, I would like to thank for their immediate help, whenever I asked for something. To be honest I sometimes felt bad asking you for stuff, because I knew that you would drop what you were doing to help me. In several cases, I only came by, saw you were busy, I tried to solve my problem alone, because I did not want to disturb you. For all prompt answers you helped me with throughout the years, I would like to thank you from my heart.

The students of nuclear medicine, Ramya Sankaranarayanan, Prachi Bharat, Julius Sigl, Amelie Heesch, Betül Altunay, Sara Sanchez, and Laura Schäfer, I would like to thank for all the nice times we had during our PhD in the lab and outside. I always enjoyed discussing our results together and debating on which is the best way to present it to Agnieszka and Prof. Mottaghy. Ramya, Prachi, Julius, Amelie, Betül, Sara, Laura, I hope to always remain in touch with you and start interesting collaborations when we each get our research group.

Our research coordinator Dr. Fabian Hertel and to the two secretaries of Prof. Mottaghy, Ute Rau and Laura Knoth, I would like to thank for their invaluable help in all organisational aspects throughout my PhD.

Actually, I would like to thank the entire team from nuclear medicine for being so incredibly open and willing to give out advice and help throughout my time here. I always had the feeling that any issue or question I have, I will never have to leave the department, as there was always someone able to help me figure it out. Special thanks would also go to Monika Rohner, Sonja Bruchmann, Brigitte Dannenberg, and Sevinc Kocaman for always helping me every single time when I needed radioactivity and for make me available the amount I always needed, and sometimes even more.

Moving also outside Aachen, I would like to thank the INTRICARE consortium and especially to each and every early-stage researcher (ESR). Dear all, I think that throughout our 3 years together we have grown so close (despite the physical distance between Aachen, Maastricht, and Stockholm). I will never forget the time most of us stayed in the same apartment in Stockholm; those were the times…:)

Coming back to Aachen I would also thank to the Institute of Laboratory Animal Science (*i.e.*, "Institut für Versuchtierkunde") of RWTH Aachen. As most of my work was based on animal research in the start I was always going and asking how to proceed with things and especially the people from the so-called control centre (*i.e.*, "Leitstelle") always helped me as fast as possible. My thank need to go also to the animal welfare officers that taught me how to correctly document, how to treat and handle animals with problem, and how to write animal ethical proposals.

To the Institute of cardiovascular molecular research (IMCAR), my former institute, where I was an intern, I would like to thank for still being there for me, although I moved. Great thanks to Prof. Dr. Elisa Liehn, Roya Soltan, Dr. Adelina Băleanu-Curaj, and Dr. Zhuojun Wu for remaining in contact (also on a personal level) after so many years.

To my first collaboration partners, Dr. Carina Stegmayr, Dr. Rogerio Craveiro, and Dr. Barbara Klinkhammer, I would like to thank and show my appreciation for taking the leap of faith with me and trusting me to perform the required analysis and design the nuclear medicine part of their experiments.

As from the start, the collaboration with Dr. Matthias Bauwens was fruitful, as he wanted to write a review together. Dear Matthias, thank you for the top-notch scientific input you always offered me. I always enjoined the scientific and not-so-scientific talks we had, especially during lunch.

In our one year together, Dr. Masoud Sadeghzadeh and I formed a strong bond, which I think is the base for our future very prosperous collaboration. Masoud, thank you for all your help and for having my back in all projects we are involved.

To the dynamic trio of Sabri Sahnoun, Dr. Pardes Habib, and me I wish to have the most fruitful of collaborations; for the help and support you two have given me, I can only say thank you from the depths of my heart and that I hope I will also be able to help you in the same quality and quantity. To Sabri special thanks for being my rock in all radiochemical aspects and for all syntheses; I could always count on you, day and night,

to get the best, most radio-chemically pure tracers I needed. Pardes and Sabri thank you for our great collaboration and friendship.

Last but not least, I would like to thank my family, my mother, Roxana Florea, and my father Niculae Florea for their motivation, emotional support, and for keeping me focused when I needed it the most. Special thanks to my fiancée, Ana-Maria Gheorghe (Love) for being next to me in my journey to the highest professional achievements. I really regret the missed nights, late evening, and changed vacation because of my work and am very grateful for your emotional support.

Affidavit according to § 5 (1) for Data Retention

Hiermit erkläre ich, dass die dieser Dissertation zu Grunde liegenden Originaldaten (I hereby declare that the original data forming the basis of this doctoral thesis are stored) in der ***Klinik für Nuklearmedizin*** des Universitätsklinikums Aachen hinterlegt sind.

Affidavit according to § 5 (1) § 11 (3) 12 of the doctoral studies regulations

I, **Alexandru Florea,** hereby declare on oath that I independently collected and prepared the following results portrayed in the dissertation "**Sodium [18F]Fluoride positron emission tomography for non-invasive identification of micro-calcifications as marker of arterial plaque vulnerability**".

I had the following assistance with completing the dissertation. These are listed in the acknowledgments.

Names-→	Alexandru Florea	Sabri Sahnoun	Agnieszka Morgenroth	Jan Bucerius	Leon J. Schurgers	M. Eline Kooi	Felix M. Mottaghy	Sum (%)
Study supervision			20	20	20	20	20	100
Study design/conception	55		10	5	10	10	10	100
Examination of the study participants	55		10	5	10	10	10	100
Data evaluation	100							100
Performing experiments:								
• Animal work	100							100
• *in vivo* scans	100							100
• *ex vivo* work	100							100
Statistical evaluation	80			5	5	5	5	100
Delivery of materials			20	10	30	20	20	100
Interpretation of data evaluation	55	5	5	5	10	10	10	100
Performing experiments:								
• Tracer synthesis		100						100

Here, if necessary, list experiments or statistical evaluations, which were not performed on one's own accord but by respective, other persons.

_____

Signature of the doctoral candidate

As the supervisor of the above dissertation, I confirm the statements of Alexandru Florea.

_____

Signature of the doctoral supervisor

About the author

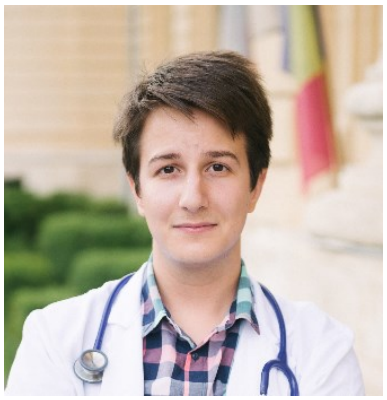

Alexandru Florea was born on Wednesday, 6th of May 1992 in Bucharest, Romania. He graduated the Central School of Bucharest in 2011, after which he enrolled to "Carol Davila" University of Medicine and Pharmacy, where he studied medicine and in his second year, he met the love of his live, Ana-Maria. As of March 2012, he also started going to the nearby "Victor Babeş" National Institute of Pathology, where he began being interested not only in medicine, but also in research. During the summer breaks of 2014, 2015, and 2016, he applied for an internship under the supervision of (at the time) Dr. Elisa Liehn, in Institute of cardiovascular molecular research (IMCAR), Aachen, Germany, to further advance his research skills. In September 2017 he obtained his medical degree and with Ana's support he applied for a Marie Currie early-stage researcher within the INTRICARE consortium.

At the beginning of 2018, the two moved to Germany and Alex started his new position as a Marie Currie fellow, while Ana began her medical career. Under the supervision of Prof. Felix M. Mottaghy from the Department of nuclear medicine of Uniklinik RWTH Aachen, he explored novel ways on how to detect inflammation and micro-calcification as markers for vulnerable plaque development and investigated the influence of vitamin K within these processes. During his PhD, he gained vast amounts of preclinical experience while working with research animals and using the small animal imaging equipment from Aachen. In the meantime, he also started networking in Maastricht University Medical Center, Maastricht, the Netherlands, where he put the basis for a clinical trial to try to translate his animal findings into the human scenario.

Outside his own research project, Alex was involved in several other collaborations, which kick started with his involvement in a research training group with the focus on tumour targeted drug delivery. Within this project he expanded his nuclear medicine expertise from cardiovascular imaging to cancer theragnostic. Throughout the years, he would get involved in other projects, spanning from non-invasive imaging of tooth movement, kidney fibrosis, triple negative breast cancer, pancreatic cancer, stroke to cancer treatment and developing a novel tracer for epilepsy and other associated neurological disorders. In May 2022, he also obtained his German licence to practice

medicine, flowing in the footsteps of his fiancée, in order to test in the future those imagining tracers in clinical trials.

Since 2019, Ana and Alex adopted a cat, named Storm, that was rescued from the streets of Bucharest, the city they met in. Currently, outside of work, they are growing fruits and vegetables in their newly acquired garden and discover together a new passion.